Adaptative mechanisms of cereals to climate change: the importance of nitrogen sources in soils

PhD. Thesis

Fernando Torralbo Cerro

Leioa, 2018

eman ta zabal zazu
Universidad del País Vasco
Euskal Herriko Unibertsitatea
NAZIOARTEKO BIKAINTASUN CAMPUSA
CAMPUS DE EXCELENCIA INTERNACIONAL

A mis padres,

mi hermana y

Belén

Cuando un científico eminente pero anciano afirma que algo es posible, es casi seguro que tiene razón. Cuando afirma que algo es imposible, muy probablemente está **equivocado**.

La única manera de descubrir los límites de lo posible es aventurarse un poco más allá, hacia lo **imposible**.

Cualquier tecnología lo suficientemente avanzada es indistinguible de la **magia**.

Arthur C. Clarke

Agradecimientos

Quisiera agradecer al Laboratorio de Fisiología Vegetal del Departamento de Biología Vegetal y Ecología de la Universidad del País Vasco (UPV/EHU) y, especialmente a mis directores de tesis, la Dra. Carmen González Murua y el Dr. Iker Aranjuelo Michelena por darme la oportunidad de realizar esta tesis.

También quisiera agradecer a:

Prof. Stefanie Wienkoop from the University of Vienna for the opportunity to make a four month stay in her research group.

Dra. Azucena González del Servicio Fitotrón e Invernadero SGIKer UPV/EHU por el apoyo técnico y humano.

Dra. Edurne Baroja del Instituto de Agrobiología (IdAB)-CSIC de Pamplona por apoyo técnico en la determinación de los metabolitos y actividades del ciclo del almidón.

Dra. Rosa Morcuende del Instituto de Recursos Naturales y Agrobiología-CSIC de Salamanca por el ayuda en el análisis de los datos de cebada.

Este trabajo de investigación ha recibido la financiación del Ministerio de Economía y Competitividad (AGL2012-37815-C05-02, AGL2015-64582-C03-02-R y AGL2016-79868-R) y del Gobierno Vasco (IT-932-16).

El autor de la tesis doctoral ha disfrutado de un Contrato Predoctoral para la formación de doctores del Ministerio de Economía y Competitividad (BES-2013-065418).

¿Cómo resumir cuatro años de trabajo? Fácil, escribe la tesis, presenta tus resultados en congresos y publica los resultados. Pero, ¿cómo agradecer rápidamente a todas las personas que han estado a tu lado durante todo este tiempo? Para mí, esto es más difícil.

En primer lugar, quisiera volver a agradecer a mis directores de tesis Carmen e Iker toda la ayuda, esfuerzo y dedicación que me habéis prestado. Carmen, gracias por tu energía y por enseñarme que hay que mirar más allá del resultado. Iker, gracias por tu inagotable perseverancia.

Gracias a todos los profesores del laboratorio de Fisiología Vegetal, Txema B, Alberto, Nacho, Usue, Amaia y Antonio, por brindarme ayuda cuando la he necesitado. Bego, gracias por tus consejos y toda la ayuda que me has dado cuando más la he necesitado.

A Miren y Txema por ser cómo sois, por vuestra cercanía, por vuestros consejos y, en general, por todos los ratos que hemos compartido. Porque entrar a vuestro despacho, a veces, es dar un paso hacia lo desconocido sin saber exactamente cuándo saldrás o con cuántas ideas nuevas.

A toda la flora (y fauna) del laboratorio de Fisiología Vegetal que tantas horas hemos compartido. Porque entre pipetas, actividades enzimáticas y muestreos siempre nos ha quedado un rato para echarnos unas risas (o unas broncas).

Asier, durante poco tiempo fuiste compañero, el resto del tiempo has sido, y eres, un amigo. ¡Qué tu buen rollísmo no se pierda nunca!

Teresa y Unai, de mayor quiero ser como vosotros. Poco más se puede decir de vosotros que no se sepa ya. No cambiéis nunca, qué sería de nosotros sin poder entrar a por vuestro consejo y ayuda, o solo a darle a la lengua. Al final hasta os he cogido cariño a pesar de que “mira que eres chorra” y “¿cómo te aguanta Belén?” son algunas de las frases diarias más bonitas que me dedicáis. ¡A por el papelito!

Isabel, mi PPAS favorito, gracias por tus multifunciones entre las que, además, te he incluido los desahogos a la hora del café. A Sergio, por los buenos momentos y mala música. Ximena gracias por no perder nunca en ánimo y, ¡por enseñarme el Euskadi tropical! Dani gracias por tu ayuda, implicación y empeño en todo lo que haces. Fátima sin ti el laboratorio es una anarquía, ¡necesitamos tu mano de hierro! Jana, ¡nos vemos al otro lado! A Iskander, por enseñarme que las diferencias entre nitrificación y desnitrificación van más allá del "des", pero sobre todo por saber que puedo contar contigo. A Izargi, ¡porqué lo mismo me enseñas de Fisiología Vegetal que de Harry Potter! Iskan, Izargi gracias por "corregirme" el euhkera!

Y en general a toda la siguiente hornada, Rafa, Marlon, Marta, Ander, Mario y Adrián, Iraide, Marina, Theo, y a la no tan reciente, Raquel, Maite, Jon, Inma y Bea gracias por estar siempre ahí y por todos los buenos ratos.

Dicen que los vascos sois fríos, ¡y menos mal! porque si fueseis más cariñosos ahora sería carbón para el Olentzero.

To the department of molecular systems of plant biology from University of Vienna, many thanks for the opportunity of being one more of yours. Especially, many thanks to Stefanie, Lena, Thomas, Reinhard, Manuela and Sebastian. Luis, todo un placer conocerte, espero que volvamos a cruzarnos algún día.

A Manolo Pineda, por abrirme las puertas a este mundo. Pepa, gracias por todos los consejos y enseñanzas que tanto me han ayudado a empezar a recorrer con buen paso esta carrera de fondo.

A mis padres, porque mi parte buena es gracias a vosotros y la mala, a pesar de vosotros. Porque me habéis enseñado a no dejar de mirar hacia adelante y a no rendirme nunca. A mi hermana por estar siempre ahí y (casi) siempre tener una sonrisa. Gracias por escucharme, por animarme y por preguntarme si he comido. Porque sin vosotros no hubiese llegado hasta aquí. A mi familia en general. Os quiero.

A mis apátridas, gracias por compartir nuestras penas y alegrías. Porque no dejemos de criticarnos en la vida. Porque acabe donde acabe sé que necesitaré espacio de sobra para alojaros.

Belén, a quien más fácil tendría que resultarme agradecerle cada momento en el que me ha ayudado, aguantado, levantado el ánimo y un eterno etcétera y quien más me ha costado encontrar las palabras. Tu apoyo incondicional y tu sonrisa me han salvado más de un día. Y, tenerte cerca hace que a lo que llamamos problemas pasen a un segundo, tercer o vigésimo plano. Eres el cobre del AMO, el Mo de la NR, el lúpulo de la cerveza. Gracias por hacerme funcionar.

Contents

Abstract / Resumen / Laburpena 25
1. Introduction 31
    1.1. Climate change 33
    1.2. Impact of human activity on atmospheric gas composition (CO_2 and N_2O) 36
        1.2.1. Carbon dioxide 36
        1.2.2. Nitrogenous gas emissions 37
        Nitrogen cycle in soils 37
        Use of N fertilisers in past, current and future agricultural practices 39
        Crop management and nitrogenous greenhouse gasses 40
    1.3. Plant performance under elevate CO_2 conditions 43
        1.3.1. Carbon fixation 43
        1.3.2. Role of nitrogen metabolism 45
2. Objectives 49
3. Dimethyl pyrazol-based nitrification inhibitors effect on nitrifying and denitrifying bacteria to mitigate N_2O emission 55
    3.1. Introduction 57
    3.2. Material and methods 61
    3.3. Results 67
    3.4. Discussion 76
4. Elevated CO_2 and nitrate supply overcomes the ammonium toxicity and improves photosynthetic parameters in wheat plants 83
    4.1. Introduction 85
    4.2. Material and methods 89
    4.3. Results 94
    4.4. Discussion 102
5. C/N metabolism in leaves and last stem internodes modulates the responsiveness of barley to changing CO_2 conditions 111
    5.1. Introduction 113
    5.2. Material and methods 117
    5.3. Results 122
    5.4. Discussion 132
6. Exposure to elevated CO_2 delays the senescence and permits the extension of the vegetative stage and the later remobilisation of metabolites toward ears 141
    6.1. Introduction 143
    6.2. Material and methods 146
    6.3. Results and Discussion 149
7. General conclusions 157
8. References 161
9. Supplemental information 189

Abstract

The human activity and, more specifically, industry, agriculture, fossil fuels consumption, deforestation, vegetable litter burning and livestock farming have caused a rapid increase in greenhouse gases (GHG) in the last century. The Intergovernmental Panel on Climate Change (IPCC) is promoting strategies to reduce these GHGs, as well as promoting the use of new crop varieties well adapted to future atmospheric conditions.

In this work, both strategies have been studied trough different approaches: a) use of nitrification inhibitors associated with ammonium-based fertilisers to reduce N_2O emissions derived from fertilization and b) study the impact of nitrogen on the C source-sink balance and the adaptation capacity of cereal varieties to the CO_2 increase. The obtained results confirm that the use of the analysed inhibitors (DMPP and DMPSA) is an effective strategy to reduce N_2O emission due to the inhibition of nitrifying bacteria. In addition, it was possible to describe how these compounds stimulate a complete denitrification, mitigating the emission of N_2O by means of a greater reduction to N_2. At plant level, in was studied the response of wheat to different sources of nitrogen (nitrate, ammonium and ammonium nitrate) under ambient (400 ppm) and elevated (700 ppm) CO_2 conditions. At elevated CO_2 conditions, ammonium nitrate or ammonium nutrition permitted better foliar carbohydrates adjustment, opposite to nitrate nutrition. Finally, the importance of developing C sinks under elevated CO_2 conditions and the C source-sink balance adjustment in leaves was studied in barley plants with different peduncle-storage capacity for carbon and nitrogen compounds. The results confirm the necessity to identify varieties with greater C sink capacity in order to allow a greater adjustment of carbon leaf, with the consequent improvement of photosynthetic activity under elevated CO_2 conditions.

Resumen

La actividad humana y más concretamente, la industria, la agricultura, el consumo de combustibles fósiles, la deforestación, la quema de restos vegetales y la ganadería han provocado un rápido aumento de gases de efecto invernadero (GEI) en el último siglo. El Panel intergubernamental para el cambio climático (IPCC) está impulsando estrategias centradas en la reducción de estos GEI, así como promoviendo el empleo de nuevas variedades (de los principales cultivos) que mejor se puedan adaptar a las futuras condiciones atmosféricas.

En ese trabajo se han abordado ambas estrategias mediante diferentes aproximaciones: a) empleo de inhibidores de la nitrificación asociados a fertilizantes de base amoniacal para reducir las emisiones de N_2O derivadas de la fertilización y b) identificar el impacto del nitrógeno en las relaciones fuente-sumidero de C y en la capacidad de adaptación de variedades de cereales al incremento de CO_2.

Los resultados obtenidos permiten confirmar que el uso de los inhibidores analizados (DMPP y DMPSA) es una estrategia efectiva para reducir la emisión de N_2O debido a la inhibición de las bacterias nitrificantes. Además, se pudo describir cómo estos compuestos estimulan una completa desnitrificación, mitigando la emisión de N_2O por medio de una mayor reducción a N_2. Por otro lado, se ha estudiado la respuesta de trigo frente a diferentes fuentes de nitrógeno (nitrato, amonio y nitrato amónico) en condiciones de CO_2 ambiental (400 ppm) y elevado (700 ppm). Bajo condiciones de elevado CO_2, la fertilización mixta o amoniacal permitió un mejor ajuste de carbohidratos foliares, al contrario que la fertilización nítrica. Por último, la importancia del desarrollo de sumideros de C en condiciones de elevado CO_2 y el ajuste de la relación fuente-sumidero de C en hoja se estudió en plantas de cebada con diferente capacidad de almacenar compuestos carbonados y nitrogenados en el pedúnculo. Los resultados descritos confirman la necesidad identificar variedades con mayor capacidad de sumidero de C para así permitir un mayor ajuste del C foliar con la consiguiente mejora en la actividad fotosintética bajo condiciones de elevado CO_2.

Laburpena

Giza jarduerak, eta zehatzago, industriak, nekazaritzak, erregai fosilen kontsumoak, deforestazioak, landare hondakinen erretzeak eta abeltzaintzak berotegi-efektuko gasen areagotze azkarra eragin dute azken mende honetan. Klima aldaketarako gobernu-arteko taldea (IPCC) berotegi-efektuko gasak murriztea ardatz duten hainbat estrategia sustatzen dabil, etorkizuneko atmosferako baldintzetara egokituta dauden kultibo barietate berrien erabilera bultzatzearekin batera.

Lan honetan aipatutako estrategia horiek ikuspuntu ezberdinetatik aztertu dira: a) amonio-oinarridun ongarrietara lotutako nitrifikazioaren inhibitzaileen erabilera ongarriketatik datozen N_2O izurpenak murrizteko eta b) nitrogenoak karbonoaren iturri-isurbide erlazioengan eta CO_2-aren areagotzearekiko zereal barietateek duten egokitzapen gaitasunarengan duen eragina aztertzea.

Eskuratutako emaitzek aztertutako nitrifikazioaren inhibitzaileen (DMPP and DMPSA) erabilera N_2O izurpen-murrizketarako estrategia egokia dela egiaztatzen dute bakteria nitrifikatzailearen inhibizioa dela eta. Gainera, konposatu hauek desnitrifikazio osoa suspertzen dutela deskribatu ahal izan da, N_2O izurpena murriztuz N_2-rako erredukzioaren areagotzearen bitartez. Bestalde, gariak nitrogeno iturri ezberdinekiko (nitratoa, amonioa eta nitrato-amonikoa) duen erantzuna aztertu da inguruneko CO_2 (400 ppm) zein CO_2 altuko (800 ppm) baldintzatan. CO_2 altuko baldintzatan, ongarritze mistoak zein amoniozkoak hostoko karbohidratoen doikuntza hobea baimentzen dute, nitrato ongarritzeak ez bezala. Azkenik, CO_2 altuko baldintzatan karbono-isurbideak garatzearen garrantzia eta hostoetako karbono iturri-isurbide erlazioaren doikuntza aztertu dira pedunkuluan karbono eta nitrogeno konposatuak metatzeko gaitasun ezberdina aurkezten duten hainbat garagar landareetan. Lortutako emaitzek karbono isurbide gaitasun handiagoko barietateak identifikatzearen beharra berresten dute, horren bitartez hostoetako karbonoaren doikuntza hobea lortu eta CO_2 altuko baldintzatan fotosintesi aktibitatea areagotzea baimenduz.

1

Introduction

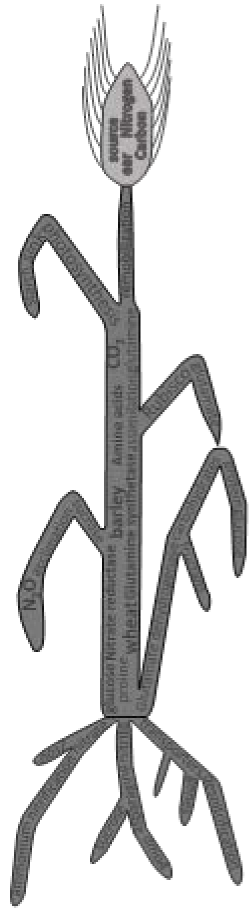

1.1. Climate change

Climate change and its implications for Earth's environmental processes have been of particular relevance in the last few decades. According to the Intergovernmental Panel on Climate Change (IPCC, 2014), climate change refers to alterations in the state of the climate that can be identified (e.g., by using statistical tests) by changes in the mean and/or variability of its properties and that persist for an extended period, typically decades or longer.

The main consequence (although not the only one) of anthropogenic climate change is stimulation of the "Greenhouse Effect". It is important to highlight the word "stimulation" because there is also a natural greenhouse effect that is due to greenhouse gases of natural form and concentration present in the atmosphere. In the absence of any atmosphere, the surface temperature of the earth would be approximately -18 °C, better known as the effective temperature of terrestrial radiation. However, the average temperature of the earth's surface is 15 °C. The terrestrial temperature is the result of the balance maintained by the earth and the atmosphere in terms of the absorption of solar radiation that reaches the earth and the emissions of longwave (infrared) radiation emitted into space. Part of the shortwave radiation from the sun is reflected by clouds and aerosols from the atmosphere, some of it is retained by the atmosphere, and the rest reaches the earth's surface where it is absorbed. The earth radiates shortwave radiation in the form of infrared radiation, which is retained by the greenhouse gases present in the atmosphere and causing the atmosphere's warming, a phenomenon known as the "Greenhouse Effect".

The amount of longwave radiation retained, and therefore responsible for the temperature increase, will depend on the atmospheric constituents (mainly greenhouse gases). The atmospheric gas composition determines the physical properties of absorbance, reflection and transmission of solar radiation to the earth's surface, and influences emission of the Earth's own radiation into space.

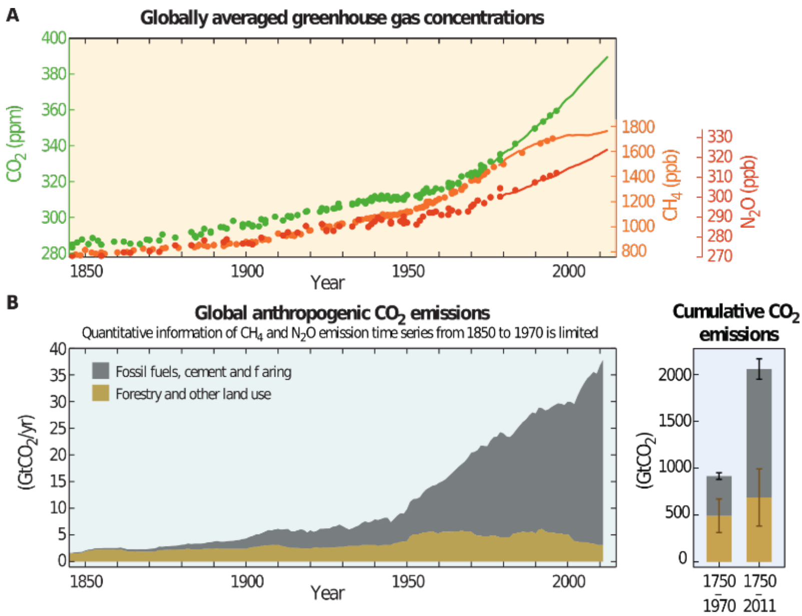

Figure 1. (A) Observed changes in atmospheric greenhouse gas concentrations of CO_2 (green), CH_4 (orange) and N_2O (red) since 1850. (B) Global anthropogenic CO_2 emissions from forestry and other land use (green) and from burning of fossil fuel, cement production and flaring. (IPCC, 2014).

The main greenhouse gases are water (H_2O), carbon dioxide (CO_2), methane (CH_4), nitrous oxide (N_2O), ozone (O_3), and halocarbons (chlorocarbons and fluorocarbons). Natural and anthropogenic processes alter the Earth's atmosphere, being responsible for climate change. Although the atmospheric gas concentration has fluctuated across different geological periods, since the start of the Industrial Revolution around 1750 the atmospheric concentrations of CO_2, CH_4 and N_2O have increased 40%, 150% and 20%, respectively (Figure 1A). Considering a time horizon of 100 years, N_2O

and CH_4 show a global warming potential 265 and 28 times higher than for CO_2 (IPCC, 2014). For CO_2 emissions, about 40% of these emissions have remained in the atmosphere and the rest has been stored on land and in the oceans or removed from the atmosphere. In addition, it has been estimated that about half of the anthropogenic CO_2 emissions have been emitted in the last 40 years (Figure 1B).

During the second half of the 20th century, a preoccupation about the impact of greenhouse gas accumulation in the atmosphere increased and following the growing scientific evidence many nations have accepted that climate change is a looming crisis. In response, the United Nations Environment Programme (UNEP) and the World Meteorological Organization (WMO) set up the Intergovernmental Panel on Climate Change in 1988 to bring together scientific data on the current state of knowledge of climate change and its potential environmental and socio-economic impacts. Based on IPCC information, the United Nations Framework Convention on Climate Change (UNFCCC) was created in 1992 to fight against the problem of climate change. A few years later 156 parties signed the Kyoto Protocol with the objective of addressing climate change and reducing carbon emissions. Currently, 197 countries are members of the IPCC and 192 countries participate in the Kyoto Protocol. More recently, during the 21st Conference of the Parties celebrated in December 2015 in Paris, the UNFCCC reached an historic landmark agreement, taking ambitious efforts to combat climate change and adapt to its effects. For the first time in the history, through the Paris Agreement signed in 2017, all nations have set the main objective of keeping the global temperature rise during this century to below 2°C with respect to pre-industrial levels.

1.2. Impact of human activity on atmospheric gas composition (CO_2 and N_2O)

1.2.1. Carbon dioxide

Carbon dioxide is considered the major greenhouse gas produced by anthropogenic causes. The increase in the concentration of CO_2 has been due, mainly, to the burning of fossil fuels and the massive felling of trees (Ussiri and Lal, 2013). Deforestation and the burning of large areas of the planet, represent a loss in global CO_2 fixation capacity. Cereal crops, which are planted in these areas, retain the fixed carbon for only a short time whereas the trees accumulate and store it for substantial periods of time. Besides of the loss of forest mass causes the loss of an important carbon sink, it disappearance alters chemical, physical, and biological conditions related to these forest ecosystems, which consequently modulate the general greenhouse gas emissions (Barrena *et al.*, 2013; Stange *et al.*, 2013). Despite numerous climate change mitigation polices, anthropogenic greenhouse gas emissions have continued increasing. The relative contribution of anthropogenic practices differs from sector to sector, with energy production and agriculture, forestry and other land use (AFOLU) sectors being the most important drivers of increases in CO_2 emissions (Figure 2).

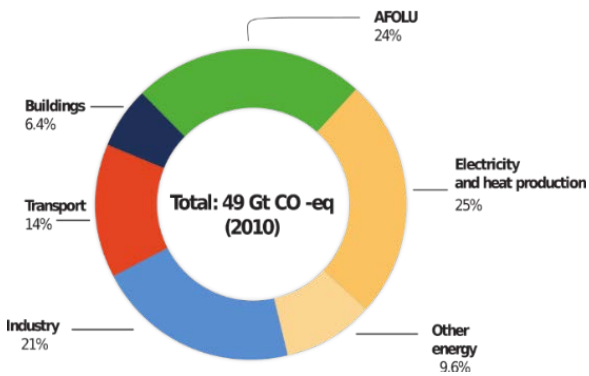

Figure 2. Total anthropogenic greenhouse gas (GHG) emissions from economic sectors in 2010. Adapted from (IPCC, 2014).

According to the IPCC (2014), agricultural practices are responsible for about 24% of CO_2 gas emissions. Since the "Green Revolution" there have been increases in grain yields through the introduction of external inputs such as irrigation, herbicides, pesticides or fertilisers but also reductions in forestry areas for increases in agricultural area (FAO, 2015). For these yield increases to occur, modified land management strategies have been necessary and therefore soil biological and chemical processes such as nitrification, denitrification or leaching have been altered.

1.2.2. Nitrogenous gas emissions

Nitrogen cycle in soils

The use of fertilisers in agriculture represents a major source of greenhouse gas emission. The intensive use of N fertilisers by farmers leads to increase crop profits, but also enhances N losses in the form of NO_3^- leaching, ammonia volatilisation (NH_3) or emission of nitric oxide (NO), N_2O or atmospheric nitrogen (N_2) gas.

Soil major N forms are ammonium (NH_4^+) and nitrate (NO_3^-). Although the main source of N input to agricultural soils is synthetic fertilizer, mineral nitrogen input comes from different sources. The plant-microbe symbiosis in legumes permit incorporate atmospheric N into ammonium by the N fixation though nitrogenase activity. Decomposition of microbial and plant biomass leads to the breakdown of complex organic matter into inorganic ammonium (mineralization) by soil microorganisms. Autotrophic nitrification is an aerobic process that consists of a two-step process where NH_4^+ is firstly oxidised under aerobic conditions to hydroxylamine (NH_2OH) by the ammonia monoxygenase enzyme (AMO) of ammonia-oxidising bacteria (AOB) and archaea (AOA) (Arp and Stein, 2003). Hydroxylamine oxidoreductase (HAO) and nitrite oxidoreductase oxide NH_2OH into nitrite (NO_2^-) and nitrate (Figure 3), respectively. Nitrification and denitrification are produced at the same time in soils; however, it is in water-saturated soils where O_2 availability is limited that optimal conditions are found for denitrifying microbes (Saggar *et al.*, 2013). Denitrification consists of the sequential reduction of NO_3^-, NO_2^- nitric oxide (NO) and N_2O ending in the formation of molecular nitrogen by the enzymatic activities of nitrate reductase (Nar, Nap), nitrite reductase (Nir), nitric oxide reductase (Nor) and nitrous oxide reductase (Nos) (Zumft, 1997; Philippot and Hallin, 2005).

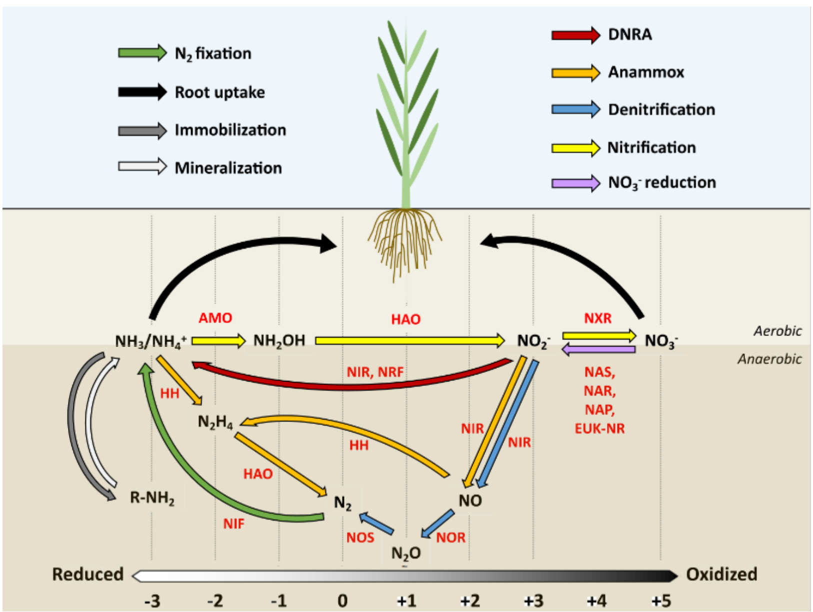

Figure 3. The soil Nitrogen Cycle. Adapted from Coskun *et al.*, (2017).

Although bacterial nitrification and denitrification are the main sources of NO and N_2O emission from soils, there are other microbial processes with ecological importance in N soil cycling (Hallin *et al.*, 2018). Nitrate can be reduced to NH_4^+ by dissimilatory nitrate reduction to ammonium (DNRA) by a specific group of bacteria and archaea, which reduce nitrate under strictly anaerobic conditions and compete directly with denitrification. Another process that also occurs under anaerobic conditions is the anammox process, where the oxidation of NH_4^+ is coupled to nitrite reduction to release N_2, with the consequent return of N_2 back to the atmosphere (Figure 3). Bacterial denitrification has been extensively studied (Philippot and Hallin, 2005; Philippot *et al.*, 2011; Jones *et al.*, 2013); however, fungal denitrification has gained more attention due to the lack of nitrous oxide reductase gene that coding for the enzyme responsible for reducing N_2O to N_2 (Mothapo *et al.*, 2015). Thus, although knowledge about the composition and diversity of the denitrifying fungal community is still limited, the importance of the N_2O-producing activity of fungi is being evaluated under specific scenarios (Mothapo *et al.*, 2013; Chen *et al.*, 2014*a*).

Use of N fertilisers in past, current and future agricultural practices

Agricultural practices have changed since the domestication of plants and animals 10000 years ago. Since the discovery of N as an essential nutrient for plants and the capacity of legumes for fixing atmospheric N by Jean-Baptiste Boussingault in 1836, many efforts have been driven to amplify our knowledge of the N cycle (Galloway *et al.*, 2013). Farmers from the nineteenth century usually employed crop rotation with legumes, organic fertilisation with manures or mineral nitrate deposition to obtain the N necessary for crop production. However, it was not until one hundred years later that the Haber-Bosch process permitted industrial quantities of ammonia production and enabled increasing N inputs in agriculture (Galloway *et al.*, 2013). Nowadays it is estimated that the production of synthetic fertiliser by this process feeds about 50 per cent of the world´s population. The consumption of N-fertiliser in 2014 reached 113147 thousand tonnes and it is estimated that in 2018 its consumption will be near to 120000 thousand tonnes (FAO, 2015; Timilsena *et al.*, 2015).

Table 1. World demand for fertiliser nutrient between 2014 and 2018 (FAO, 2015).

Year	2014	2015	2016	2017	2018
Nitrogen (N)	113147	115100	116514	117953	119418
Phosphate (P_2O_5)	42706	43803	44740	45718	46648
Potash (K_2O)	31042	31829	32628	33519	34456
Total (N + P_2O5 + K_2O)	186895	190732	193882	197190	200522

The N input in agricultural soils permits increased crop production, but its use is not equally distributed across the world's surface. By far the largest N-fertiliser consumption coincides with developing countries, being the poor countries with a severe famine where the use of N-fertiliser is lower. Many farmers do not have access to mineral fertiliser, requiring the use of other techniques such as biological nitrogen fixation or application of manure and slurries to increase N in soils, but these are not always enough to cover needs.

In addition, the estimated increase in the global population predicts that at the end of the 21st century the world's population may surpass 11 billion (Unite Nations, 2015). Moreover, the projections estimate that more than 80% of the world's population will live in Asia and Africa. Therefore, not only will it be necessary to increase food production but this will also require optimisation and adaption of crops and land use management to improve agricultural efficiency and ensure food security (Chien *et al.*, 2009; Snyder *et al.*, 2009; Sanz-Cobena *et al.*, 2016). Furthermore, the existing agricultural system makes supplementation with external N inputs indispensable, mainly in the form of manures, crop residues and synthetic fertilisers to maintain crop yields.

Crop management and nitrogenous greenhouse gasses

In order to reduce the emission of nitrogenous greenhouse gases such as N_2O and NH_3, several strategies are focussed on controlling the N in soils to reduce the main environmental impacts of water eutrophication and N_2O

emission. The IPCC (2014) has estimated that the gaseous emission factor in agricultural soils is about 1% of the applied N. Thus, the optimisation of fertiliser formulations and agronomic practises are essential to reduce N losses (Sanz-Cobena *et al.*, 2016). Moreover, reducing these losses would allow increased nitrogen use efficiency (NUE) by plants that it is estimated that only 47% of the nitrogen applied is recovered by cereal crops (Lassaletta *et al.*, 2014). Among the mitigation strategies employed, those that stand out are modifying N application rates to match crop N needs, combining synthetic and organic fertilisers, and optimising water management with land and fertiliser uses (Sanz-Cobena *et al.*, 2016). One of the objectives to better manger N fertilisers and reduce N losses from agricultural soils is to maintain N in the soil for longer periods. There are many strategies focussed towards this objective, one of them consisting of replacing (complete or partially) synthetic fertilisers with organic fertilisers. This provides not only N and other essential nutrients, but is also a source of organic C. However, it is usually difficult to provide adequate N application rates with this strategy (Rees *et al.*, 2013; Sanz-Cobena *et al.*, 2016).

In order to maintain N for longer periods, the use of urea or ammonium-based fertilisers combined with urease inhibitors and/or nitrification inhibitors, respectively, is a strategy employed across the globe (Menéndez *et al.*, 2008, 2012; Pfab *et al.*, 2012; Huérfano *et al.*, 2015, 2016). These compounds deactivate the enzyme responsible for the first step of nitrification, reducing the oxidation of ammonium to nitrite, and subsequently the substrate for denitrification. The inactivation of these processes reduces N_2O emissions and retains N in the soil for longer periods. There are many biological or synthetic nitrification inhibitors used for this purpose (Subbarao *et al.*, 2006; Ruser and Schulz, 2015); however, among them the most widely used are synthetic, including dicyandiamide (DCD) and 3,4-Dimethylpyrazol-phosphate (DMPP)

(Figure 4A). The effectiveness of nitrification inhibitors depends on their physicochemical properties, which condition their solubility, volatility, mobility and persistence in soils (Zerulla *et al.*, 2001; Marsden *et al.*, 2016; Li *et al.*, 2017), and is subject to soil parameters such as pH, temperature or soil water content (Menéndez *et al.*, 2012; Liu *et al.*, 2015; Qiao *et al.*, 2015). These chemical compounds should be chemically stable, efficient at low concentrations, innocuous for plants and competitive in cost. Several works have evaluated the effectiveness of these nitrification inhibitors in maintaining crop yields while keeping NH_4^+ in soils and mitigating N_2O emissions (Menéndez *et al.*, 2008; Huérfano *et al.*, 2015, 2016; Guardia *et al.*, 2017). Although both DCD and DMPP have shown similar efficiency, their use shows global variation (Di and Cameron, 2016; Yang *et al.*, 2016). DCD applications are the most widely used around the world due to it being cheap, having low volatility and being relatively soluble in water. DMPP is mainly applied in China and Europe, and despite its higher economic cost DMPP has the advantage of lower application rates than DCD and minor eco-toxicological side effects for ecosystems (Marsden *et al.*, 2015). More recently, 2,3-dimethylpyrazol-succini acid isomeric mixture (DMPSA) (Figure 4B) has been developed to confer more stability and reduce pyrazole ring volatility. Therefore, DMPSA can be combined with other fertilizers like calcium ammonium nitrate or diammonium phosphate, which were previously not compatible.

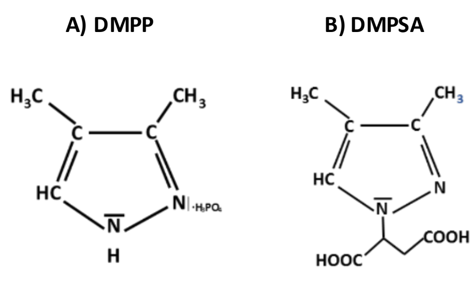

Figure 4. Chemical structures of DMPP (A) and DMPSA (B).

1.3. Plant performance under elevate CO_2 conditions

The effects of elevated CO_2 on crops are well studied due to the strong concern for future food security (Long *et al.*, 2004; Aranjuelo *et al.*, 2011). In plants with C_3 photosynthetic metabolism such as wheat, ambient CO_2 concentration is limiting; therefore, photosynthesis and growth in wheat is expected to be enhanced by elevated CO_2 resulting in higher yields (Drake and Gonzàlez-Meler, 1997; Kimball *et al.*, 2002; Ainsworth and Rogers, 2007; Schmid *et al.*, 2016). Although the current CO_2 in the atmosphere is generally limiting for C_3 photosynthesis, the available information suggests that the predicted CO_2 increase will enhance photosynthetic rates in plants (Long *et al*., 2004). Despite an expected increase in cereal production from the projected increase in CO_2, the interaction of CO_2 with other limiting factors like nitrogen availability, temperature and/or low water availability might decrease or eliminate the positive effect of elevated CO_2 on plant production (Kimball *et al.*, 2002; Aranjuelo *et al.*, 2011, 2013*b*).

1.3.1. Carbon fixation

It has been noted that while exposure to elevated CO_2 might induce photosynthetic activity at first, the initial stimulation of photosynthetic capacity in C_3 plants is often reduced when exposure to elevated CO_2 is prolonged (Ainsworth and Rogers, 2007; Xu *et al.*, 2016). According to the predicted increase in atmospheric CO_2 (IPCC, 2014), the carboxylation reaction of Rubisco should be enhanced by the greater availability of substrate thus augmenting photosynthetic capacity and then leading to increased crop yield (Drake and Gonzàlez-Meler, 1997; Sharkey *et al.*, 2007; White *et al.*, 2015). As mentioned above, a number of studies have shown that prolonged exposures to elevated CO_2 causes stomata or Rubisco limitations, which impedes increase photosynthetic capacity and provokes the well-known photosynthetic acclimation. Plants adjust their carbon fixation and photoassimilates utilisation capacity, and the coordination between these two parameters has been described as being key to regulation of photosynthesis under elevated CO_2. The most popular hypothesis to explain acclimation to elevated CO_2 is known as the "source-sink hypothesis", and it states that photosynthetic rates are limited by an insufficient plant sink strength (Arp, 1991). The accumulation of non-structural carbohydrates is sensed by hexokinase, and this represses expression of genes coding the photosynthetic apparatus and finally, induces acclimation (Long *et al*., 2004; Moore *et al*., 1999). At the whole plant level, photosynthetic rates are tightly coordinated with the ability to maintain and develop new non-photosynthetic plant tissues.

A wide range of physiological and developmental mechanisms control plant growth. Internally, plant C source-sink interactions are modulated at the molecular, physiological, and developmental levels. The plant developmental transition from vegetative to reproductive growth has important implications for the sink-source balance. The relationship between sink and source organs is conditioned by the rate at which external nutrients are taken up and transformed internally into organic compounds and the remobilisation of these resources to others organs.

Source organs are generally tissues that provide C and N resources to other developing organs where nutrients are required (Coskun *et al.*, 2016; Tegeder and Masclaux-Daubresse, 2017). Regarding carbon sink-source, it is well known that the C fixed by photosynthesis is usually stored/translocated from leaf (source) to other sink organs such as roots and stems. As mentioned before, sink strength is considered a key parameter conditioning crop responsiveness to elevated CO_2 (Ainsworth *et al.*, 2004; Aranjuelo *et al.*, 2009). Under elevated CO_2 conditions, the greater availability of C can increases leaf photoassimilates such as sucrose. When leaf carbohydrate content exceeds leaf C demand, usually linked to the impossibility of remobilising these photoassimilates to sink organs, plants suffer sink-source imbalance. Therefore, plants with a large sink size (i.e. large ears in the case of cereals) should be capable of overcoming leaf carbohydrate build-up and consequently benefit from CO_2 enrichment. On the other hand, plants with a small sink size would be more susceptible to leaf C sink-source imbalance and consequently photosynthetic acclimation(Aranjuelo *et al.*, 2009; White *et al.*, 2015).

Since the Green Revolution, agricultural practices have increased the yield potential of many crops. Furthermore, wheat and rice yields the actual rate of crop profits through traditional plant breeding programs is not enough for provide food for the current estimates of the growth in the human population. This world population increase together with the projections for climate change indicate that a special effort will be required to search for more productive and well-adapted cultivars for the future. In addition, current plant breeding programs use elite crop cultivars with selected agronomic characteristics that may lack some alleles that were not previously considered interesting but in the future may be important adaptations to climate change (Maydup et al., 2012; Serrago et al., 2013; Dawson et al., 2015). For that, it is necessary to integrate others ecotypes such as wild cultivars that might provide with these alleles lacked (Ellis *et al.*, 2000).

1.3.2. Role of nitrogen metabolism

Nitrogen is an essential component for plant growth and crop productivity, being a component of nucleic acids, amino acids, chlorophylls, proteins, and secondary metabolites among others (Hawkesford *et al.*, 2012). Both nitrate and ammonium are the main N-mineral forms taken up by plants

(Masclaux-Daubresse *et al.*, 2010) but also, plants can take up N-organic forms or even fix N_2 via symbiosis with rhizobium.

Nitrogen availability and management determines photosynthetic performance under raised CO_2 (Langley & Megonigal, 2010; Stitt & Krapp, 1999). It has been reported that photosynthesis acclimation is tightly dependent on N dosage: the effect is evident when plants are N-limited, but not observed in well-fertilised conditions (Reich & Hobbie, 2012; Geiger et al., 1999). Under elevated CO_2 it has been documented that N content is reduced (in varying degrees) in all plant tissues (Cotrufo et al. 1998) under all culture conditions (Poorter et al. 1997) and has been corroborated as a conserved response across many plant species (Loladze, 2014). The reduction in nitrogen content in plants exposed to elevated CO_2 has been the subject of an intense debate. Different studies published during the last decade have highlighted that the form of N applied plays a crucial role in the responsiveness of plants to elevated CO_2 (Vega-Mas *et al.*, 2015; Coskun *et al.*, 2016; Rubio-Asensio and Bloom, 2017). When both N inorganic sources (nitrate and ammonium) are available for plant uptake, ammonium, which is the reduced form, would be preferred for assimilation due avoidance of the cost of reduction (Bloom *et al.*, 1992; Andrews *et al.*, 2013). Nevertheless, in many plants species when ammonium is supplied as the sole N source, "ammonium toxicity" may appear (Britto and Kronzucker, 2002; Ariz *et al.*, 2011).

Most plant species cannot grow or develop adequately when NH_4^+ is present at high concentrations in the soil and especially when it is the sole N source (Britto and Kronzucker, 2002; Bittsánszky *et al.*, 2015). So, a substantial effort has been made to elucidate the mechanisms determining plant ammonium tolerance/sensitivity. However, the physiological and molecular mechanisms involved are still not completely clear (Esteban *et al.*, 2016; Liu and

Wirén, 2017). The adverse effects of NH_4^+ range from visible symptoms such as leaf chlorosis, early flowering and a general loss of plant biomass, to physiological disorders, which include disruption of hormonal homeostasis, decreases in photosynthesis, oxidative stress, alterations in intracellular pH, osmotic imbalance and mineral nutrient deficiency among others (Britto and Kronzucker, 2002; Esteban *et al.*, 2016). Roots most likely play a "barrier" role in preventing ammonium translocation to photosynthetic organs. In fact, the main strategies plants have evolved to avoid ammonium toxicity are to increase NH_4^+ efflux from the cell, to enhance NH_4^+ assimilation (mainly in roots), and to store NH_4^+ inside the vacuole. The energetic cost of these processes is considered a cause of the growth impairment often observed under ammonium nutrition. At the same time, increases in the activity of TCA anaplerotic enzymes have been related to a better adaptation to using NH_4^+ as an N source (Setién *et al.*, 2013, 2014; Vega-Mas *et al.*, 2015; Sarasketa *et al.*, 2016). Moreover, the external provision of succinate and 2-oxoglutarate, key carbon sources for NH_4^+ incorporation into amino acids, enhances its assimilation and alleviates toxicity symptoms (Magalhaes *et al.*, 1992). In the context of increasing concentrations of atmospheric CO_2, an understanding of the complexity of plant responses to ammonium nutrition and mixed ammonium nutrition will help translate our knowledge of plant physiological responses to elevated CO_2 (Vega-Mas *et al.*, 2015; Jauregui *et al.*, 2017; Nimesha *et al.*, 2017) into approaches that will benefit crop production.

2

Objectives

The Intergovernmental Panel on Climate Change (IPCC) highlights different strategies to evaluate and mitigate the effects of Climate Change. More specifically, the IPCC has developed two Working Groups (II and III) focused on studying the impacts, adaptation and vulnerability to climate change and evaluating different strategies of mitigation to Climate Change. Within this context, the IPCC has proposed, among other actions, the use of nitrification inhibitors jointly with ammonium-based fertiliser to reduce greenhouse gas emission (such as N_2O) from agricultural soil. On the other hand, IPCC urges to deepen the knowledge of the atmospheric CO_2 increase effect in the crop development. Therefore, within this context, a deeper understanding on the use ammonium-based fertilizer under elevated CO_2 concentration conditions could be a goal of great relevance for crop performance during the next decades.

After all this, the general purpose of the current PhD. project was to evaluate the impact of nitrification inhibitors (contextualized in a strategy to mitigate the N_2O gas emission derived from N-fertilisation), the N fertilization form and C sink/source balance in crops exposed to elevate CO_2 conditions.

The specific objectives of this study have been:

- To study the effectiveness of nitrification inhibitors (DMPSA and DMPP) in mitigating N_2O emissions together with the behaviour of nitrifying and denitrifying microbial populations under two contrasting soil water-content conditions (40% and 80% WFPS). This objective is addressed in chapter 3.
- To evaluate the physiological and molecular response of wheat plants to elevated CO_2 in relation to nitrogen source in order to clarify the connection between the photosynthetic apparatus and the assimilation of nitrogen in leaves. This objective is addressed in chapter 4.

- To determine the relevance of the C sink-source balance in response to elevated CO_2 in two barley cultivars with different capacity to store C/N compounds in the internodes. This objective is addressed in chapter 5.
- To evaluate the importance of elevated CO_2 on the remobilisation of leaf metabolite compounds of wheat at vegetative stages and grain filling periods. This objective is addressed in chapter 6.

3

Dimethyl pyrazol-based nitrification inhibitors effect on nitrifying and denitrifying bacteria to mitigate N_2O emission

SCIENTIFIC REPORTS | 7: 13810 |

3.1. Introduction

Nitrous oxide (N_2O) represents an important environmental threat due to its high global warming potential (298 times that of CO_2 for a 100-year time horizon), together with its involvement in the destruction of the ozone layer. Moreover, its total global emissions to the atmosphere have increased 6% since 2005 (IPCC, 2014). Soil, both natural and managed, is considered the primary source of N_2O in global greenhouse gas budgets (Syakila *et al.*, 2010). Furthermore, it has been estimated that the agricultural contribution to anthropogenic N_2O emissions represents around 70-80% (Ussiri *et al.*, 2009; IPCC, 2014). Autotrophic nitrification and heterotrophic denitrification are responsible for most of these emissions (Braker and Conrad, 2011). Under aerobic conditions, nitrification is driven by ammonia-oxidising bacteria (AOB) and archaea (AOA), which oxidise NH_3 into hydroxylamine (NH_2OH) through the ammonia monoxygenase enzyme (AMO) encoded by the *amoA* gene (Arp and Stein, 2003). During the nitrification process, N_2O can be produced as a secondary product. N_2O can be also emitted by the nitrifiers denitrification, which reduces nitrite (NO_2^-) directly to nitric oxide (NO), N_2O or N_2 (Wrage *et al.*, 2001). However, although both nitrification and denitrification processes can occur in wet soils where there is limited O_2 availability, the main source of N_2O is usually the denitrification of NO_3^- by denitrifying microbes (Li *et al.*, 2016). The denitrification pathway consists of four sequential reactions initiated by NO_3^- reduction and carried out by nitrate reductase (Nar, Nap), followed by nitrite reductase (Nir), nitric oxide reductase (Nor), and nitrous oxide reductase (Nos), leading to the generation of N_2 as an end-product (Zumft, 1997; Philippot and Hallin, 2005).

In agriculture, the magnitude of N_2O emissions depends greatly on both the application of nitrogen fertilisers and the effect of edaphoclimatic conditions on microbial activity, including O_2 levels as well as temperature, pH, and the soil carbon:nitrogen ratio (Ussiri and Lal, 2013; Benckiser *et al.*, 2015). Nitrification inhibitors (NIs) have been extensively applied to keep N available, in the form of ammonium, in the soil for longer periods while lessening NO_3^- leaching and mitigating N_2O gas emission. In this sense, the use of NIs in conjunction with ammonium-based fertilisers has been proposed as an excellent strategy for reducing N_2O emissions (Menéndez *et al.*, 2006; Pfab *et al.*, 2012; Huérfano *et al.*, 2015). A great number of molecules with the capacity to inhibit nitrification have been identified (Subbarao *et al.*, 2013; Ruser and Schulz, 2015). At present, the commercialised dicyandiamide (DCD) and 3,4-dimethylpyrazole phosphate (DMPP) are the most widely used NIs. The mode of action of DCD and DMPP has not been completely elucidated, but both of them are supposed Cu-selective metal chelators that may remove this AMO co-factor, therefore avoiding the oxidation of NH_4^+ to NO_2^- (Ruser and Schulz, 2015). Several studies have demonstrated similar efficacy for DMPP and DCD in mitigating N_2O emissions (Yang *et al.*, 2016). However, DMPP reduces the ecotoxicological and leaching problems related to DCD, as it is applied at approximately one-tenth lower concentration than DCD and is less mobile in the soil (Pasda *et al.*, 2001; Zerulla *et al.*, 2001; Macadam *et al.*, 2003; Liu *et al.*, 2013). The persistence of NIs and their capacity to reduce the microbial oxidation of NH_4^+ to NO_2^-, thus mitigating N_2O emissions, have been shown to be affected by soil conditions including soil temperature, moisture (Menéndez *et al.*, 2012; Di *et al.*, 2014; Barrena *et al.*, 2017), and pH (Shi *et al.*, 2016*a,b*). A very recent development is the new DMP-based inhibitor 2-(N-3,4-dimethyl-1H-pyrazol-1-yl) succinic acid isomeric mixture (DMPSA). The use of pyrazole compounds as nitrification inhibitors have the disadvantage of the highly volatility of the pyrazole rings. Instead of the phosphate from DMPP, the succinic residue holds to the pyrazole ring from the DMPSA form a salt that confer stability and reduces its volatility. Therefore, DMPSA is stable with other fertilizers such as calcium ammonium nitrate or diammonium phosphate that would not be able to use with nitrification inhibitors such as DMPP. Both DMPP and DMPSA are structurally very similar but it is not still clear if these inhibitors have the same mode of action and efficiency when targeting soil nitrifying organisms. In fact, there are almost no studies on DMPSA (Huérfano *et al.*, 2016; Guardia *et al.*, 2017). To our knowledge, only Huérfano *et al.*(2016) have compared DMPSA and DMPP in a wheat-field. These authors found that both inhibitors exhibited a similar N_2O-emissions-reducing capacity while maintaining crop yield and quality.

It is accepted that the nitrification inhibition action of DCD and DMPP reduces nitrifying bacterial populations. This is generally observed as a reduction in *amoA* gene copy number in AOB, although the effect on AOA *amoA* is less evident (Ruser and Schulz, 2015). It is also probable that NIs mitigate N_2O emissions through indirectly limiting denitrification processes by decreasing the availability of NO_3^- (Menéndez *et al.*, 2012; Florio *et al.*, 2014; Kou *et al.*, 2015). Finally, in the framework of reducing N_2O emissions from agriculture, the last denitrification step by Nos (encoded by *nosZ*) becomes crucially important since this is the only enzyme capable of reducing N_2O to N_2. Most studies describing the *nosZ* gene copy number after the application of NIs are related to organic fertilisation, and there is no consensus on how the *nosZ* gene abundance is affected (Di *et al.*, 2014; Florio *et al.*, 2014; Domeignoz-Horta *et al.*, 2015). Additionally, until now, no-one has looked at how DMPSA affects populations of soil nitrifying and denitrifying microbes. Therefore, a greater understanding of how these molecules reduce the negative effect associated with nitrogen fertilisation is crucial to optimising land managements.

Moreover, the determination of where NIs are actuating is interesting to comprehend their effect over ground microbial populations.

In this context, the main objectives of this work were to study how the effectiveness of DMPSA compared to DMPP in mitigating N_2O emissions, and quantify the behaviour of nitrifying and denitrifying microbial populations under two contrasting soil water-content conditions (40% and 80% water-filled pore space; WFPS). Moreover, since NIs are highly efficient at reducing N_2O emissions in soils under low oxygen availability; in this work, we also explored the hypothesis that denitrification could be directly affected by DMP-based inhibitors.

3.2. Materials and methods

Soil sampling and experiment setup

Soil was collected in June 2014, from a 0-30 cm layer of clay loam soil in a wheat field (Table 1), in the Basque Country (Spain). In the laboratory, any roots and stones were removed and the soil was passed through a 2 mm sieve. After this, it was air-dried, homogenised and kept at 4°C until the start of the experiment.

Table 1. Physical and chemical properties of the soil (0–30cm depth). OM means organic matter.

Soil texture	Sand (%)	36
	Silt (%)	28
	Clay (%)	36
Soil chemical properties	pH	8.4
	OM (%)	2,9
	N (%)	0.23
	C:N	7.31
	Carbonate (%)	2.01
	P (ppm)	106
	Ca (ppm)	1295
	Mg (ppm)	171.4
	K (ppm)	516

In order to reactivate the soil microorganisms, fourteen days prior to the onset of treatments, the soil was rehydrated with deionised water up to 10% below the final water filled pore space (WFPS) and activated by adding 500 mg of carbon in the form of glucose, and 3 mg of NH_4NO_3 per kg of dry soil (equivalent to 10 kg N ha^{-1}) (Singh *et al.*, 2010; Menéndez *et al.*, 2012). The experiment was set up as a soil microcosm incubation study. 272 1 litre glass flasks were prepared with 300 g of dried soil per flask; 3 technical replicates per treatment and time point were sampled destructively for mineral N and pH determinations (a total of 240 bottles), and the remaining 32 flasks were used for N_2O emissions and soil nitrifying and denitrifying bacterial population analyses (4 technical replicates per treatment). The trial was designed as a split plot arrangement in which eight treatments were established as a result of combining the different soil water content and fertilisers. The treatments were: unfertilised control (C); ammonium sulphate (AS); AS+DMPP (DMPP); and AS+DMPSA (DMPSA). Ammonium sulphate [$(NH_4)_2SO_4$] was applied at a rate of 42.8 mg N kg^{-1} dry soil (equivalent to 140 kg N ha^{-1}); DMPP and DMPSA (EuroChem Agro Iberia S.L.) were both added at 1% N. In order to achieve a homogeneous distribution of the fertilisers in the soil, the AS (with or without inhibitor) was dissolved in deionised water, and subsequently 5 ml were added to the corresponding treatments. For unfertilised treatments, 5 ml of deionised water were added. Each treatment was then subdivided into two sub-treatments with different moisture conditions expressed as water filled pore space (WFPS 40% and 80%). Water was added to every flask in order to reach the humidity defined for each soil water content according to the equation by Aulakh *et al*. (1991): [(gravimetric water content X soil bulk density)/total soil porosity], where soil porosity = [1 — (soil bulk density/particle density)], soil bulk density =1.14 g cm^{-3}, and particle density is assumed to be 2.65 g cm^{-3}. In order to maintain the humidity while allowing gas diffusion, the flasks were covered with Parafilm (Oshkosh, WI, USA) throughout the entire study. Twice per week each flask was weighed to check the soil water content, deionised water being added whenever necessary. The microcosms were incubated in the dark at 20°C throughout the 51 days of the experimental period.

N_2O emissions measurement

Daily N_2O emissions were determined every two days for the first 16 days, as well as on days 31 and 51. To do this, four independent flasks for each microcosm treatment were closed hermetically and 20 ml of gas from the atmosphere of the hermetic flasks were sampled after 30, 60 and 90 minutes, and stored at pressure in 12 ml vials for later N_2O analysis. Emission rates were calculated taking into account the increased concentration of N_2O during the 90 minutes of incubation. The gas samples were analysed an Agilent 7890A gas chromatograph (GC; Agilent Technologies, Santa Clara, CA, USA) equipped with an electron-capture detector (ECD). The gas samples were injected into a capillary column (IA KRCIAES 6017: 240 °C, 30 m x 320 µm) by means of a headspace auto-sampler (Teledyne Tekmar HT3, Mason, OH, USA) connected to the GC. On every measurement day, N_2O standards were analysed as internal controls. Cumulative N_2O production throughout the entire experiment was calculated by multiplying the length of time between two measurements by the average emissions rate for that period, and adding that amount to the previously accumulated N_2O.

Geochemical analyses

In order to monitor soil pH and mineral nitrogen (NH_4^+ and NO_3^-), three samples per treatment and time point were sampled, each from an independent flask. Soil pH is a key factor affecting biological processes as well as the diversity and structure of bacterial populations (Šimek and Cooper, 2002), and the addition of DMPP may affect this pH (Liu *et al.*, 2015). For this reason, we monitored the evolution of soil pH throughout the entire incubation period. To determine soil pH, 10 g of dry soil were suspended in deionised water (1:2, w:v) and shaken for an hour at 165 rpm (KS501D, IKA, Staufen, Germany) to properly homogenise the mixture. Soil suspensions were left to settle for 30 min, to decant the particles, and the pH was determined from the solution. No significant differences were observed between the fertilised treatments (Supplementary Figure 1).

To analyse soil mineral nitrogen, 100 g of dry soil were mixed with 1 M KCl (1:2, w:v) and shaken for an hour at 165 rpm to properly homogenise the mixture. This soil solution was filtered twice; first through Whatman no. 1 filter paper (GE Healthcare, Little Chalfont, Buckinghamshire, UK), and then through Sep-Pak Classic C18 Cartridges 125 Å pore size (Waters, Milford, MA, USA) to eliminate organic carbon. The filtered soil solution was used to determine the NO_3^- content, as described by Cawse (1967), and NH_4^+ content using the Berthelot method (Patton and Crouch, 1977).

Nucleic acid isolation

Ten grams of soil were collected from the same flasks as used for N_2O determination on each measurement day, immediately frozen in liquid nitrogen and stored at -80 °C until use. To quantify bacterial populations, DNA was extracted from 0.25 g of soil using the PowerSoil DNA Isolation Kit (MO BIO Laboratories, Carlsbad, USA) following the manufacturer's recommendations. DNA was quantified spectophotometrically (Nanodrop, Thermo Scientific, Walthan, MA, USA). For total RNA isolation, 1.5 g of frozen soil was extracted with a RNA PowerSoil Total RNA Isolation Kit following the manufacturer's protocol (MO BIO Laboratories, Carlsbad, USA). The quantity of RNA was determined spectrophotometrically using a NanoDrop (Thermo Scientific), and the RNA was quality checked with a Bioanalyzer 2100 (Agilent Technologies). For each sample, 100 ng of RNA were retrotranscribed into complementary DNA using the PrimeScript™ RT reagent Kit (Takara-Bio Inc., Otsu, Shiga, Japan). The absence of contamination with genomic DNA was tested in all RNA samples by PCR using *16S rRNA* gene primers.

Quantification of nitrifying and denitrifying gene a*bundance and expression analysis using qPCR*

Total bacterial and archaeal abundances (*16S rRNA*), and genes involved in nitrification (*amoA*) and denitrification (*narG*, *nirK, nirS*, *nosZI* and *nosZII),* were amplified by qPCR using SYBR® *Premix Ex Taq*™ II (Takara-Bio Inc.) using

StepOnePlus™ Real-Time PCR System and StepOnePlus™ Software v2.3 (Thermo Scientific). Detailed information about gene-specific qPCR primers, thermal programs and plasmid standard efficiencies are refereed in Supplementary Table 1. Standard curves were prepared from serial dilutions of 10^7 to 10^2 gene copies μl^{-1} linearised p-GEMT plasmids with insertions of target gene fragments (Promega Corporation, Madison, WI, USA), following the equations detailed in Correa-Galeote *et al.* (2013). The copy number of target genes per gram of dry soil was calculated from the equation: [(number of target gene copies per reaction X volume of DNA extracted) / (volume of DNA used per reaction X gram of dry soil extracted)] described in Behrens *et al*. (2008). To determine gene expression levels, the same primers and PCR programs were used (Supplementary Table 1). Target gene expression was quantified relative to *16S rRNA* gene expression calculated with the $2^{-\Delta\Delta Ct}$ method, using the unfertilised soil as calibrator.

Denitrification assay

In order to determine the effect of both NIs on the nitrous oxide reductase activity (Nos activity), 100 g of dried soil were loaded into 500 ml bottles. The treatments applied were: potassium nitrate (KNO_3), KNO_3 + DMPP, and KNO_3 + DMPSA. In order to favour the denitrification, KNO_3 was applied at a high rate of 300 mg N kg^{-1} dry soil, NIs were added at 1% of N applied, glucose was added at a rate of 180 mg Kg^{-1} dry soil and the humidity was adjusted to 80% WFPS. The bottles were maintained in the dark at 20°C and measurements were made 0, 24, and 48 hours after fertilisation. At each time point, 8 bottles per treatment were closed hermetically with rubber septa (Sigma-Aldrich, Inc, USA) and the inner atmospheric headspace was evacuated and fluxed with N_2 three consecutive times to create an anoxic environment and thus, impel denitrification. To inhibit Nos activity, in four bottles per treatment 10% of the atmosphere was replaced with acetylene (C_2H_2) (Yoshinari *et al.*, 1977). Then, 5 ml of gas from the headspace of each bottle, either with or without added C_2H_2, were sampled 30, 60 and 90 min after the C_2H_2 had been added. Finally, the samples were measured by GC, as detailed previously. The N_2O production throughout the entire experiment was represented as cumulative emission of N_2O.

Statistical analyses

The data was analysed using the IBM SPSS statistics 22 software (Armonk, NY, USA). Normality and homogeneity of variance were analysed using the Kolmogorov-Smirnov and Levene tests. Analysis of significant differences in daily N_2O emissions, mineral nitrogen, and gene expression levels was carried out by comparison of means (t-test). For bacterial gene copy number, N_2O cumulative emissions and denitrification assay, significant differences between treatments were analysed using one-way ANOVA with a Duncan post hoc test. Additional details and significance levels are described in the figure captions.

3.3. Results

DMPP and DMPSA reduced nitrous oxide emissions and ammonium oxidation under both WFPS conditions.

Fertilisation with ammonium sulphate (AS) generated a clear N_2O emissions peak during the first 12 days of incubation (Figure 1). The magnitude of the N_2O emitted was dependent on soil water content, since under 80% WFPS greater than ten times more N_2O was emitted than at 40% WFPS (Figure 1A, C). When NIs were applied together with AS, almost no N_2O was emitted under either soil water content (Figure 1). However, under 80% WFPS conditions, although both NIs reduced N_2O emissions, in DMPSA-treated soils the cumulative N_2O emission was significantly higher than both the control and DMPP treatment; therefore, DMPP was more efficient at 80% WFPS (Figures 1C, D). The unfertilised control treatments maintained low and constant values of both NH_4^+ and NO_3^- regardless of soil WFPS. The higher nitrification rates expected under the more aerobic conditions (40% WFPS) provoked rapid oxidation of NH_4^+, which in AS-treated soils dropped to the level of the unfertilised-soil after six days of incubation (Figure 2A). In contrast, the application of NIs led to a higher NH_4^+ content being maintained until day 16 (Figure 2A). In agreement with the dynamics of NH_4^+ content, the level of NO_3^- at 40% WFPS in AS-treated soils underwent a faster and more pronounced increase than in those with DMPP and DMPSA (Figure 2B). At 80% WFPS, due to the limited oxygen availability that impairs nitrification, the NH_4^+ content stayed at relatively high levels until day 14 in all fertilised treatments; however, in the presence of NIs the higher NH_4^+ content was evident from day 10, and this was maintained until the end of the incubation period (Figure 2C). Nitrate contents remained low throughout the entire experiment in all soils under 80% WFPS conditions (Figure 2D).

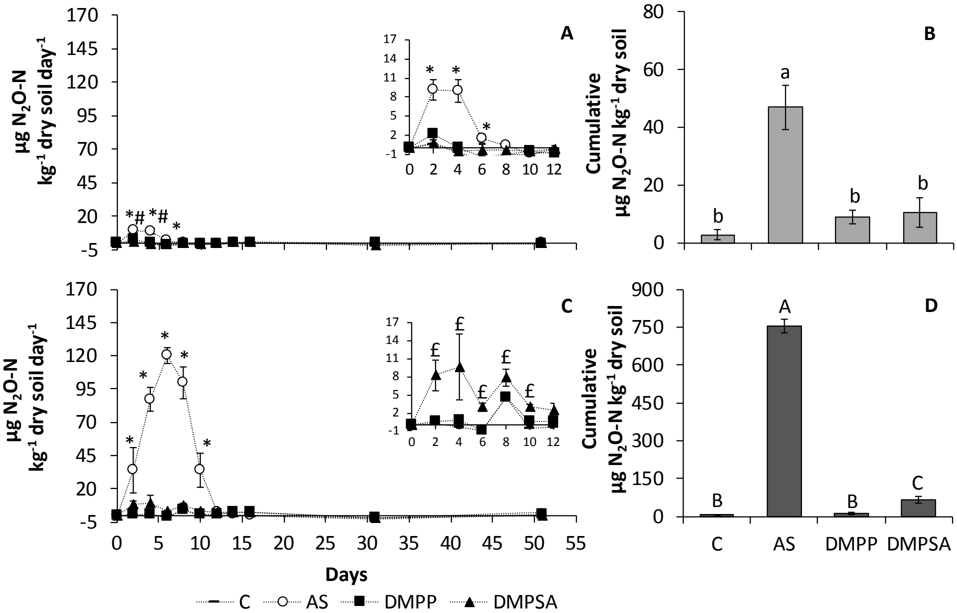

Figure 1. Daily (A, C) and cumulative (B, D) N2O emissions at 40% WFPS (A, B) and 80% WFPS (C, D) soil microcosms during the experiment. The inset graphs in sub-figures A and C show an amplified view of the daily N2O emissions for the first 12 days. For daily emissions, significant differences ($p<0.05$) between DMPP and DMPSA with respect to AS are represented by * and #, respectively, and significant differences ($p<0.05$) between DMPP with respect to DMPSA are represented by £. For cumulative emissions, significant differences ($p<0.05$) are represented by different letters. Values represent the mean ±SE (n=4). C = unfertilised control; AS = ammonium sulphate; DMPP = ammonium sulphate + DMPP; and DMPSA = ammonium sulphate + DMPSA

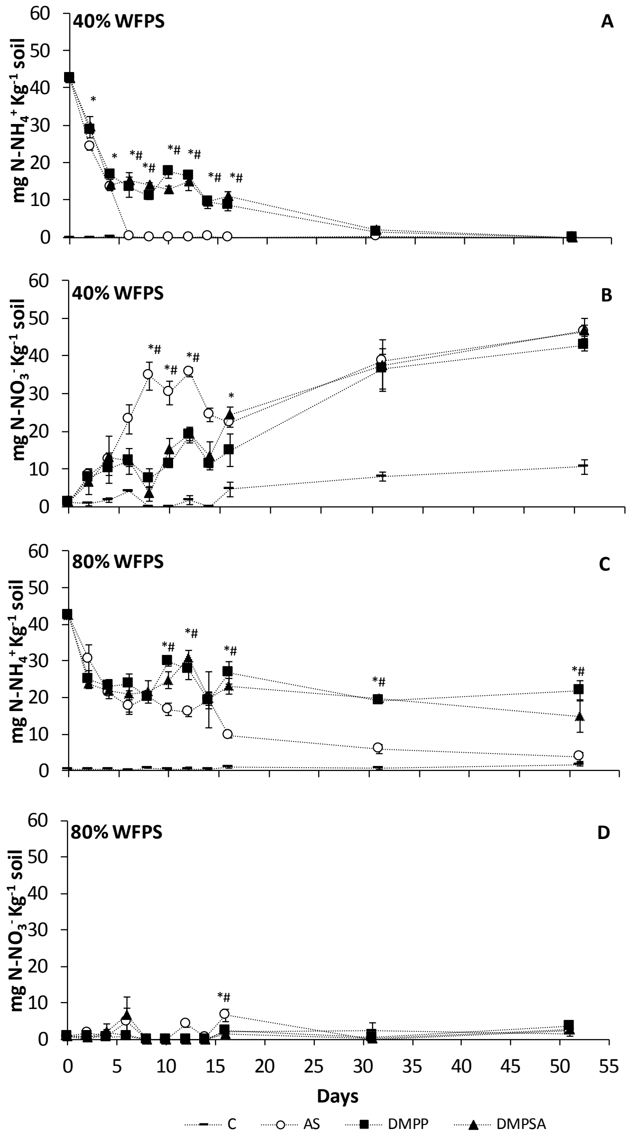

Figure 2. Evolution of soil ammonium (A, C) and nitrate content (B, D) at 40% WFPS (A, B) and 80% WFPS (C, D). Significant differences ($p<0.05$) between DMPP and DMPSA with respect to AS are represented by * and #, respectively. Values represent mean ± SE (n=3). Ammonium content for day 0 represents the total amount of NH_4^+ added to the samples.

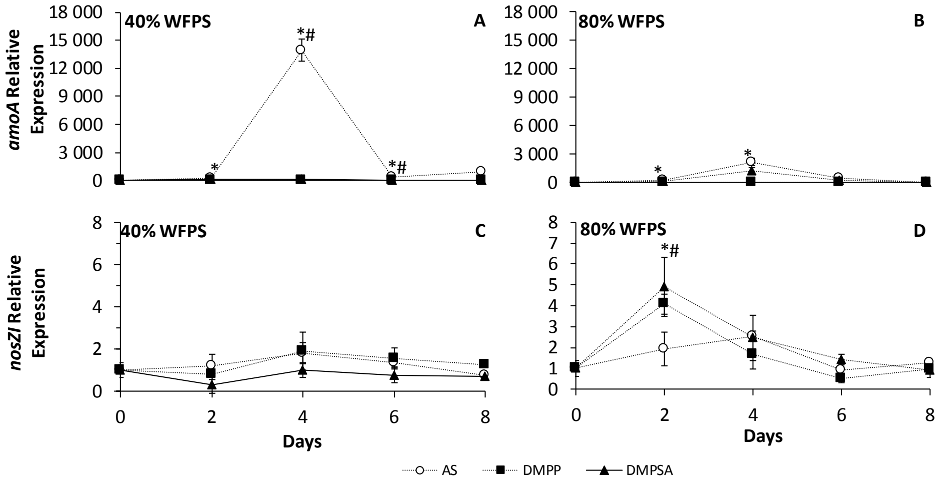

Figure 3. Relative expression of bacteria *amoA* (A, B) and *nosZI* (C, D) at 40% WFPS (A, C) and 80% WFPS (B, D) for the first 8 days. Significant differences ($p<0.05$) between DMPP and DMPSA with respect to AS are represented by * and #, respectively. Values represent mean ± SE (n=3).

Expression and abundance of nitrification and denitrification genes.

To check how the different fertilisation regimes were affecting soil bacteria, we measured the expression of nitrifying and denitrifying genes in the first days of incubation. Under 40% WFPS conditions, bacterial *amoA* expression experienced a striking induction in AS-treated soils concomitant with N_2O emissions, and this induction was completely blocked when DMPP or DMPSA were applied together with AS (Figure 3A). Under 80% WFPS conditions, the magnitude of bacterial *amoA* expression in AS-treated soils was almost six times lower than with 40% WFPS on day 4 (Figure 3A, B). DMPP also impeded *amoA* expression induction at 80% WFPS. In contrast, although the expression values recorded with DMPSA were not as high as when only AS was applied, the differences between these two treatments were not significant (Figure 3B).

The expression of the denitrifying genes *narG*, *nirK* and *nirS* did not vary substantially, regardless of the fertilisation type (Figure 4). Only *nirK* expression increased on day 4 after AS fertilisation at 40% WFPS (Supplementary Figure 2C). Interestingly, *nosZI* gene expression was induced 2 days from the onset of the incubation, when nitrification inhibitors were applied; this induction was exclusive to the 80% WFPS conditions, where denitrification is favoured due to low levels of O_2 availability (Figure 3D). The low intensity of the *nosZII* amplification signal meant we were unable to quantify its expression in any of the fertilisation regimes.

To confirm the results obtained through gene expression analysis, we also quantified the nitrifying and denitrifying abundances 16 and 51 days after fertilisation. The abundance of bacteria, quantified as *16S rRNA* gene copy number per gram of dry soil, did not vary among the fertilised treatments at any of the incubation times (Supplementary Figure 3). The abundance of archaea did not vary between treatments at day 16 (Supplementary Figure 3C); however, at day 51 under 40% WFPS conditions, archaea abundance in AS-treated soils was lower than in the unfertilised control (Supplementary Figure 3D). Nitrifying microbial abundances (AOB and AOA) were quantified by determining bacterial and archaeal *amoA* gene copy number per gram of dry soil. As shown in Figure 4A, 16 days after fertilisation and regardless of soil WFPS, AS treatment stimulated the AOB population, which was around five times more abundant than in the unfertilised control. This stimulation was completely abolished when NIs were applied together with the fertiliser. Interestingly, the effect of AS on AOB dropped 51 days after fertilisation and was only evident at 40% WFPS (Figure 4B). No differences were detected in AOA abundance among the fertilised treatments, regardless of WFPS and incubation time (Figure 4C, D). The ratio of AOA gene copies over AOB gene copies (AOA / AOB) gives us an idea of the response of the community in the microcosm. AOA gene copies was not affected by the addition of AS. Nevertheless, NI-treated soils reduced AOB gene copies number and thus, which resulted in a higher ratio AOA/AOB than in the soil treated only with AS (Supplementary Figure 4).

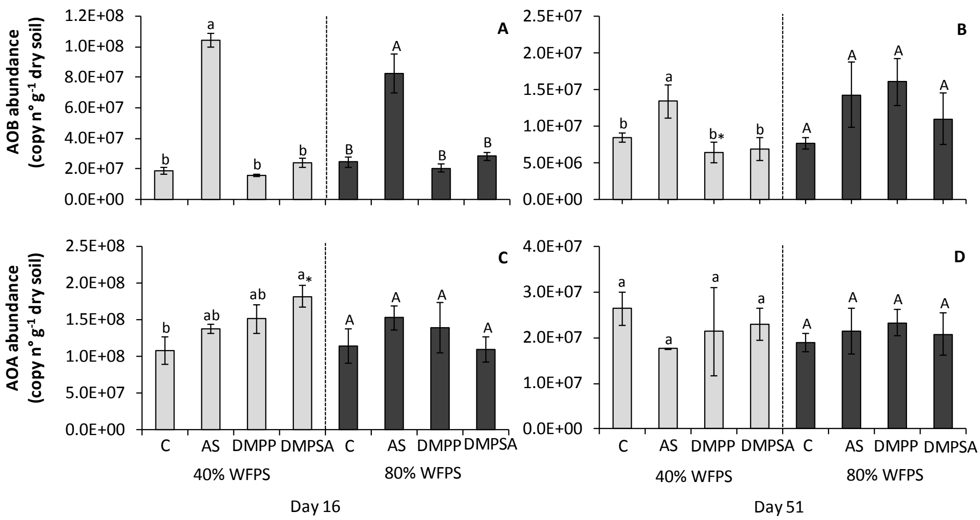

Figure 4. Abundance of AOB (A,B) and AOA (C,D) expressed respectively as bacteria and archaea *amoA* gene copy number per gram of dry soil at 40% WFPS (grey bars) and 80% WFPS (black bars), 16 (A, C) and 51 days (B, D) after treatment application. Significant differences ($p<0.05$) between treatments within each WFPS condition are indicated with different letters. Asterisk (*) indicates significant WFPS effect for each fertilised treatment ($p<0.05$). Values represent the mean ± SE (n=4). C = unfertilised control; AS = ammonium sulphate; DMPP = ammonium sulphate + DMPP; and DMPSA = ammonium sulphate + DMPSA.

Nitrate and nitrite-reducing bacteria were quantified by determining the copy number of *narG*, *nirK* and *nirS* genes per gram of dry soil. None of these gene abundances varied between the different treatments

(Supplementary Figure 5A-F). The abundance of nitrous oxide-reducing bacteria was determined by quantifying the *nosZI* and *nosZII* gene copy number per gram of dry soil. As shown in Figure 5, the *nosZ* gene copy numbers did not differ between the fertilised treatments at 40% WFPS. However, 51 days from the onset of the incubation at 80% WFPS, the abundance of both genes increased when DMPP or DMPSA were applied together with AS (Figure 5B, D).

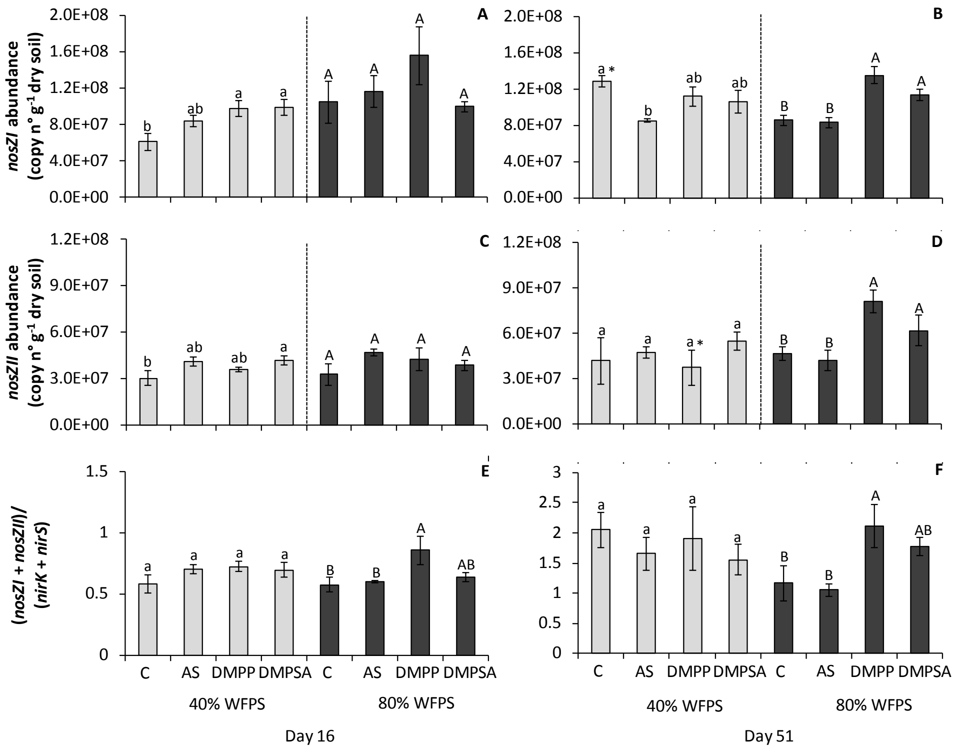

Figure 5. Abundance of *nosZI* (A, B), *nosZII* (C, D) expressed as gene copy number per gram of dry soil, and the ((*nosZI* + *nosZII*) / (*nirK* + *nirS*)) ratio (E, F) at 40% WFPS (grey bars) and 80% WFPS (black bars), 16 (A, C, E) and 51 days (B, D, F) after treatment application. Significant differences ($p<0.05$) between treatments within each WFPS condition are indicated with different letters. Asterisk (*) indicates significant WFPS effect for each fertilised treatment ($p<0.05$). Values represent the mean ± SE (n=4). C = unfertilised control; AS = ammonium sulphate; DMPP = ammonium sulphate + DMPP; and DMPSA = ammonium sulphate + DMPSA.

The ratio of the sum of *nosZI* and *nosZII* gene copies over the sum of *nirK* and *nirS* gene copies ((*nosZI* + *nosZII*) / (*nirK* + *nirS*)) gives us an idea of potential N_2 *versus* N_2O production; a higher ratio means a greater potential for N_2O reduction. At 80% WFPS, the ratio was higher with DMPP application compared to AS treatment, this difference being emphasised at day 51 (Figure 5E-F). This fact suggests that although the potential for completing the denitrification pathway to N_2 is enhanced in the presence of both NIs, DMPP is more effective than DMPSA at promoting the N_2O reduction.

DMPP and DMPSA induce nitrous oxide reductase activity under denitrifying conditions.

In order to confirm the effect of DMPP and DMPSA as potential inducers of N_2O to N_2 reduction under 80% WFPS conditions, we aimed to determine the activity of the denitrifying enzymes through a soil incubation experiment in denitrifying conditions after nitrate was added in a high concentration to induce the denitrification process. As shown in Figure 6, Nos activity was inhibited in acetylene-treated bottles; thus, higher N_2O emissions were detected compared to non-acetylene-treated bottles. Moreover, in non-acetylene-treated bottles, where Nos activity was active, DMP-inhibitors stimulated this activity reducing significantly N_2O emissions (Figure 6B). The ratio of acetylene-treated bottles over non-treated ones ((N_2O + N_2) / N_2O) ratio was higher when DMPP or DMPSA were applied jointly with KNO_3, supporting the hypothesis that these NIs induced the reduction of N_2O to N_2 (Figure 6C).

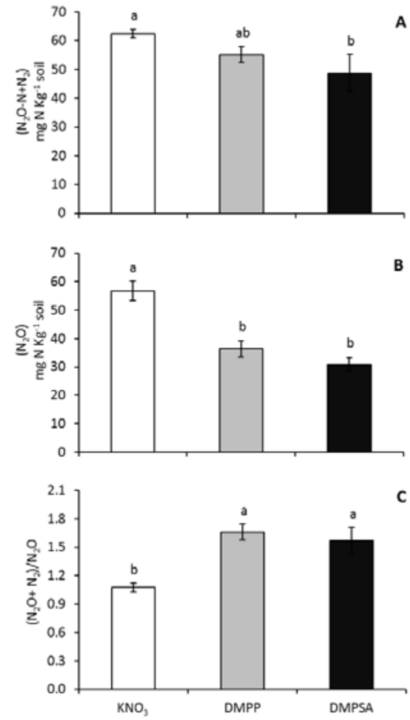

Figure 6. Denitrification activity up to N_2O+N_2 (A) (acetylene) or up to N_2O (B) (non-acetylene) and nitrous oxide reductase activity (Nos activity) (C) expressed by the ratio of acetylene incubation over non-acetylene incubation ((N_2O + N_2)/N_2O) in KNO_3, KNO_3 + DMPP, and KNO_3 + DMPSA treatments. Significant differences ($p>0.05$) are indicated with different letters. Values represent the mean ± SE (n=4).

3.4. Discussion

NI mode of action is not completely understood; however, it is generally accepted that their function is related to the inhibition of the AMO enzyme (Subbarao *et al.*, 2013; Ruser and Schulz, 2015). The effectiveness of NIs in reducing N_2O emissions varies with land use, soil type, environmental conditions, and the type of fertiliser employed (Gilsanz *et al.*, 2016; Yang *et al.*, 2016). Indeed, NIs are also able to decrease N_2O emissions under low O_2 conditions, where the activity of nitrifying bacteria is limited and the main source of N_2O is denitrification (Menéndez *et al.*, 2012; Di *et al.*, 2014).

Several studies have reported that the efficiency of DMPP in reducing N_2O emissions is related to the inhibition of ammonium oxidation associated with AOB control (Di and Cameron, 2011; Chen *et al.*, 2014*b*; Kou *et al.*, 2015). In this work we also observed that DMPP reduced N_2O emissions to the unfertilised control level (Figure 1) concomitantly with ammonium oxidation inhibition (Figure 2). This was further evidenced by the inhibition of AOB proliferation on day 16 (Figure 4), and correlation analysis indicated that the cumulative N_2O emissions (Figure 1B) were positively correlated with the AOB abundance ($r=0.526$, $p<0.05$). Huerfano *et al*. (2016) observed the same N_2O-emission-reducing behaviour of DMPP and DMPSA in a wheat field. Here we report a similar effect of both DMPP and DMPSA, observed under 40% WFPS conditions. Besides the commonly reported lower AOB population after NI application (Di and Cameron, 2011; Di *et al.*, 2014; Kou *et al.*, 2015), in this work we also found that both DMPP and DMPSA completely blocked the rapid induction of bacterial *amoA* gene expression provoked after fertilisation with AS (Figure 3A, B). Similar results were also obtained recently when DMPP was added to soils amended with cattle effluent (Florio *et al.*, 2014), and plant residues (Duan *et al.*, 2017). This evidences the fact that NIs affect AOB, not only by inhibiting AMO activity (Ruser and Schulz, 2015), but also by regulating *amoA* transcription. However, NIs were not observed to affect *amoA* from AOA as reported in previous studies (Di and Cameron, 2011; Shen *et al.*, 2013; Di *et al.*, 2014). Indeed, it has been suggested that the substantial cellular and genetic differences between AOB and AOA could explain the minor efficiency of Nis in targeting AOA (Shen *et al.*, 2013; Shi *et al.*, 2016*a*). Finally, as expected, gene expression levels and the gene copy number of denitrification pathway marker genes showed no significant variation caused by the use of NIs under 40% WFPS (Supplementary Figures 2, 5), in accordance with the specificity of nitrification inhibitors targeting AOB described by Kong *et al.* (2016*a*).

When the available oxygen is limited, denitrification is the dominant force responsible for N_2O production (Khalil *et al.*, 2004; Butterbach-Bahl *et al.*, 2013; Gilsanz *et al.*, 2016). In our study, at 80% WFPS, the near lack of nitrate (Figure 2D), accompanied by the huge increase in N_2O emissions with respect to 40% WFPS conditions (Figure 1), evidences that NO_3^- consumption by denitrifiers is principally responsible for N_2O emission. Nevertheless, nitrification does take place under low oxygen conditions, although at much lower rates (McTaggart and Tsuruta, 2003; Menéndez *et al.*, 2008; Harter *et al.*, 2013). In addition, although not completely understood, NIs have also been shown to efficiently mitigate N_2O emissions under denitrifying conditions (Hatch *et al.*, 2005; Menéndez *et al.*, 2012; Barrena *et al.*, 2017; Wu *et al.*, 2017). In our study, the stimulation of AOB abundance after AS application (Figure 4A), together with *amoA* gene expression induction (Figure 3B) and NH_4^+ content depletion through time (Figure 2C), corroborates the presence of nitrifying activity at 80% WFPS, which provides the substrate for denitrification. However, it must be noticed that the decrease in NH_4^+ takes place much more slowly than at 40% WFPS (Figure 2); moreover, *amoA* induction by AS fertilisation was around 6 times lower than at 40% WFPS, evidencing the expected lower nitrification rate under 80% WFPS conditions, where O_2 availability is restricted. At 80% WFPS, both NIs reduced N_2O emissions and inhibited nitrification, evidenced by the persistence of NH_4^+ in the soil (Figure 2C), together with the decrease in the AOB population (Figure 4A). Surprisingly, DMPSA proved to be less efficient than DMPP at reducing N_2O emissions (Figure 1D). Indeed, no significant *amoA* expression inhibition was observed with DMPSA (Fig 3B). In view of the low level of nitrification induction observed after the application of AS at 80% WFPS, together with the significant efficiency of NIs in reducing N_2O emissions, the effect of NIs on the denitrification process was analysed in order to corroborate our hypothesis that NIs could also be acting on denitrification.

We found that both DMPP and DMPSA stimulated the expression of the *nosZI* gene at 80% WFPS (Figure 3D), and provoked an increase in the bacterial abundance of both clades of *nosZ* at the end of the experiment (Figure 5B, D). This induction was not observed in other denitrification pathway genes, since the gene expression and gene copy number of *narG*, *nirK* and *nirS* did not vary with the addition of NIs (Supplementary Figures 2, 5). Recent studies have concluded that one-third of all denitrifiers lack *nosZ* and their abundance is affected by different soil properties (Philippot *et al.*, 2011; Domeignoz-Horta *et al.*, 2015). Moreover, the increase in the ((*nosZI* + *nosZII*) / (*nirK* + *nirS*)) ratio (Figure 5E, F) suggests specific induction of N_2O reduction to N_2 in soils treated with DMPP or DMPSA, which must contribute to the reduction in N_2O emissions observed after the application of both NIs (Figure 1). Indeed, we found that *nosZI* and gene abundance were negatively correlated with N_2O emissions ($r=-0.373$, $p<0.05$). This specificity in promoting N_2O reduction to N_2 after adding DMPP or DMPSA at 80% WFPS was confirmed by means of a complementary denitrification assay (Figure 6). Several studies have proposed that elevated

NO_3^- content increases the N_2O:N_2 ratio (Saggar *et al.*, 2013) and the effect of NIs on denitrification is indirect, probably due to the shortage of NO_3^- (Müller *et al.*, 2002; Di *et al.*, 2014; Florio *et al.*, 2014). In contrast, Barrena *et al*. (2017) speculated that DMPP may reduce N_2O emissions by inducing either gene expression or Nos activity. In agreement with that, in our denitrification assay, which provided the same NO_3^- rate in all treatments, the reason for the increased N_2O reduction to N_2 must have been a direct effect of the NIs. Therefore seems to be an alternative NI effect on denitrification that provokes a transient induction of *nosZ* expression (Figure 3D), which finally stimulates the complete reduction of N_2O to N_2 through the action of Nos (Figure 6). Interestingly, the increase in the ((*nosZI* + *nosZII*) / (*nirK* + *nirS*)) ratio was lower with DMPSA than with DMPP (Figure 5) and this was in complete agreement with the lower efficiency of DMPSA compared to DMPP in mitigating N_2O emissions at 80% WFPS (Figure 1D). In line with our results, Hatch *et al*. (2005) observed that N_2O production decreased during anaerobic soil incubation with DMPP, concomitant with an increase in N_2 production, compared to non-DMPP-treated soils.

Interestingly, the action of other types of soil amendments with the capacity to reduce N_2O emissions, such as biochar, has also been related to a rapid and transient induction of *nosZ* gene expression (Harter *et al.*, 2013). Overall, our results evidence the fact that the decrease in N_2O emissions from NI-treated soils at 80% WFPS is not only caused by nitrification inhibition but also by the stimulation of N_2O reduction to N_2 by nitrous oxide reductase during the denitrification process. Our results therefore lead the way towards future studies on the mechanisms underlying the direct effect of DMP-based NIs over nitrous oxide reductase enzymes and *nosZ* gene induction.

To our knowledge, this work is the first microcosm study using DMPSA and the first description of the effect of DMPSA on populations of soil microbes. As stated above, we observed that DMPSA and DMPP behaved differently under 80% WFPS conditions. Both molecules are structurally similar and it is difficult to comprehend why the presence of a phosphate compared to a succinic group should have this kind of impact on inhibitor efficiency. In this sense, further work focusing on the mechanism of action of the NIs is essential to elucidate how DMPSA and DMPP behave in the soil.

4

Elevated CO_2 and nitrate supply overcomes the ammonium toxicity and improves photosynthetic parameters in wheat plants

4.1. Introduction

The increase in the world's population predicted for the end of the 21st century (http://www.fao.org) requires that intensive agriculture employ large amounts of nitrogen (N) to increase maximum cereal yield. Furthermore, the worldwide nitrogen fertilizer consumption reached 109 million tonnes in 2014 (Timilsena *et al.*, 2015). Despite the larger N inputs, the nitrogen use efficiency (NUE) is low with less than 47% of the nitrogen applied recovered by crops (Lassaletta *et al.*, 2014). The remaining soil N resulting from the intensive agriculture may cause environmental problems, which include the contamination of aquatic systems though nitrate leaching or the emission of nitrous oxide gas by nitrification and denitrification processes (Fowler *et al.*, 2013). In order to reduce these pollutant problems and increase NUE, nowadays several strategies are focused on minimizing N losses and optimizing fertiliser formulation. Between others, to replace the use of ammonium-based fertilizers instead of nitrate-based fertilizers (Sanz-Cobena *et al.*, 2016) and to understand the biochemical and physiological mechanisms employed by plants for use external N (Tegeder and Masclaux-Daubresse, 2017) are propose as strategies to reduce the environmental problems associated with agricultural N inputs and improving NUE by plants, respectively.

Both nitrate and ammonium are the major N-forms available in soils for plants uptake (Andrews *et al.*, 2013; Tegeder and Masclaux-Daubresse, 2017). Nitrogen absorbed by root require to be assimilated into amino acids in either roots or shoot, with the subsequent energetic cost (Masclaux-Daubresse *et al.*, 2010; Andrews *et al.*, 2013). Nitrate assimilation in plants requires the reduction of nitrate to ammonium by the enzymes nitrate reductase (NR) and nitrite reductase (NiR) to ammonium. The ammonium, either coming from primary nitrate reduction or taken-up by the plant directly from the soil is incorporated into amino acids by glutamine synthetase (GS) and glutamine:oxoglutarate aminotransferase (GOGAT), in the so-called GS/GOGAT cycle (Lea and Miflin, 1974). Although agriculture practises tend to apply a sole N source (ammonium, nitrate or urea), under natural conditions microbial processes in soils favoured a mixed nutrition. In addition, when both inorganic-N sources are available for plant uptake, ammonium is preferred for incorporation due to its more reduced status than nitrate and thus, requiring less energy for its assimilation (Andrews *et al.*, 2013). Nevertheless, the application of ammonium as the sole N source generally provokes ammonium toxicity symptoms in many plants species (Britto and Kronzucker, 2002). Besides the visual symptoms observed as a reduced plant growth or leaf chlorosis, the toxic action of ammonium provokes alteration on expression and activity of N assimilating enzymes, disruptions in photosynthesis and hormonal homeostasis, deficiency in ion balance or induces higher photorespiration rates (Guo *et al.*, 2007; Esteban *et al.*, 2016). The ammonium effects over photosynthesis are typically related with declines in Rubisco and NADP-dependent glyceraldehyde-3-phosphate dehydrogenase or changes in chloroplast ultrastructure; however, these effects are depending on plant species and ammonium concentration (Britto and Kronzucker, 2002; Esteban *et al.*, 2016). In addition, environmental factors such as light intensity (Ariz *et al.*, 2011; Setién *et al.*, 2013), pH conditions (Sarasketa *et al.*, 2016), the external N concentration (Vega-Mas *et al.*, 2015) and atmospheric CO_2 concentration (Nimesha *et al.*, 2017; Rubio-Asensio and Bloom, 2017; Vega-Mas *et al.*, 2017) determine the threshold for ammonium toxicity. According to these studies, an adequate availability of carbon skeletons, coming lately from photosynthates and derived through Krebs cycle, is essential to maintain the internal ammonium homeostasis in the plant cell, thus avoiding toxic effects associated to ammonium nutrition.

Plant growth stimulation by elevated atmospheric CO_2 has been previously described to enhanced CO_2 fixation (Evans, 1983; Drake and González-Meler, 1997; Coskun *et al.*, 2016). Among others, limitations in N assimilation and the consequent lower N availability have been pointed out as a target factor conditioning crop responsiveness to elevated CO_2. During the last decade, several authors have studied the plant responsiveness to elevated CO_2 in function of the N-form (nitrate, ammonium and ammonium nitrate) (Bloom *et al.*, 2014; Jauregui *et al.*, 2015, 2017; Vega-Mas *et al.*, 2015). In case of nitrate-fertilised plants, previous studies show that as a consequence of the increase in CO_2 fixation rates, leaf carbohydrate sink/source balance is altered (Stitt *et al.*, 2002). The accumulation of non-structural carbohydrates such as starch induces the down-regulation of the gene expression, specifically of those coding the photosynthetic apparatus, with the consequent decrease in the photosynthetic carboxylation capacity (Long *et al*., 2004; Moore *et al*., 1999). The inhibition of leaf nitrate assimilation in wheat and *Arabidopsis thaliana* plants grown under elevated CO_2 has been related with a depletion in photorespiratory rates (Rachmilevitch *et al.*, 2004). Therefore, Bloom *et al.* (2010) hypothesized the depletion of nitrate assimilation under elevated CO_2 would be produced by lower photorespiration rates, by the increase in CO_2 fixation that produces stromal acidification or by a higher competition between C and N metabolism enzymatic activities for ATP and ferredoxin/NAD(PH) reductant equivalents. According to these authors, under low photorespiratory conditions, the decrease of NO_3^- assimilation diminishes plant organic N compounds and reduces the energy provision to photosynthesis and N assimilation, which comprises plant growth.

According to previous studies, it could be expected that plants might vary the strategy of N assimilation into organic compounds under elevated CO_2. In addition, the predicted raise of atmospheric CO_2 would favour plant developments under nutrition based on ammonium-fertilisation by a larger C-skeletons availability supported for permit ammonium assimilation (Vega-Mas *et al.*, 2015) and overcome the associated ammonium toxicity. In this study, we have grown durum wheat plants (*Triticum durum* Def. cv. Amilcar) at two different concentrations of atmospheric CO_2 (400 and 700 ppm) and under different N nutrition (NO_3, NH_4 and NH_4NO_3) in order to evaluate the relevance of N fertilization form in plant responsiveness to elevate CO_2. For that, we grew wheat plants during 5 weeks under nitrate as N-source (10 mM). Afterwards, the following 2 weeks N-source was supplied in form of ammonium or nitrate ammonium, whereas plant subgroups were kept growing under nitrate, as control. The present work has been conceived with the objective of evaluate the effect of elevated CO_2 conditions on wheat plants fertilised under the mixed ammonium nitrate fertilisation for improving photosynthesis, metabolism and biomass, without present the N-limitations associated to individual N-nutrition forms.

4.2. Materials and Methods

Plant material and experimental design

Seeds of wheat plants (*Triticum durum* L. cv. Amilcar) were germinated on trays filled with perlite-vermiculite 1:1 (v/v) and watered with deionised water. In order to synchronize the germination, seeds were maintained for 10 days in darkness and at 4 °C. After thus, seedlings were transferred to 5 litres hydroponic pots in two independent controlled environmental chambers (Phytotron Service, SGIker, UPV/EHU), under 550 µmol m^{-2} s^{-1} of light intensity, 25/17 °C of temperature, 50-60% of relative humidity during the light and dark periods, respectively, with a 14 h photoperiod. Plants grown under two different controlled atmosphere CO_2 of 400 ppm and 700 ppm CO_2 levels and Hoagland solution (Arnon and Hoagland, 1940) were replaced three times by week. Wheat plants grown for 5 weeks under nitric nutrition based on calcium nitrate. Afterwards, for the following 2 weeks the N source was modified by ammonium sulphate (NH_4^+) or ammonium nitrate (NH_4NO_3), keeping control plants under nitrate nutrition (NO_3^-). The N source was supplied at a rate of 10 mM total N. After measuring photosynthesis in flag leaves of four plants from each CO_2 condition, wheat plants were harvested and dried in an oven at 80 ℃ for 72 h for biomass determination. For metabolic analysis, totally expanded flag leaves of at least three plants were harvested and stored at −80 °C until further measurements.

Gas exchange determinations

Gas-exchange measurements were conducted in totally expanded flag leaves using a Li-COR 6400XP portable photosynthesis system (LI-COR Inc., Lincoln, NE, USA). The rate of CO_2 assimilation (A_N), stomata conductance (g_s) and intercellular CO_2 (Ci) parameters were determined at both 400 and 700 ppm CO_2 in light-saturated conditions with a photosynthetic photon flux density (PPFD) of 1200 µmol m^{-2} s^{-1} at 25°C. For the estimation of thee maximum carboxylation velocity of Rubisco (Vc_{max}), the CO_2 in the leaf chamber was decreased in three steps from 400 to 100 ppm of CO_2, followed by an increase from 400 to 1200 ppm of CO_2 in five steps. The estimation of Vc_{max} was done using the equation developed by Sharkey *et al.*, (2007). The dark respiration measurements were conducted after 45 min the dark period started and simultaneously, the thylakoid electron transport rate (J_T) and the maximal PSII photochemical yield (Fv/Fm) were measured using a Leaf Chamber Fluorometer (LFC 6400–40; Li-COR) coupled to the Li-COR 6400XT portable photosynthesis system. Photorespiratory CO_2 release (R_l) was estimated according the equation: $V_o/2=1/12[J_T - 4\ (A_N + R_d)]$ provided by (Valentini *et al.*, 1995).

Metabolites determination

Soluble sugars were measured from 10 mg of lyophilised powdered samples by modified hydroalcoholic extraction described in Fuertes-Mendizábal *et al.*, (2010). Soluble carbohydrates (glucose, fructose, and sucrose) were measured by using a test kit (Boehringer Mannheim, Germany) from the hydrated extract resultant from evaporating the ethanol fraction (Speed Vac, Thermo Savant). For starch determination, the dry residue obtained in the hydroalcoholic extraction was resuspended and starch was determined as glucose equivalents by using the test kit (Boehringer Mannheim, Germany) after α-amylase and amyloglucosidase digestion. For maltose determination, 0.1 g of plant-frozen powder was resuspended in 1 mL of 90% ethanol and incubated for 90 min at 70°C. After thus, the extract were centrifuged at 13000 g for 10 min. For glucose-6-phosphate, glucose-1-phosphate, fructose-6-phosphate determinations, 0.5 g plant-frozen powdered was resuspended in 0.4 ml of 1 M $HClO_4$, incubated for 2 h at 4°C and centrifuged at 10000 g for 5 min. The supernatants were neutralized with K_2CO_3 and maltose, glucose-6-phosphate, glucose-1-phosphate and fructose-6-phosphate were determined by HPLC with pulsed amperometric detection on a DX-500 Dionex system. N-inorganic forms of nitrate and ammonium were determined according to materials described by Patton and Crouch, (1977) and Cataldo *et al.*, (1974), respectively.

Single amino acid profile was quantified at the Scientific and Technological Center of the University of Barcelona (CCiT UB). Amino acids were extracted from flag leaves homogenized with 1:20 (w/v) of 1M HCl. After 16 hours of incubation at -20 °C, the extracts were centrifuged at 10000 g for 15 min and filtered. 2.5 mM Norleucine were added as internal standard to the five times diluted amino acid extraction. Afterwards, 20 µl of derivatized sample were injected for amino acids determination by HPLC using Waters Delta 600 chromatographic system with a column (Nova-Pak C18 4 µm, 3.9 x 150 mm) and an absorbance detector (Waters 2487 Dual λ) coupled to an auto sampler (Waters 717plus) using the AccQTag pre-column derivatization method. The reaction of amino acids with 6-aminoquinolyl-N-hydroxysuccinimidyl carbamate yields derivatives were detected at 254 nm and its concentration was calculated according to internal standard (Cohen and Michaud, 1993; Cohen and De Antonis, 1994).

C cycle enzymatic activities

Leaves powder were homogenised with in a extraction buffer consisting [100 mM HEPES pH 7.5, 2 mM EDTA and 2 mM dithiothreitol, 1 mM PMSF, 10 µl ml^{-1} protease inhibitor cocktail (Sigma P9599)], and centrifuged at 14000 g for 20 min. The supernatant was desalted by ultrafiltration on Vivaspin 500 centrifugal concentrator (Sartorius) and the protein extract thus obtained was assayed for enzymatic activities. ADP-Glucose pyrophosphorylase (AGPase) activity was measured following the two-step assay method described by Li *et al.*, (2012). Phosphoglucose isomerase (PGI) and phosphoglucomutase (PGM) were measured as described by Bahaji *et al.*, (2015). Starch phosphorylase and amylolytic activities were assayed as described by Sweetlove *et al.*, (1996). Starch synthase activity was measured in two steps: (1) in a buffer reaction [50 mM HEPES pH 7.5, 6 mM $MgCl_2$, 3 mM dithiothreitol, 1 mM ADPG, 3% glycogen] for 5 min at 37°C. After stop the reaction by boiling for 2 min, (2) the ADP produced was measured by HPLC on a Waters Associate's system fitted with a Partisil-10-SAX column. One unit (U) is defined as the amount of enzyme that catalyzes the production of 1 µmol of product per min.

N cycle enzymatic activities

Soluble protein was extracted from powdered frozen flag leaves homogenised with 1:20 (w/v) extraction buffer based on Sarasketa *et al.*, (2014). Soluble protein was measured according to Bradford, (1976) from extract recovered after centrifugation at 4000 g for 30 min at 4 °C. Nitrate reductase (NR) maxim activity was determined incubating 50 µl of protein extract for 30 min at 30 °C according to Baki *et al.*, (2000). Glutamine synthetase (GS) and aminating-Glutamate dehydrogenase activity (NADH-GDH) were determined as described by Sarasketa *et al.*, (2016).

RNA extraction and Quantitative real-time PCR

Total RNA was isolated from pulverized leaves using the Nucleospin RNA plant kit (Macherey-Nagel) according to the manufacturer's recommendations. RNA integrity and purity were checked on a 1.5% (v/v) agarose gel and 1 µg of RNA was retrotranscribed into cDNA using the PrimeScript™ RT reagent Kit (Takara Bio Inc.). Gene expression was determined using a StepOne Plus Real Time PCR System (Applied Biosystems) in a 15 µL reaction using the SYBR Premix ExTaq™ (Takara Bio Inc.), 200 nM of each-gene specific primer and 2 µL of cDNA diluted 1:10. The PCR thermal profile was: 95°C for 10 min, 40 cycles (95°C for 15 s and 60°C for 1 min) and a final step to obtain the melting curve. The data was expressed as the log_2-fold change after the quantification of the relative gene expression using the comparative C_t method $2^{-\Delta\Delta Ct}$ (Schmittgen and Livak, 2008).

Statistical analysis

Data were analysed using IBM SPSS statistic 22 software (Armonk, NY, USA). Normality and homogeneity of variance were analysed by Kolmogorov-Smirnov and Levene test. Analysis of significant differences between N treatments on both CO_2 condition were analysed by one-way ANOVA with a Duncan post hoc-test. For both analyses, differences were considered significant at $p<0.05$. Differences between N treatments under both CO_2 conditions were analysed by t-test.

4.3. Results

Growth of durum wheat cv. Amilcar showed different behaviour depending on the N-form supplied in the nutrient solution and CO_2 environmental conditions. Both nitrate and ammonium nitrate nutrition showed the highest biomass production, whereas plant biomass did not increased under exclusive ammonium nutrition . Moreover, under elevated CO_2 condition, the mixed ammonium nitrate nutrition allowed increasing the shoot biomass in the same extent as nitrate nutrition when they were compared with their respective controls at ambient CO_2 (Table 1); but no effect was observed for ammonium nutrition due to elevated CO_2 concentrations in terms of shoot biomass. In addition, ammonium-fed plants biomass was reduced about 40% with respect to treatment fertilised with nitrate (Table 1).

Table 1. Nitrogen source effect on shoot biomass of wheat plants grown under ambient and elevated CO_2 conditions (400 and 700 ppm CO_2). Data represent mean values (g DW) ± SE (n=5). Significant differences ($p<0.05$) between N treatments are indicated with different letters. Asterisk (*) indicates significant CO_2 differences ($p<0.05$). Values represent mean ± SEM (n=5).

	400 ppm CO_2				700 ppm CO_2			
NO_3^-	21.77	±	2.73	a	26.26	±	1.10	A
NH_4^+	14.64	±	1.23	b	15.14	±	2.32	B
NH_4NO_3	20.80	±	0.53	a	26.56	±	1.90	A*

Gas-exchange parameters measured on flag leaves of 7-week-old wheat plants showed that ammonium- and ammonium nitrate-fertilised plants grown under ambient CO_2 conditions presented a strong stomata closure, that reduced the intercellular CO_2 concentration (C_i) and thus, the CO_2 assimilation rate (Fig 1A, C, D). Under nitrate nutrition, the exposure to elevated CO_2 reduced the stomata conductance (g_s), but it did not affect the photosynthetic rate (A_N). On the contrary, the exposure to elevated CO_2 stimulated the stomata conductance in ammonium nutrition with a reflect on the assimilation rate; and interestingly, ammonium nitrate-fertilised plants avoided the stomatal closure observed under nitrate, stimulating the A_N rate to be on a par with that of nitrate-fertilised plants (Figure 1C). Ammonium–fertilised at ambient CO_2 plants showed the lowest values for maximum carboxylation velocity of Rubisco (Vc_{max}); and regardless the nitrogen nutrition, the exposure to elevated CO_2 maintained or even increased the maximum carboxylation velocity of Rubisco (Vc_{max}) respect to their controls grown at ambient CO_2 (Figure 1B).

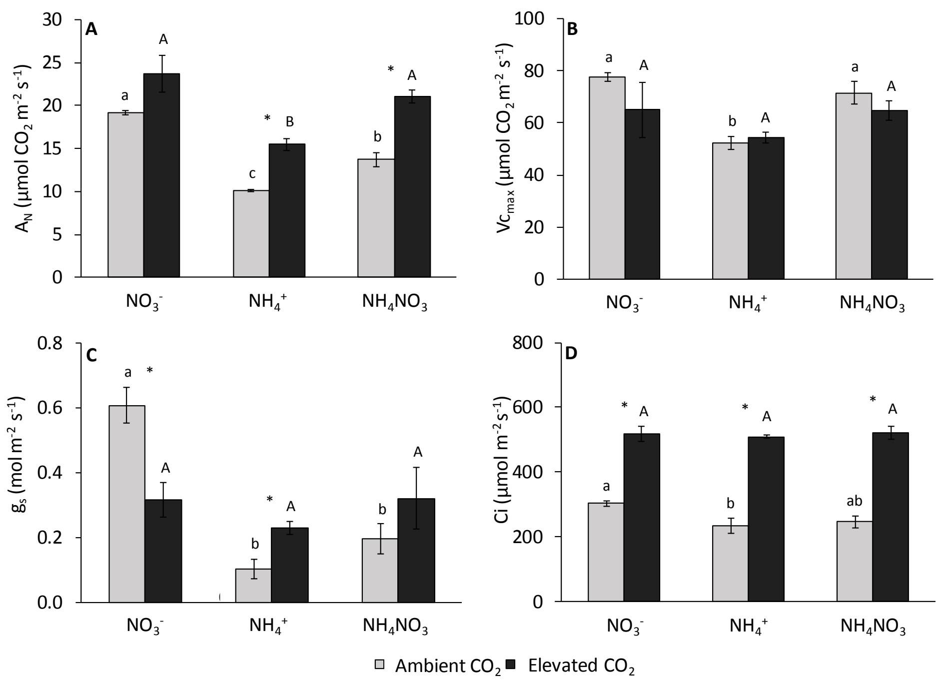

Figure 1. Nitrogen source (NO_3^-, NH_4^+ and NH_4NO_3) effect on net photosynthesis rate (A), maximum velocity of RuBP carboxylation (B), stomatal conductance (C), intercellular CO_2 mole fraction (D), under ambient (grey bars) and elevated (black bars) CO_2 conditions. Data represent mean values ±SE (n=3). Letters represent significant differences between treatments analysed by Duncan's test ($p<0.05$). Asterisk (*) indicates significant CO_2 differences ($p<0.05$).

Both ammonium and ammonium nitrate nutrition reduced thylakoid electron transport rate (J_T), but only ammonium nutrition depleted the maximum photochemical yield of PSII (Fv/Fm) (Figure 2A, C). The exposition of elevated CO_2 allowed ammonium-fed plants to recover Fv/Fm to normal values; and the electron transport rate (J_T), at the same time the photorespiratory CO_2 release, increased (Figure 2) for both ammonium nutrition treatments, either exclusive ammonium or mixed nutrition.

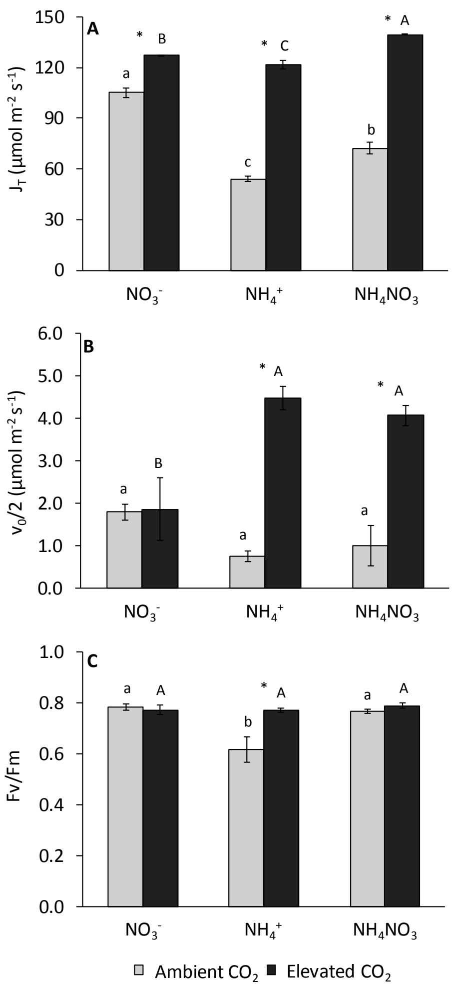

Figure 2. Nitrogen source (NO_3^-, NH_4^+ and NH_4NO_3) effect on net total electron transport through PSII (A), photorespiratory CO_2 release (B) and maximal photochemical yield of PSII (C), under ambient (grey bars) and elevated (black bars) CO_2 conditions. Data represent mean values ± SE (n=3). Letters represent significant differences between treatments analysed by Duncan's test ($p<0.05$). Asterisk (*) indicates significant CO_2 differences ($p<0.05$).

At the carbohydrate level, the exposure to elevated CO_2 reduced contents of sucrose, fructose-6-phosphate and glucose-6-phosphate6 in nitrate-fertilised plants while increased the starch content (Figure 3). However, the enzymatic activities of (PGI), (PGM) and (AGPase), involved in the conversion of fructose-6-phosphate into ADP-glucose, did not vary when they were compared with their nitrate controls at ambient CO_2 conditions. Concomitantly with the starch accumulation, these plants showed a higher starch synthase activity and a lower amylase activity (Figure 3). Ammonium nutrition under ambient CO_2 condition also showed a higher starch synthase activity, but also an elevated amylase activity (Figure 3) that might prevent the starch accumulation in leaves. Moreover, in ammonium-fertilised plants grown under ambient CO_2 condition the maltose content was higher (Figure 3). Ammonium nitrate-fertilised plants grown at ambient CO_2 showed lower sucrose, Fructose-6-phosphate and glucose-6-phosphate content than nitrate-fertilised plants. At elevated CO_2 conditions, ammonium nitrate-fed plants increased PGI, PGM, AGPase, Starch synthase and total amylase activities compared with nitrate-fed plants, favouring the synthesis and degradation of starch and avoiding its accumulation (Figure 3). The single amino acids profile showed that predominant amino acids were asparagine + serine (asn+ser), glutamate (glu) and glutamine + histidine (gln+his) (Figure 4 and Supplementary Table 2). Wheat plants exposed to elevated CO_2 conditions reduced the amino acids content under exclusive ammonium in wheat leaves (Figure 4A). More concretely, the amino acids more depleted under elevated CO_2 were Asn+Ser, Glu, His+Gln and Pro. Moreover, proline was also presented in high levels in ammonium and ammonium nitrate-fertilised plants grown at ambient CO_2, however, it was not accumulated under elevated CO_2 conditions in these treatments (Figure 4E). Exposure to elevated CO_2 increased total soluble proteins, being statistically significant when N-source was in form of exclusive nitrate or ammonium (Figure 4F).

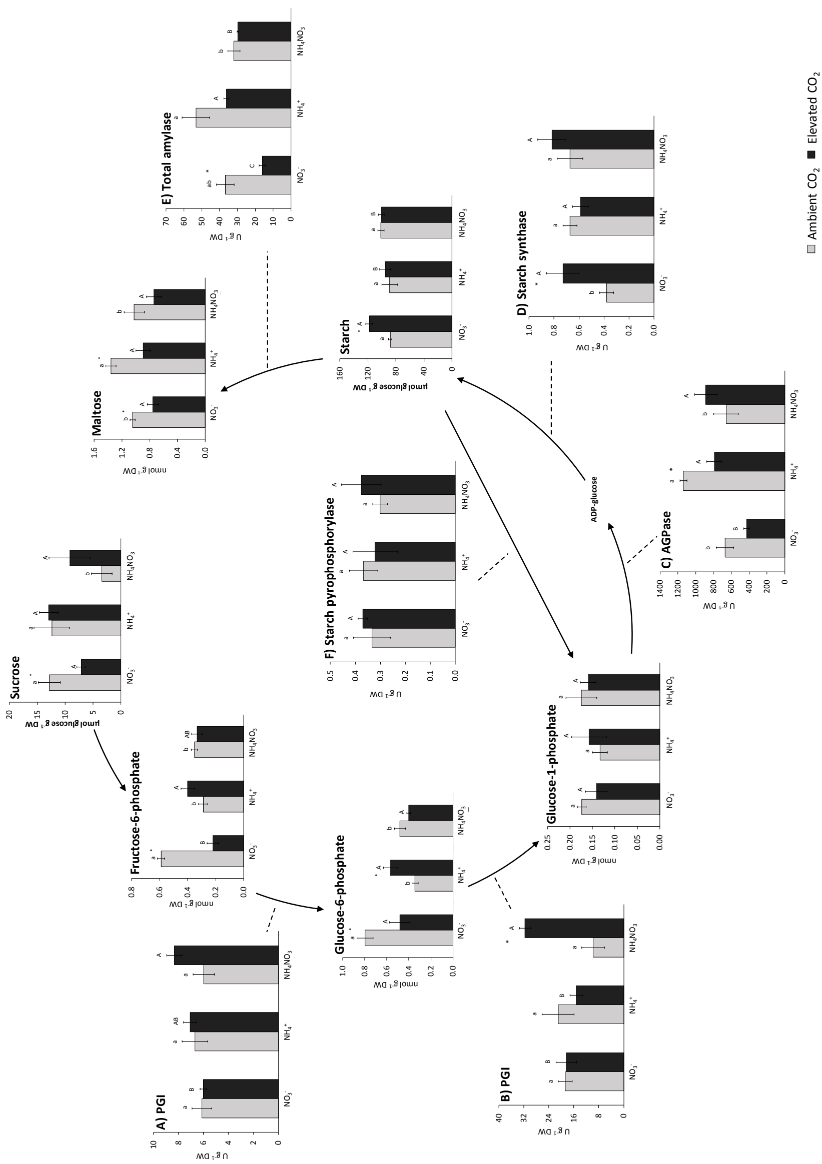

Figure 3. Nitrogen source (NO_3^-, NH_4^+ and NH_4NO_3) effect on phosphoglucose isomerase (A), phosphoglucomutase (B), ADPGlc pyrophosphorylase (C), starch synthase (D), total amylase (E) and starch pyrophosphorylase (F) activities and on the carbohydrates sucrose, fructose-6-phosphate, glucose-6-phosphate, glucose-1-phosphate, maltose and starch content under ambient (grey bars) and elevated (black bars) CO_2 conditions. Data represent mean values ± SE (n=4). Letters represent significant differences between treatments analysed by Duncan's test (P<0.05). Asterisk (*) indicates significant CO_2 differences (p<0.05).

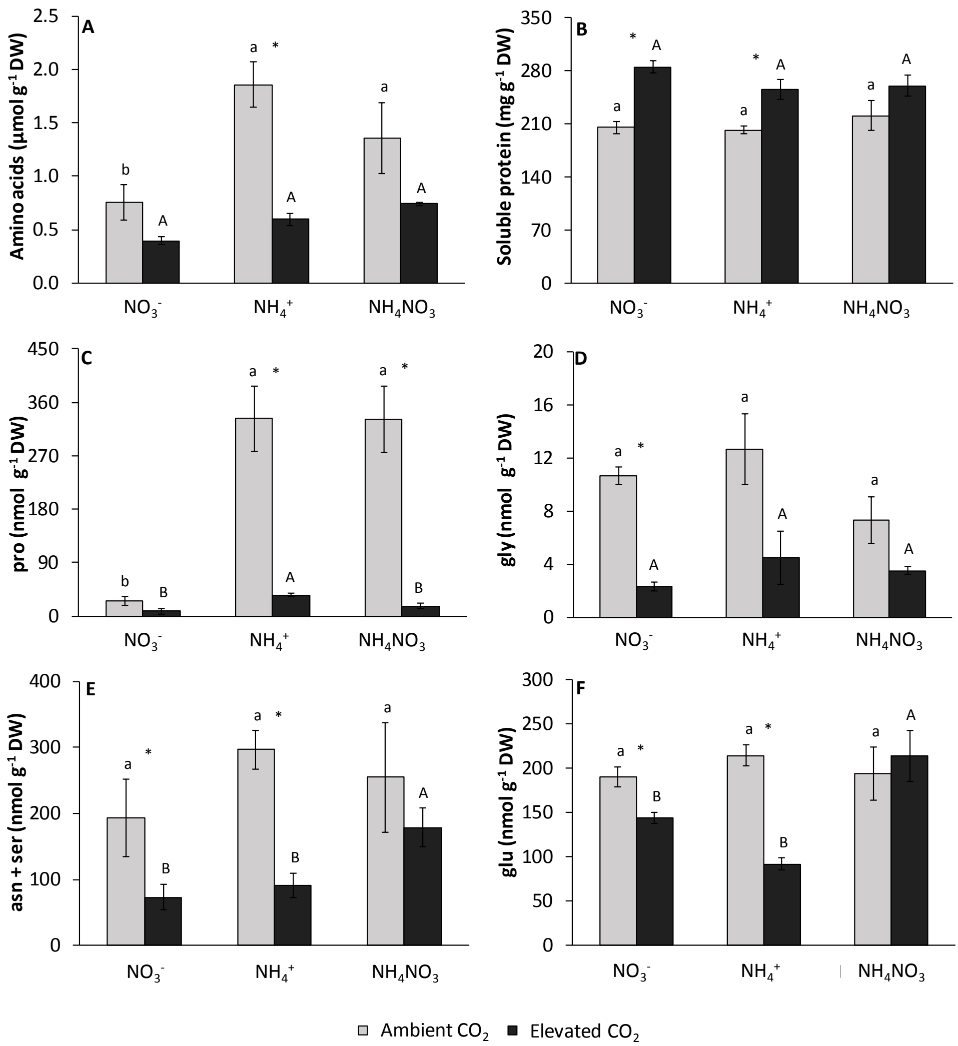

Figure 4. Nitrogen source (NO_3^-, NH_4^+ and NH_4NO_3) effect on total amino acids (A), total soluble protein (B), proline (C), glycine (D), aspartate and serine (E) and glutamine (F) under ambient (grey bars) and elevated (black bars) CO_2 conditions. Data represent mean values ± SE (n=3-4). Letters represent significant differences between treatments analysed by Duncan's test ($p<0.05$). Asterisk (*) indicates significant CO_2 differences ($p<0.05$).

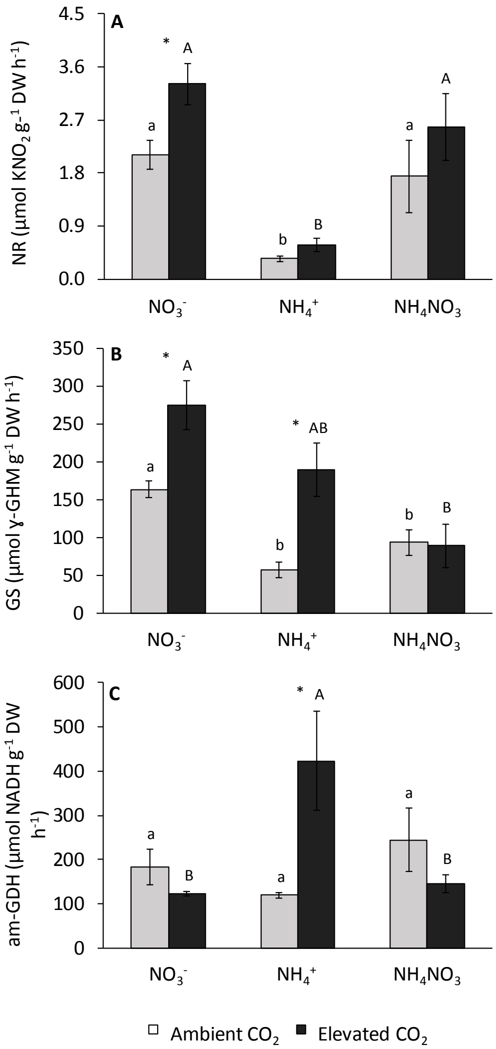

Figure 5. Nitrogen source (NO_3^-, NH_4^+ and NH_4NO_3) effect on nitrate reductase (A), glutamine synthethase (B) and glutamate dehydrogenase aminating (C) activities under ambient (grey bars) and elevated (black bars) CO_2 conditions. Data represent mean values ± SE (n=4). Letters represent significant differences between treatments analysed by Duncan's test ($p<0.05$). Asterisk (*) indicates significant CO_2 differences ($p<0.05$).

Together with nitrogen metabolites content in wheat leaves, the activity of N-cycle enzymes changed depending CO_2 conditions and N nutrition (Figure 5). Comparing the effect of N-source, ammonium-fertilised plants only showed less GS activity under ambient CO_2 condition respect to nitrate-fertilised plants; whereas ammonium nitrate nutrition reduced GS activity regardless the CO_2 conditions (Figure 5B). The exposure to elevated CO_2 stimulated NR and GS activities of nitrate-grown plants, without disturb GDH activity (Figure 5A-C).

For ammonium-fertilised plants, exposure to elevated CO_2 stimulated GS activity; at the same time that these plants presented the maximum activities for aminating GDH (Figure 5B-C).

Exposure to elevated CO_2 and N nutrition modulated the gene expression (Table 2). Under ambient CO_2 conditions, ammonium- and ammonium nitrate-fertilised plants down-regulated the gene expression of carbonic anhydrase, CA1, CA2 y CA3, but up-regulated that of CA4 (only for ammonium nitrate-nutrition). However, under elevated CO_2 this down-regulation in carbonic anhydrase was detected only under ammonium nutrition. Under elevated CO_2, ammonium nitrate-fertilised plants up-regulated the expression of carbonic anhydrases compared with plants grown under ambient conditions. Ammonium fertilisation stimulated the expression of aquaporins (PIP1.1 and PIP2.3), but decreased the expression of TIP1 under ambient CO_2 conditions. Moreover, the expression of ammonium transporter was down-regulated under elevated CO_2 conditions (Table 3) for nitrate and mixed ammonium nitrate nutrition.

Table 2. Heat map of transcript abundance in flag leaves of wheat grown under different nitrogen source (NO_3^-, NH_4^+ and NH_4NO_3) and under ambient and elevated CO_2 conditions (400 and 700 ppm CO_2). Data represent mean values ± SE (n=3). Letters represent significant differences between treatments analysed by non-parametric test (p<0.05).

		400 ppm CO_2			700 ppm CO_2		
		NO_3^-	NH_4^+	NH_4NO_3	NO_3^-	NH_4^+	NH_4NO_3
BE213258	Putative carbonic anhydrase, plastidial, CA1	a	a	b	B*	C	A*
TC389217	Putative carbonic anhydrase, plastidial, CA2	a	b	b	A	B	A*
TC393400	Putative carbonic anhydrase, plastidial, CA3	a	b	b	A	B	A*
TC442386	Putative carbonic anhydrase, plastidial, CA4	b	b*	a*	A	A	A
AY428038	Ammonium transporter, AMT2;1	a	a	a	A*	B	B*
HF544985	Low affinity nitrate transporter, NRT1.1A	a*	a	a	A	A	A
AY587264	Low affinity nitrate transporter, NRT1.2	a	a	b	A	A	A
HF544995	Low affinity nitrate transporter, NRT1.7B	a	b	ab	A	A	A
DQ345446	Aquaporin, PIP 1.1	b	a*	b	A	A	A
AY525641	Aquaporin, PIP 2.3	b	a*	ab	A	A	A
EU177566	Aquaporin, TIP 1	a	b	a	A	A	A

-4 +4

4.4. Discussion

Previous studies revealed that the N forms provided to plants have a differential effect on plant photosynthesis, C and N metabolism (Stitt *et al.*, 2002; Masclaux-Daubresse *et al.*, 2010; Coskun *et al.*, 2016; Rubio-Asensio and Bloom, 2017), with the consequent impact on the plant growth. As it is highlighted in the current study, the type of N fertilization has a target impact on gas exchange parameters, expression of proteins linked with CO_2 and H_2O diffusion together with C and N metabolism.

Exposure to elevated CO_2 usually increase the plant growth due to an enhanced CO_2 fixation, but also it has been documented that prolonged exposure to elevated CO_2 causes stomata closure affecting the initial photosynthetic stimulation, with the consequent plant growth acclimation (Ainsworth and Rogers, 2007; Xu *et al.*, 2016). In accordance with this, nitrate-fertilised plants grown under elevated CO_2 suffered a strong stomata limitation that avoided a stimulation of the photosynthetic rate over ambient CO_2 rates. Moreover, the exposure to elevated CO_2 did not enhance the Rubisco carboxylation despite the higher intercellular CO_2 concentration detected. In accordance with Zhu et al. (2012), both Vc_{max} activity and g_s indicated that nitrate-fertilised plants would suffer from photosynthetic acclimation under elevated CO_2. Opposite to earlier studies that described a decrease of NR activity under elevated CO_2 in nitrate-fertilised plants (Bloom *et al.*, 2002, 2010; Vicente *et al.*, 2015), data obtained for wheat var. Amylcar indicated that CO_2 enrichment far from reducing leaf nitrate pool, increased the nitrate uptake and its assimilation into proteins, through an activation of NR and GS activities. Thus under these conditions, free amino acids contents were lower since they were destined to synthesis of total soluble protein. These results would indicate that nitrate-fertilised plants were able to coordinate both C fixation and N assimilation at high rates due to an efficient energy balance.

C fixed during the photosynthesis is commonly assimilated in form of starch or sucrose. The starch accumulation observed in nitrate-fertilised leaves at elevated CO_2 suggest a C imbalance (MacNeill *et al.*, 2017), and has been commonly correlated with the photosynthetic acclimation (Drake and Gonzàlez-Meler, 1997). In our case, the starch accumulation in photosynthetic tissues could be considered as a symptom of C overflow generated when the rate of photosynthesis exceeds the rate of leaf C demand (Stitt *et al.*, 2010). The data underline the fact that the excess of atmospheric C stimulated the starch synthase activity, and as consequence of a lower sink demand, the starch degradation was reduced. Thus, the excess of C was stored as starch in leaves (Ainsworth *et al.*, 2004; Aranjuelo *et al.*, 2011, 2013*b*; White *et al.*, 2015) would suggest a slight C imbalance although apparently no photosynthetic acclimation was observed, contrasting our results with those reported by Bloom *et al.* (2010). Overall, elevated CO_2 exerted a positive effect on wheat plant growth and this variety could gain benefit from an increasing CO_2 atmospheric concentrations.

Ammonium fertilisation often causes many toxicity symptoms when it is supplied as the sole N source. These effects are reflected in overall in biomass terms, as it is shown by lower photosynthetic performance and growth of wheat plants. The alteration of hormonal and ion homeostasis, the stimulation of photorespiration or oxidative stress, are among others effects of ammonium toxicity (Britto and Kronzucker, 2002; Ariz *et al.*, 2011; Esteban *et al.*, 2016). Those symptoms have been linked with oxidative stress that cause an intracellular redox imbalance, affecting over the mitochondrial electron transport chain (Jauregui *et al.*, 2017; Liu and Wirén, 2017). In agreement with other studies, our data showed that under ambient CO_2 conditions, ammonium contents was accumulated in leaf tissue under ammonium, reflecting an imbalance between its uptake and its assimilation (Setién *et al.*, 2013; Sarasketa *et al.*, 2016). Besides, it is shown that ammonium nutrition strongly impaired the photochemical processes, since the depletion of maximal photochemical yield electron (Fv/Fm) is an indicator of photoinhibition of photosynthetic apparatus; and accordingly a lower photosynthetic electron transport rate (J_T) occurs. Besides, ammonium nutrition also limited photosynthetic CO_2 assimilation as consequence of the strong stomatal limitation (stomatal opening depleted 88% respect to nitrate-fertilised plants), with the concomitant depletion in the intercellular CO_2 concentration. The limited diffusion of CO_2 to carboxylation place depletes the maximum velocity of Rubisco carboxylation. Thus, at ambient CO_2 grown conditions, the CO_2 assimilation was limited as the electron sink, which might cause the over-excitation of photosystem II, favouring the appearance of reactive oxygen species (ROS) and the onset of oxidative stress. The strong increase in proline content was concordant with the fact that ammonium plants were subjected to a severe stress under ambient CO_2 conditions. Enhanced proline contents in leaves may reduce the damaging effects of ROS produced by an inadequate electron flow between both photosystems, thus protecting cell homeostasis (Szabados and Savouré, 2009). Proline can act as osmolyte required for protecting proteins, membranes and the photosynthetic electron transport in the plant cell under certain abiotic stresses, such as temperature stress or osmotic stress (Szabados and Savouré, 2009). The synthesis of proline is mainly derived from glutamate, however under stress conditions, the degradation of transitory starch in maltose with would be connected with the biosynthesis of proline (Zanella *et al.*, 2016). In this sense, the high contents of maltose observed in ammonium fertilised plants could be linked with its role in supporting the biosynthesis of proline (Baslam *et al.*, 2017). Besides, wheat leaves are able to derive part of carbohydrates to increase the ammonium assimilation into other amino acids, as Asn+Ser, Gln+His.

The fact that ammonium-fertilised plants showed lower evapotranspiration rates, than nitrate-fertilised plants, might be explained by the drastic stomata closured, but also over absorption and translocation of ammonium. Aquaporins (AQP) that coordinates the plant–water relations at all levels of organization also are implicated in the transport of other molecules, such as ammonium (Coskun *et al.*, 2013; Bittsánszky *et al.*, 2015; Esteban *et al.*, 2016) or CO_2 (Flexas *et al.*, 2006; Maurel *et al.*, 2008). In this context, other functions are attributable to AQP members that facilitate CO_2 transport, affecting directly over photosynthesis and stomatal opening. The higher expression values detected in PIP 1.1 and 2.3 of ammonium treated plants at ambient CO_2, would reflect the necessity to overcome potential limitations on chloroplast CO_2 availability associated with the stomatal and mesophyll conductance (Flexas *et al.*, 2006).

Interestingly, contrasting with the stomata closure under exposure to elevated CO_2 observed for nitrate-fertilised wheat plants, elevated CO_2 induces the opening of stomata at elevated CO_2. The enhancement of ammonium tolerance has been reported under different changing condition such as high irradiance (Setién *et al.*, 2013), higher external pH in the growth medium (Sarasketa *et al.*, 2016), increasing atmospheric CO_2 (Rubio-Asensio *et al.*, 2015; Vega-Mas *et al.*, 2017) or fertilising with a mixed ammonium nitrate-nutrition (Zaghdoud *et al.*, 2016). This is apparently the case for ammonium-fertilized plants growing under elevated CO_2. The exposition to non-limiting C atmosphere would ameliorate the oxidative stress derived from ammonium toxicity, since plants do not present photoinhibition, as they show similar Fv/Fm to nitrate-fed plants. The recovery of a high electron transport rates and low proline contents would discard the appearance of stress oxidative conditions. Thus, due to the higher electron transport efficiency we would have expected an improvement of maximum carboxylation velocity of Rubisco under elevated CO_2 condition, but no stimulation of CO_2 assimilation took place, and consequently the biomass growth remained low. Besides, higher flux of carbon skeletons would be destined via Krebs cycle (Setién *et al.*, 2013) in order to maintain ammonium assimilation. Due to the higher ammonium assimilation rates, C was accumulated in form of proteins and not as carbohydrates (sucrose or starch).

Under normal conditions, the commonly described incorporation of ammonium into amino acids via GS and GOGAT activities provides glutamine and glutamate, respectively. In addition, an alternative pathway to reduce ammonium excess is the aminanting GDH activity, which catalyses the amination of α-ketoglutarate into glutamate (Setién *et al.*, 2013; Vega-Mas *et al.*, 2015). The photoinhibition and the lower electron transport efficiency observed for ammonium-fed plants when they grow under ambient CO_2 indicates that these plants were not able to balance C and N assimilation. However, the disappearance of oxidative stress observed at elevated CO_2 conditions would stimulate a higher ammonium detoxification. The increased GS and GDH activities would be contributing to assimilate ammonium levels finally in form of proteins, at the same time no excess free amino acids were detected. In addition, the absence of significant differences on AQPs and N-transporter expressions would remark that in absence of a stressing context, ammonium fertilized plants grown at elevated CO_2 conditions did not require an adjustment of CO_2 and H_2O diffusion.

Ammonium toxicity can be modulated by different environmental conditions such as CO_2, nitrate supplementation or pH regulation (Britto and Kronzucker, 2002; Vega-Mas *et al.*, 2015, 2017; Esteban *et al.*, 2016; Sarasketa *et al.*, 2016) . The presence of reduced forms of nitrogen limits the nitrate uptake by the plant, because of the decreased requirements of reductant equivalents for primary nitrogen assimilation and thus, photosynthesis does not suffer energetic-limitations (Hachiya and Sakakibara, 2017). In the case of ammonium nitrate nutrition interesting differences were observed: regarding photochemical, gas exchange parameters and metabolism, they were more similar to ammonium-fed plants, especially at ambient CO_2. Under these CO_2 conditions, photosynthetic parameters and the electron transport flux followed the same pattern, reaching intermediate values, a bit higher than in ammonium-fed plants but lower than in nitrate-fed plants. Thus, ammonium nitrate-fed plants are more effective in the efficiency of carboxylation, since they shows high Vc_{max}. Indeed, ammonium nitrate-fed plants showed similar growth pattern than under nitrate, even having lower photosynthesis. However, under non-limiting C availability at elevated CO_2, ammonium nitrate-fed plants are able to equalise their photosynthetic parameters to respond as nitrate-fed plants. Under these conditions, ammonium nitrate-fed plants presented a high electron transport rates recovery that permitted increase photosynthetic parameters. Moreover, the coexistence of ammonium together with nitrate permitted adapt C/N metabolisms in wheat plants. Despite a decrease in carbonic anhydrase expression is often described in plants exposed to elevated CO_2 (Fukayama *et al.*, 2011; Vicente *et al.*, 2015), our data suggest that the overexpression of carbonic anhydrase genes together with the maintenance of nitrate transporters in ammonium nitrate-fertilised plants grown under elevated CO_2 allowed increasing the photosynthetic assimilation and the nitrate uptake. These plants stimulated the synthesis of starch, at expense of sucrose and others monosaccharides (fructose-6-phosphate and glucose-6-phosphate), but the higher demand of carbohydrates prevented the starch accumulation in flag leaves. The results suggest that mixed ammonium nitrate nutrition could prevent photosynthetic acclimation in plants (Stitt *et al.*, 2010) in comparison to nitrate nutrition, making a more efficient use of carbohydrates and nitrogen in shoot biomass.

Ammonium nitrate-fed plants showed similar photochemical response than ammonium-plants. In this sense, both ammonium- and ammonium nitrate-nutrition reduced the efficiency in electron transport, but only under ammonium-nutrition were observed stress symptoms. Both ammonium- and ammonium nitrate-nutrition presented higher photorespiratory rates under elevated CO_2 conditions. The higher C and N assimilation provide with more amino acids as alanine that permitted to enhance photorespiration. This was consistent with the fact that these plants did not increase carboxilatory activity under elevated CO_2 despite larger C availability. Furthermore, high photorespiratory rates detected in ammonium- and ammonium nitrate-fed plants would be related with an energy dissipation strategy in order to reduce oxidative stresses. Ammonium nitrate-fed plant presented similar growth parameters than nitrate-fed plants despite they showed lower C assimilation by photosynthesis. In addition, ammonium nitrate-fed plants grown under elevated CO_2 conditions were able to increase CO_2 assimilation while no starch accumulation was detected in photosynthetic tissues, which suggests that these plants had a better nutrient utilisation for synthetize amino acids and proteins. Moreover, the fact that did not show ammonium toxicity and permitted to those plants had a growth parameters similar than nitrate-fed plants.

5

C/N metabolism in leaves and last stem internodes modulates the responsiveness of barley to changing CO_2 conditions

Under revision in Journal of Experimental Botany

5.1. Introduction

Atmospheric carbon dioxide (CO_2) has increased from around 280 ppm recorded at the beginning of the Industrial Revolution (1780) to approximately 400 ppm at present, and depending on the climate change emissions scenario, is expected to increase to over 900 ppm by the end of the 21st century (IPCC, 2014). While it would be logical to assume an enhanced photosynthetic assimilation in C_3 plants due to the increase in Rubisco´s substrate, CO_2, several studies have shown that leaf carbohydrate build-up linked to higher CO_2 availability might induce a reduction in carboxylation efficiency (Ainsworth *et al.*, 2006; Bloom *et al.*, 2010; Aranjuelo *et al.*, 2015). Processes that induce stomatal closure with a consequent impact on CO_2 diffusion into the chloroplast would partly explain the diminishment of photosynthetic carboxylation capacity derived from exposure to elevated CO_2 (Xu *et al.*, 2016). Regarding the non-stomatal processes involved in photosynthetic down-regulation, previous studies have shown that this phenomenon is accompanied by a reduction in Rubisco activity and content (Pérez *et al.*, 2005; Córdoba *et al.*, 2017). Enhanced leaf C content caused by greater photosynthetic rates in plants exposed to elevated CO_2 could lead to repression of photosynthetic related genes and for a down-regulation of photosynthetic capacity (Ainsworth *et al.*, 2004; Aranjuelo *et al.*, 2009, 2011). The leaf carbohydrate build-up has been associated with a high/low capacity to develop strong C sinks, such as developing organs (Lewis *et al.*, 2002; Aranjuelo *et al.*, 2013*b*). Therefore, higher C sink strength could contribute to preventing photosynthetic down-regulation via a better redistribution and allocation of carbohydrates from leaves to sinks under elevated CO_2 conditions (Ainsworth *et al.*, 2004; Aranjuelo *et al.*, 2013*b*). Indeed, plants with higher capacity to remobilise the "extra" photoassimilates to organs with a higher demand for C could overcome the photosynthetic down-regulation that would result from exposure to elevated CO_2.

Nitrogen (N) assimilation limitations have also been identified as being central to photosynthetic performance under elevated CO_2. Photosynthesis provides C skeletons for assimilating N into amino acids to form proteins and other nitrogenous compounds. An imbalance between C fixation and N assimilation has been claimed as being responsible for photosynthetic down-regulation under elevated CO_2 (Ainsworth and Long, 2005; Bloom *et al.*, 2010). Moreover, limitations to N reduction and assimilation observed in plants grown under elevated CO_2 have been associated with a reduction in energy availability in such plants, which would have effects on C and N assimilation (Rachmilevitch *et al.*, 2004; Bloom *et al.*, 2010; Aranjuelo *et al.*, 2013*b*). Under this context of energy availability limitations, prolonged exposure to elevated CO_2 would modify the C/N ratio by increasing the carbohydrate content and decreasing the N pool due to competition for reductant (Rachmilevitch *et al.*, 2004; Bloom *et al.*, 2010).

The assimilation and remobilization of C compounds during grain filling condition the development of grains. Photoassimilates required to sustain grain filling are mainly provided by flag leaf photosynthesis (Evans, 1983), remobilization of C stored in leaves and stem internodes assimilated before anthesis (Gebbing and Schnyder, 1999) and ear photosynthesis (Tambussi *et al.*, 2007; Zhou *et al.*, 2016). Sucrose, fructans and starch, among others, are target carbohydrates that condition crop performance during the grain-filling period in barley. Sucrose is the major carbohydrate transport form that provides most of the energy and C necessary for the growth and development of non-photosynthetic organs. Together with starch, fructans have been described as the major C storage compounds in different cereal organs such as the grains, leaves, stems and roots (Morcuende *et al.*, 2004). In addition to their role as reserve carbohydrates, fructans also provide C and energy to non-photosynthetic tissues (Xue *et al.*, 2011; Van den Ende, 2013). Moreover, carbohydrates can also act as signal molecules regulating the expression of a wide variety of genes involved in different metabolic pathways and cellular functions (Osuna *et al.*, 2007; Van den Ende, 2013; Valluru, 2015). Fructan synthesis is regulated by the sucrose content, being necessary that sucrose overpass a threshold concentration (Pollock and Cairns, 1991; Koroleva *et al.*, 1998). In addition, the sucrose concentration increases fructosyltransferases gene expression, whereas nitrate inhibits the content of this protein (Morcuende *et al.*, 2004). Indeed, a close correlation between carbohydrate content and expression of carbon metabolism related genes has been reported recently (Vicente *et al.*, 2018).

Searching for more productive varieties, conventional plant-breeding programs have reduced the genetic diversity of crops by the use of elite crop varieties that have lost specific alleles relevant to specific environmental conditions (Ellis *et al.*, 2000; Dawson *et al.*, 2015). This searching of elite varieties has resulting in some sink-source limitations in comparison with ancient cultivars (Maydup *et al.*, 2012; Serrago *et al.*, 2013). To recover some of the favourable alleles lost during plant-breeding programs, Matus *et al.* (2003) developed a recombinant chromosome substitution line (RCSL) population of 140 lines using the wild ancestor of barley (*Hordeum vulgare* subsp. *spontaneum*) as a source of genes for Harrington (*Hordeum vulgare* subsp. *vulgare* 'Harrington'), which is commonly used as a malting quality standard in North America. The recovered genes in the barley line RCSL-89 showed higher tolerance to abiotic stress by accumulating more carbohydrates under drought conditions (Méndez *et al.*, 2011).

In order to adapt crop to future atmospheric condtions, a further understanding of the factors contributing to increases in C sinks will enable adjustment of leaf carbohydrate demand under elevated CO_2. In this work we performed two approaches with the purpose of evaluate the importance of C sink-source balance in the responsiveness of plants to different CO_2 conditions. The first goal was to determine the relevance of plant C sink-source balance in barley responsiveness to elevated CO_2. For that, barley cultivars with high (RCLS-89) and low (cv. *Harrington*) capacity to store C/N compounds in the internodes were exposed to elevated CO_2 for 11 weeks. Secondly, plants growing for 5 weeks under ambient CO_2 conditions (400 ppm) were exposed to elevated CO_2 for the following 6 weeks at the ear emergence growth stage, and *vice versa*, plants growing for 5 weeks under elevated CO_2 (700 ppm) were exposed to ambient CO_2 (400 ppm). The current experiments enabled us to identify mechanisms developed by plants to adapt their C sink/source balance under changing CO_2.

5.2. Materials and Methods

Plant material and experimental design

Seeds of both barley plants, *Harrington* and RCLS-89, were stored at 4°C for 10 days to synchronize germination. Once germinated, 64 plants were grown in 32 pots filled with a mixture of vermiculite:perlite (2:1; v:v). Plants were grown in two controlled environment chambers (Phytotron Service, SGIker, UPV/EHU). The environmental conditions inside the chambers were 550 µmol m^{-2} s^{-1} photosynthetic photon flux density (PPFD); 14-light/10h-darkness photoperiod; 25/17 °C and 50/60% relative humidity, respectively. Barley plants were watered twice a week with Hoagland´s solution (Arnon and Hoagland, 1940) and once a week with deionized water to avoid salt accumulation. The experimental set up was designed as two sub-experiments in parallel. For the first goal barley plants were grown at different atmospheric CO_2 (400 *vs.* 700 ppm) and environmental conditions as described above for 11 weeks. The second goal was to characterize the plasticity of plants exposed to changing environmental CO_2 to explore the adaptive mechanisms performed by plants for balancing the sink-source. For that, in the second experiment a set of 32 plants that were grown for 5 weeks at ambient CO_2 were exposed during the following 6 weeks to elevated CO_2 conditions (400-700), and vice versa, plants that were grown elevated CO_2 were exposed to ambient CO_2 conditions (700-400). In parallel, reference plants were kept growing continuously at 400 and 700 ppm CO_2 during the 11 weeks.

Biomass and gas exchange determinations

At the end of the experiment on week 11, plant sampling and gas exchange determinations were done between 2 and 4 hours after onset the photoperiod. Gas-exchange parameters were measured in the flag leaf. The net photosynthetic rate (A_N) was measured at 500 µmol m^{-2} s^{-1} PPFD with a LI-COR

6400-XT portable gas exchange system (LI-COR Inc., Lincoln, NE, USA). Simultaneously, the stomatal conductance (g_s) and intercellular CO_2 (Ci) were obtained. The curves of net CO_2 assimilation rate (An) versus intercellular CO_2 concentration (Ci) (*A–Ci*) were recorded under saturated light conditions (1000 µmol m^{-2} s^{-1} PPFD). In order to estimate the maximum carboxylation velocity of Rubisco (Vc_{max}), the CO_2 concentration was decreased in three steps from 400 to 100 ppm CO_2, followed by an increase from 400 to 1800 ppm CO_2 in five steps. For the estimation of the maximum carboxylation velocity of Rubisco (Vc_{max}) we used the equation developed by Sharkey *et al.* (2007).

After measuring photosynthesis in flag leaves, plant material was harvested for biochemical analysis. Flag leaves and last stem internodes of four plants for each treatment were immediately plunged into liquid nitrogen and stored at -80 °C until further analysis. For biomass determination, four plants per treatment were dried in an oven at 80 °C for 72 h. Harvest index (HI) was calculated by the equation: HI = Ear Biomass / Total biomass.

Carbon and nitrogen content

Flag leaves and last stem internodes dried at 80 °C for 72 h were ground for carbon and nitrogen content (%) determination. For each sample, 1 mg of dry material in small tin capsules was analysed using a Flash 1112 Elemental Analyzer (Carbo Erba, Milan).

Metabolite determinations

Frozen flag leaf and last stem internode plant material was used for ethanol/water extraction for carbohydrate determination according to Morcuende *et al.* (2004). Sucrose, starch and fructan contents were subsequently determined spectrophotometrically following the protocol described by Morcuende *et al.* (2004). In the flag leaf, total amino acids were determined by the ninhydrin method (Hare and Cress, 1997), ammonium quantification was carried out with the Berthelot method (Patton and Crouch, 1977) based on the phenol hypochlorite assay, and nitrate quantification was done according to nitration of salicylic acid as described by Cataldo *et al.* (1974).

Soluble Protein extraction and Rubisco quantification

Protein extraction from flag leaves was carried out according to Sarasketa *et al.* (2014). Total soluble proteins were quantified spectrophotometrically using the Bradford dye-binding assay (Bio-Rad, Hercules, CA, USA) with BSA as standard for the calibration curve. For relative Rubisco content (%) determination, protein extracts were denatured at 95 °C for 5 min after adding one volume of loading buffer (Laemmli, 1970). Ten µg of denatured proteins were separated by a sodium dodecyl sulfate–polyacrylamide gel electrophoresis (SDS-PAGE) system using a 1.5 mm thick gel (10% separating, 4.6% stacking). Electrophoresis was carried out in a vertical electrophoresis cell (Mini-Protean III; Bio-Rad) at room temperature and at a constant current of 120 V for 2 hours. The gels were stained with 1% Coomassie blue solution for 1 h and subsequently destained, washing 4 times in water:methanol:acetic acid (4:4:2, v:v:v) for 20 min. Finally, the gels were scanned and the densitometry of the Rubisco subunit band was estimated using Image J software.

N assimilation enzyme activities

Maximum nitrate reductase (NR) activity was determined as described by Baki *et al.* (2000). The reaction was incubated for 30 min at 30 °C after the addition of 50 µl of protein extract to 250 µl of reaction buffer. Afterwards the reaction was stopped by adding 0.5 M zinc acetate and was centrifuged at 4000 g for 30 min at 4 °C. For nitrite detection, 1% sulfanilamide in 3 M HCl and 0.02% N-naphthyl-ethylenediamine hydrochloride (NEDA) were added and the reaction formed was measured colorimetrically at 540 nm and using KNO_2 as the standard for the calibration curve. Glutamine synthetase (GS) activity was determined by incubating 50 µl of protein extract for 30 min at 30 °C with 100 µl reaction buffer (Vega-Mas *et al.*, 2015). The reaction was stopped by adding 150 µl of 0.122 M $FeCl_3$, 0.5 M TCA and 2 N HCl. Then, samples were centrifuged at 2000 g for 5 min and the absorbance of ɣ-glutamylmonohydroxamate (ɣ-GHM) in the supernatant was measured at 540 nm using ɣ-GHM as the standard for the calibration curve. Glutamate dehydrogenase (GDH) and glutamate synthase (GOGAT) activities were determined as described in Vega-Mas *et al.* (2015). Initial kinetics of changes in the NADH concentration were monitored by absorbance at 340 nm in a reaction consisting of 20 µl protein extract and 280 µl of reaction buffer NADH-dependent GDH or NADH-dependent GOGAT, respectively.

RNA extraction and synthesis of *cDNA*

RNA was isolated from pulverized frozen flag leaves using the phenol:chloroform method described by Morcuende *et al.* (1998). Ten µg of RNA for each sample were treated with DNase Turbo (Ambion) according to the manufacturer´s instructions. RNA integrity was checked on a 1.5% (v/v) agarose gel and the absence of genomic DNA contamination was confirmed by PCR using a primer pair for the gene encoding glyceraldehyde-3-phosphate dehydrogenase (GenBank ID: EF409633) designed to amplify exon-intron-exon sequence with a product size of 120 bases for RNA and 360 bases for genomic DNA. cDNA was synthesized using SuperScript III reverse transcriptase (Invitrogen GmbH) according to the manufacturer´s instructions.

Quantitative real-time PCR

Gene expression was measured as described in Vicente *et al.* (2015). Quantitative PCR was performed in an optical 384-well plate with an ABI PRISM 7900 HT Sequence Detection System (Applied Biosystems) in a 10 µl reaction volume using the SYBR Green Maxter Mix reagent (Applied Biosystems), 1 µl of diluted cDNA (1:40) and 200 nM of each-gene specific primer. The PCR thermal profile was as follows: polymerase activation (50°C for 2 min, 95°C for 10 min) amplification and quantification cycles repeated 40 cycles (95°C for 15 s and 60°C for 1 min) and a final step of 95°C for 15 s and 60°C for 15 s to obtain the dissociation curve. Three biological replicates were used for quantification analysis with two technical replicates for each biological sample.

Transcript levels for genes associated with photosynthesis, carbohydrate metabolism and nitrogen assimilation in flag leaves were determined using the primers described in Méndez (2014) and Córdoba *et al.* (2016) (Table S1). The data was presented as the log_2-fold change after the quantification of the relative gene expression using the comparative C_t method $2^{-\Delta\Delta Ct}$ (Schmittgen and Livak, 2008), and using the actin gene as a reference gene for normalizing gene expression results (Córdoba *et al.*, 2016).

Statistical analysis

Data were analysed using IBM SPSS statistic 22 software (Armonk, NY, USA). Normality and homogeneity of variance were analysed by Kolmogorov-Smirnov and Levene tests. Analysis of significant differences for the effect of CO_2 on both barley cultivars was analysed by one-way ANOVA with a Duncan post-hoc test. Differences between both cultivars in the same CO_2 condition were analysed by a t-test. For both analyses, differences were considered significant at $p<0.05$.

5.3. Results

Experiment 1: Evaluation of the relevance of plant C sink-source balance in response to elevated CO_2

Exposure to elevated CO_2 did not alter the total biomass in either barley cultivar, but increased the HI as a consequence of the higher ear biomass (Table 1). The net photosynthetic rate (A_N) with respect to 400 ppm CO_2 was not increased in Harrington plants exposed to elevated CO_2 (Figure 1A), but the Vc_{max} activity was decreased respect to 400 ppm CO_2 (Figure 1B). Harrington plants showed a similar stomatal conductance under both CO_2 conditions (Figure 1C). In RCSL-89 plants exposed to elevated CO_2, the Vc_{max} activity was higher than those grown at 400 ppm CO_2 (Figure 1B, C). Therefore, the A_N was increased in RCSL-89 plants under elevated CO_2 conditions (Figure 1A). Comparing both barley Harrington and RCSL-89 plants, the results indicated that despite there was no difference in the internal CO_2 (Ci) of Harrington leaves relative to RCSL-89, the lower Vc_{max} of Rubisco observed at 700 ppm indicates that elevated CO_2 induced the down-regulation of its activity (Figure 1B, D).

Table 1. Total biomass, ear biomass and harvest index of Harrington and RCSL-89 barley cultivars. Growth conditions were 400 ppm, 700 ppm, 400-700 (from 400 to 700 ppm) and 700-400 (from 700 to 400 ppm) CO_2. Significant differences ($p<0.05$) between each CO_2 condition are indicated with different letters. Asterisk (*) indicates significant cultivar differences ($p<0.05$). Values represent mean ± SEM (n=4).

		Total Biomass (g)				Ear (g)				Harvest Index			
Harrington	400	12.88	±	1.38	a	2.18	±	0.40	b*	0.17	±	0.02	b*
	700	13.15	±	1.76	a	3.77	±	0.36	a	0.33	±	0.03	a
	400-700	9.68	±	0.81	ab*	2.09	±	0.27	b	0.22	±	0.02	b
	700-400	8.52	±	0.53	b	1.98	±	0.32	b*	0.23	±	0.04	b
RCLS-89	400	11.40	±	1.07	A	1.05	±	0.13	C*	0.10	±	0.01	C*
	700	14.48	±	1.39	A	4.59	±	0.19	A	0.30	±	0.02	A
	400-700	12.72	±	1.24	A*	2.73	±	0.21	B	0.22	±	0.02	B
	700-400	13.62	±	1.23	A	3.81	±	0.36	B*	0.25	±	0.03	AB

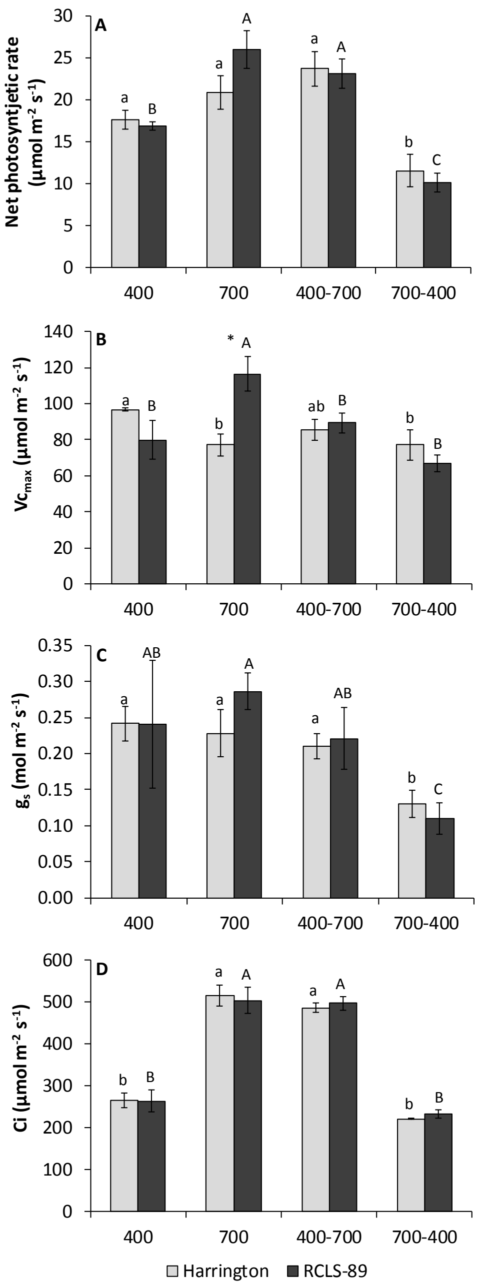

Figure 1. Effect of CO_2 on flag leaf gas exchange and photosynthesis parameters. **A**, net photosynthetic rate; **B**, maximum velocity of RuBP carboxylation by Rubisco (Vc_{max}); **C**, stomatal conductance (g_s) and **D**, intercellular CO_2 mole fraction (Ci) of Harrington (grey bars) and RCSL-89 (black bars) barley plants. Growth conditions were 400 ppm), 700 ppm, 400-700 (from 400 to 700 ppm) and 700-400 (from 700 to 400 ppm) CO_2. Significant differences (p<0.05) between each CO_2 condition are indicated with different letters. Asterisk (*) indicates significant cultivar differences (p<0.05). Values represent mean ± SEM (n=4).

In order to determine the photo-assimilates and their mobilisation to sink organs, the sucrose, starch and fructan contents were determined in flag leaves and the last stem internodes of both barley cultivars (Figure 2). Flag leaves of Harrington plants grown under elevated CO_2 showed lower sucrose levels (Figure 2A) and maintained starch and fructan contents (Figure 2C, E). Elevated CO_2 did not significantly alter the sucrose and starch contents in the flag leaves and last stem internodes of RCSL-89 plants (Figure 2A-D), but decreased the fructan contents in the flag leaves (Figure 2E). However, the fructan contents of the last stem internodes in RCSL-89 were not significantly changed compared to plants grown at 400 ppm CO_2 (Figure 2F).

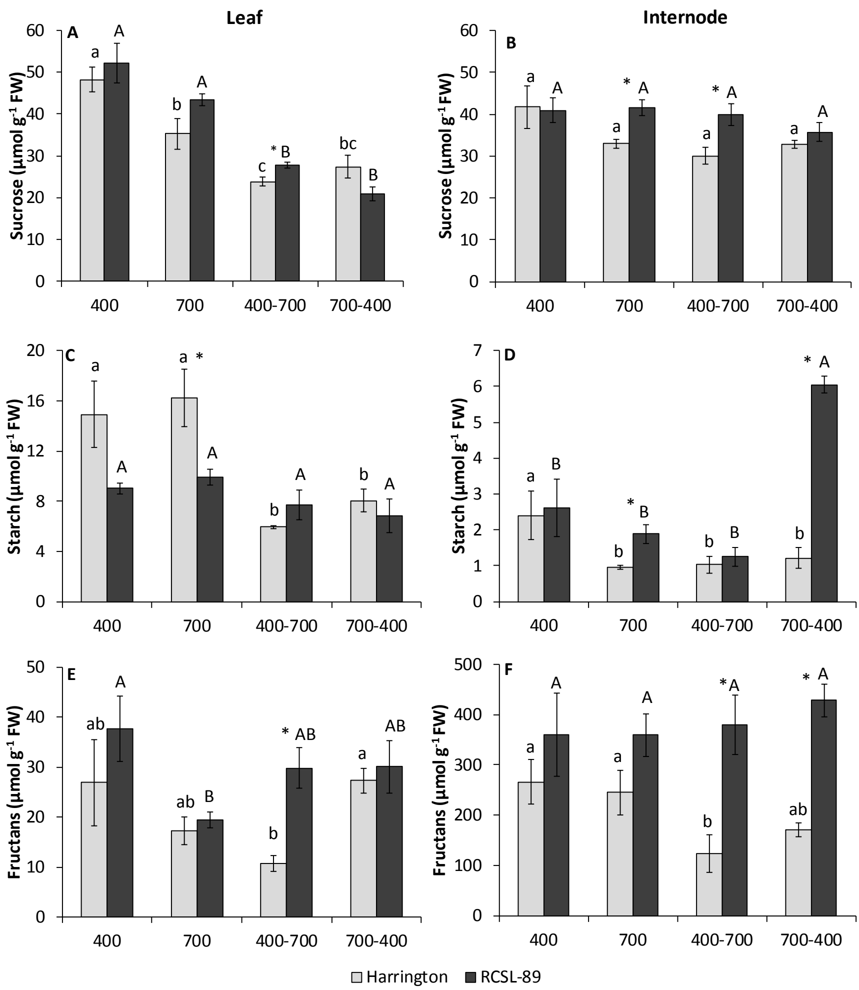

Figure 2. Effect of CO_2 in carbohydrates content in the flag leaf and last stem internode. A-B, sucrose; **C-D**, starch and **E-F** fructans of Harrington (grey bars) and RCSL-89 (black bars) barley plants. Growth conditions and significant differences are described in Figure 1.

The C and N (%) contents in the flag leaves and internodes of the two barley cultivars were not affected by the CO_2 conditions (Table 2). Interestingly, the leaf C/N ratio was higher in RCSL-89 under elevated CO_2 (13.82), this value being similar to the Harrington leaves (14.91). The nitrogen available for protein synthesis was quantified by the analysis of N forms (NO_3^- and NH_4^+), amino acids and protein content in leaves (Figure 3). Although elevated CO_2 did not reduce the amount of NO_3^- in leaves of both cultivars, the NH_4^+ content was lower in both cultivars grown under elevated CO_2 (Figure 3A-B). Interestingly, the amino acid content and relative Rubisco content in Harrington was also lower compared to 400 ppm CO_2, but no differences were observed in RCSL-89 (Figure 3C, E). In addition, elevated CO_2 increased the foliar soluble protein content in RCSL-89 but not in Harrington (Figure 3D).

Table 2. N and C content in flag leaf and last stem internode of barley Harrington and RCLS-89 cultivars grown under different CO_2. Growth conditions and significant differences indications are described in Table 1.

		Leaf N (%)	Leaf C (%)	Internode N (%)	Internode C (%)
Harrington	400	3.47 ± 0.26 a	45.19 ± 0.16 a	1.37 ± 0.99 a	42.36 ± 0.23 a*
	700	3.00 ± 0.14 a	44.57 ± 0.24 a	0.95 ± 0.67 ab	42.39 ± 0.35 a*
	400-700	3.16 ± 0.49 a	43.47 ± 0.36 b	0.90 ± 2.49 b	44.60 ± 2.03 a
	700-400	3.14 ± 0.25 a	44.46 ± 0.36 a	1.17 ± 1.33 ab	41.53 ± 0.10 a*
RCLS-89	400	4.08 ± 0.47 A	45.22 ± 0.71 A	1.34 ± 0.22 A	43.34 ± 0.05 A*
	700	3.25 ± 0.12 AB	44.93 ± 0.29 A	1.01 ± 0.11 A	43.52 ± 0.07 A*
	400-700	4.08 ± 0.09 A	43.53 ± 0.16 B	1.36 ± 0.20 A	42.95 ± 0.31 A
	700-400	3.00 ± 0.20 B	43.23 ± 0.31 B	1.46 ± 0.30 A	42.79 ± 0.51 A*

Determinations of N assimilation enzyme activities revealed that the exposure to elevated CO_2 did not significantly affect the NR and GOGAT activities in either of the barley cultivars (Figure 4A, C). Moreover, exposure to elevated CO_2 decreased GS and GDH activities in Harrington but not in RCSL-89, which maintained similar activities to plants grown at 400 ppm CO_2 (Figure 4B, D).

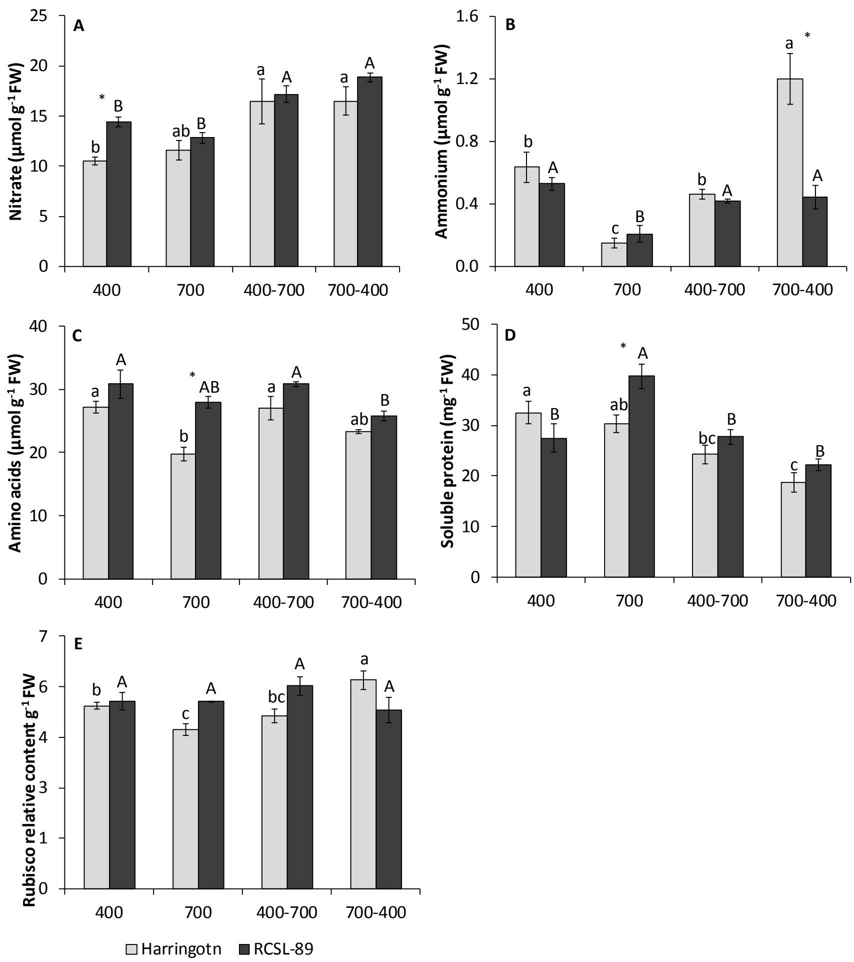

Figure. 3. Effect of CO_2 on N forms (nitrate and ammonium), amino acids and soluble proteins of flag leaves. **A**, nitrate; **B**, ammonium; **C**, amino acids; **D**, Soluble protein and **D**, Rubisco relative content of Harrington (grey bars) and RCSL-89 (black bars) barley plants. Growth conditions and significant differences are described in Figure 1.

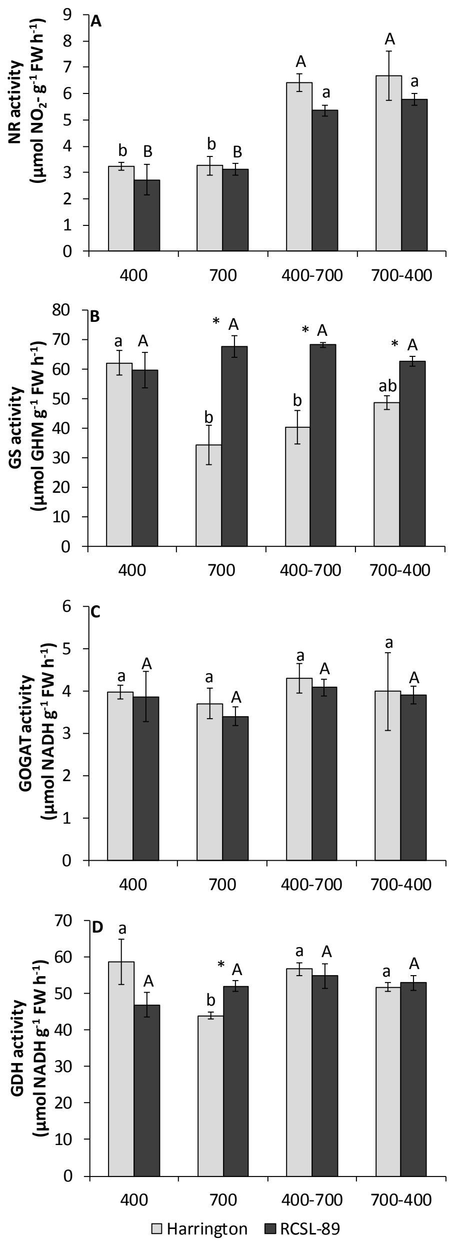

Figure. 4. Effect of CO_2 on flag leaf N enzyme activities. A, nitrate reductase; **B**, glutamine synthetase **C**, glutamate dehydrogenase and **D**, glutamate synthase of Harrington (grey bars) and RCSL-89 (black bars) barley plants. Growth conditions and significant differences are described in Figure 1.

Finally, evaluation of the abundance of transcripts for genes linked to photosynthesis and carbohydrate and nitrogen metabolism (Table 3) showed that elevated CO_2 decreased the transcripts for photosynthetic proteins, including photosystem II light-harvesting chlorophyll a/b binding protein and Rubisco large subunit in both cultivars, but it did not affect the transcripts for photosystem I related-genes. Exposure to elevated CO_2 also decreased significantly the transcripts for the Rubisco small subunit in RCSL-89 but not in Harrington. Moreover, elevated CO_2 decreased the expression of fructan related-genes 1-SST and 1-FFT in Harrington plants, while these were not changed in RCSL-89. Following the lack of changes in NR activity (Figure 4), the gene expression for NR was not altered by elevated CO_2, regardless of the barley cultivar.

Table 3. Heat map of transcript abundance in leaves of barley cultivars Harrington and RCLS-89 cultivars grown under different CO_2. Growth conditions and significant differences indications are described in Table 1.

Acc. No.	Description	400	700	400-700	700-400	*P*
Harrington						
AK356022	Photosystem II light harvesting chlorophyll a/b binding protein	b	c	a	bc	**0.003**
AK361860	Photosystem II light harvesting chlorophyll a/b binding protein	a	b	a	b	**0.009**
AK365564	Photosystem II subunit R	c	b	a	d	**<0.001**
AK360942	Oxygen evolving enhancer protein 3, PsbQ	a	a	a	a	0.055
AK252670	Photosystem II reaction center, PsbP	a	a	a	a	0.757
KC912689	Photosystem I P700 apoprotein A1, PsaA	ab	a	a	b	**0.029**
AGP50910	Photosystem I P700 apoprotein A2	a	a	a	a	0.151
X15869	Protochlorophyllide oxidoreductase, POR	b	b	a	b	**0.004**
AGP50919	Rubisco large subunit, RbcL	a	b	a	b	**0.022**
U43493	Rubisco small subunit, RbcS	a	a	a	a	0.13
AK366020	Sucrose:sucrose 1-fructosyltransferase, 1-SST	a	b	b	b	**0.004**
X83233	Sucrose:fructan 6-fructosyltransferase, 6-SFT	a	a	a	a	0.101
JQ411253	Fructan:fructan 1-fructosyltransferase, 1-FFT	a	b	b	b	**0.011**
AJ605333	Fructan 1-exohydrolase, 1-FEH	a	a	a	b	**0.012**
AK357958	Fructan 6-exohydrolase, 6-FEH	a	a	a	b	**0.022**
AJ534444	Cell wall invertase, cwinv2	a	ab	b	c	**0.001**
AK359654	Structural constituent of cell wall	a	a	a	a	0.082
X57845	Nitrate reductase, NR	b	b	a	a	**0.013**
RCSL-89						
AK356022	Photosystem II light harvesting chlorophyll a/b binding protein	A	B	A	A	**0.015**
AK361860	Photosystem II light harvesting chlorophyll a/b binding protein	A	B	A	B	**<0.001**
AK365564	Photosystem II subunit R	B	C	A	C	**<0.001**
AK360942	Oxygen evolving enhancer protein 3, PsbQ	A	A	B	C	**<0.001**
AK252670	Photosystem II reaction center, PsbP	A	B	A	B	**0.003**
KC912689	Photosystem I P700 apoprotein A1, PsaA	A	A	A	B	**0.023**
AGP50910	Photosystem I P700 apoprotein A2	A	A	A	B	**0.018**
X15869	Protochlorophyllide oxidoreductase, POR	A	B	A	B	**0.002**
AGP50919	Rubisco large subunit, RbcL	A	B	AB	AB	**0.02**
U43493	Rubisco small subunit, RbcS	A	B	A	B	**<0.001**
AK366020	Sucrose:sucrose 1-fructosyltransferase, 1-SST	A	A	A	A	0.299
X83233	Sucrose:fructan 6-fructosyltransferase, 6-SFT	A	A	A	A	0.528
JQ411253	Fructan:fructan 1-fructosyltransferase, 1-FFT	A	A	AB	B	**0.034**
AJ605333	Fructan 1-exohydrolase, 1-FEH	A	A	B	B	**0.01**
AK357958	Fructan 6-exohydrolase, 6-FEH	A	A	A	B	**0.003**
AJ534444	Cell wall invertase, cwinv2	A	B	B	C	**0.002**
AK359654	Structural constituent of cell wall	A	A	A	A	0.115
X57845	Nitrate reductase, NR	B	B	A	A	**0.016**

Experiment 2: testing the mechanisms adopted by the plants in response to changing CO_2

The total biomass of Harrington plants decreased when the CO_2 was increased after initial growth at ambient CO_2 (400-700; Table1). However, the ear biomass and HI of Harrington plants were similar to plants adapted to grown continuously at 400 ppm CO_2. On the other hand, although the total biomass of RCSL-89 was not affected when the CO_2 increased (400-700; Table 1), the ear biomass of these plants was in between the biomass of 400 and 700 ppm-adapted plants, and a similar intermediate HI was observed (Table 1). The photosynthetic parameters of Harrington plants exposed to 400-700 ppm CO_2 were similar to those in 700 ppm-adapted plants, but the Vc_{max} was lower in RCSL-89 plants exposed to elevated CO_2 after growth at 400 ppm (400-700) than those grown at 700 ppm CO_2 (Figure 1A, B).

Increasing the CO_2 of the growth chamber for 6 weeks (400-700) reduced the sucrose content in leaves of both cultivars compared to those grown at 700 ppm CO_2 (Figure 2A). The starch content was decreased in Harrington leaves compared to those grown at 700 ppm CO_2 continuously (Figure 2C). The internode fructan contents were decreased in Harrington compared to 700 ppm-adapted plants (Figure 2F). In addition, RCSL-89 maintained higher fructan contents in leaves and internodes than Harrington (Figure 2E, 2F). Thus, the fructan contents showed substantial differences depending on the cultivar and tissue analysed. The increase in CO_2 (400-700) reduced C content in leaves of both barley cultivars with respect to plants that grown continuously at 700 ppm CO_2, but this did not occur in the last stem internode (Table 2). While Harrington leaves did not show substantial changes in N content when CO_2 increasing (400-700), the internode N content decreased (Table 2). Raising the CO_2 in the growth chamber from 400 to 700 increased the ammonium and amino acid contents in Harrington plants (Figure 3B-C), whereas, in RCSL-89 the nitrate and ammonium content increased (Figure 3A-B) and the protein content decreased relative to 700 ppm-adapted plants (Figure 3D). Regarding N-metabolism enzyme activities, both barley cultivars showed higher NR activity when the CO_2 increased from 400 to 700 ppm (Figure 4A). In addition, the increased CO2 (400-700) did not affect the GS and GOGAT activities, regardless of the studied cultivars, but increased the GDH activity in Harrington while the activity in RCSL-89 was unaltered (Figure 4B-D). The main differences in the transcriptional response to the increased CO_2 (400-700) over 6 weeks were that several photosynthetic genes were induced in both cultivars, such as photosystem II light-harvesting-related genes, the Rubisco large subunit and protochlorophyllide oxidoreductase, and most of them were induced more strongly in Harrington compared to 700 ppm-adapted plants (Table 3). The gene encoding NR was also induced in both cultivars, whereas the gene encoding fructan 1-exohydrolase was repressed in RCSL-89 plants (Table 3).

Considering the response of barley plants to the decrease from 700 to 400 ppm CO_2 over 6 weeks, Harrington plants showed lower biomass than 400 ppm-adapted plants. However, both ear biomass and HI were similar to the 400 ppm-adapted plants (Table 1). Decreasing the CO_2 of the growth chamber (700-400) during the 6 weeks did not significantly affect RCSL-89's total biomass. Nevertheless, these plants showed higher ear biomass and HI relative to 400 ppm-adapted plants (Table 1). In both cultivars, the reduction in CO_2 decreased the A_N by a strong stomatal closure (Figure 1A, C) compared to plants grown at 400 ppm CO_2. In addition, the Vc_{max} was significantly decreased in Harrington but not in RCSL-89 (Figure 1B).

Reducing the atmospheric CO_2 conditions (400-700) decreased sucrose content in the leaves of both cultivars compared to the references at 400 ppm CO_2 (Figure 2A), but did not significantly change the sucrose content in internodes (Figure 2B). The starch content in Harrington leaves and internodes was reduced, whereas the starch content in RCSL-89 leaves did not changed, but increased in the last stem internodes in comparison to 400 ppm-adapted plants (Figure 2C-D). Concerning fructan content, in both Harrington and RCSL-89 cultivars there were no significant differences relative to their references at 400 ppm CO_2 and regardless of the plant tissue (Figure 2E-F). Accordingly, with the decline in the A_N, the C (%) content was lower in leaves of both cultivars than in the 400 ppm-adapted plants (Table 2). Decreasing the CO_2 of the growth chamber (700-400) increased nitrate and ammonium contents but reduced protein content in Harrington (Figure 3A-B, D). However, in RCSL-89 there was increased nitrate content but decreased amino acid contents that did not affect the protein content relative to 400 ppm-adapted plants (Figure 3A, C-D). In the case of N assimilation enzyme activities, the reduction in CO_2 led to an increase in NR activity in both cultivars (Figure 4A) and this did not affect the rest of the studied enzyme activities (Figure 4B-D). Reducing the CO_2 of the growth chamber during the 6 weeks showed that, comparing both cultivars to plants that were grown continuously at 400 ppm CO_2, several genes that encode photosynthetic proteins as well as genes involved in fructan metabolism (1-FFT, 1-FEH and 6-FEH) and cell wall synthesis were repressed (Table 3). Similar to the increase in NR activity reported above, decreasing the CO_2 of the growth chamber also induced genes for NR.

5.4. Discussion

Sink-source balance has been postulated as being key to conditioning the responsiveness of photosynthetic capacity to increasing CO_2 (Ainsworth and Long, 2005; Aranjuelo *et al.*, 2011, 2013*b*). In the present study two approaches have been carried out to test the relevance of 1) internode capacity to accumulate carbohydrates and 2) the "plasticity" of leaf C/N metabolism following modification in growth CO_2 conditions.

Experiment 1: a higher internode C-storage capacity contributes to overcoming photosynthetic down-regulation under elevated CO_2

Carbon sink-source imbalance has been claimed as being responsible for the photosynthetic down-regulation frequently observed when plants are exposed to elevated CO_2 (Aranjuelo *et al.*, 2011, 2013*b*; White *et al.*, 2015). Indeed, an insufficient demand for carbohydrates from developing C-sinks has been observed to induce leaf C imbalances (White *et al.*, 2015). The last stem internode acquires a special importance in the C storage capacity for maintaining leaf C balance during the vegetative stage (Tambussi *et al.*, 2007). Later on during the grain filling period the C stored in the internode is remobilized towards the grain. Within this context, our study noted that in both barley cultivars, higher fructan contents were detected in internodes than in leaves showing the importance of these organs for the subsequent grain filling-stage.

Inadequate C sink strength can lead to a decrease in photosynthetic activity so that C source activity and sink capacity are balanced (White *et al.*, 2015). The data obtained also revealed that there was a differential response to the elevated CO_2 over the Vc_{max} and relative Rubisco content for each barley cultivar. Exposure to elevated CO_2 decreased the Vc_{max} and relative Rubisco content in Harrington, while RCSL-89 showed an increase in the Vc_{max}. The decline observed in Harrington is consistent with the photosynthetic down-regulation response widely studied under elevated CO_2 (Pérez *et al.*, 2005; Aranjuelo *et al.*, 2011, 2013*b*; Vicente *et al.*, 2015). In addition, the depletion in Rubisco content in these plants, alongside the decrease in amino acid and soluble protein contents, reduced the levels of leaf organic N compounds (Bloom *et al.*, 2002; Pérez *et al.*, 2005; Aranjuelo *et al.*, 2011; Vicente *et al.*, 2015). By contrast, elevated CO_2 led to an increase in the soluble protein content in RCSL-89. These results suggest an improvement in leaf organic N compounds that could help to maximize photosynthetic capacity in RCSL-89, which is consistent with the higher Vc_{max} observed under elevated CO_2. Moreover, the drastic increase in ear biomass under elevated CO_2 in RCSL-89 indicates that the strong sink capacity of this organ was especially important in the photosynthetic performance under elevated CO_2 (Ziska *et al.*, 2004). The distribution of photo-assimilates from leaves to the last stem internodes may have contributed to avoidance of carbohydrate build-up under elevated CO_2. Moreover, the experimental data suggested that the improved leaf C balance in RCSL-89 may have helped to maintain N status and consequently avoid photosynthetic down-regulation of elevated CO_2. On the other hand, in the case of Harrington, the down-regulation of genes encoding the Rubisco large subunit, together with the decreased transcripts for proteins involved in light harvesting and the lower Rubisco content under elevated CO_2 (Vicente *et al.*, 2015), may have contributed to the photosynthetic acclimation found in this barley cultivar. The fact that at 700 ppm CO_2 Harrington showed higher starch content than RCSL-89 may indicate that leaves of Harrington plants were subjected to C sink-source imbalance. It should be noted that starch has been proposed as a way to store the excess C in plants, while the leaf sucrose content is suggested to represent the main form of C translocated towards developing sinks (Stitt *et al.*, 2010). This data highlights the fact that impaired N assimilation, and consequently Rubisco protein availability, could be linked to the leaf C sink-source imbalance (Ainsworth *et al.*, 2004; Aranjuelo *et al.*, 2011, 2013*b*; White *et al.*, 2015).

In our study, NR activity was not significantly affected by elevated CO_2 in the flag leaves of either Harrington or RCSL-89 plants. These data suggest that CO_2 enrichment does not restrict leaf nitrate reduction, which is at variance with the decrease reported in other plant species (Bloom *et al.*, 2002, 2010; Vicente *et al.*, 2015). In addition, the higher sucrose content in RCSL-89 could contribute to the maintenance of NR expression and activity (Morcuende *et al.*, 1998) and to sustaining the GS activity (Robredo *et al.*, 2011), with the consequent impact on amino acid and protein availability under elevated CO_2. On the other hand, GS has been described as a target enzyme involved in N and C metabolism (Vega-Mas *et al.*, 2015). The decline in GS and GDH activities decreased the nitrate assimilation pathway in Harrington leaves and in turn altered amino acids and other organic N compounds under elevated CO_2. On the other hand, the maintenance of these activities observed in RCSL-89 leaves would guarantee assimilation of inorganic nitrogen into amino acids. Indeed, total soluble protein increased in RCSL-89 leaves under exposure to elevated CO_2. These findings suggest that a limitation in N assimilation could be involved in the decline in organic N compounds and the down-regulation of photosynthetic capacity found in Harrington plants under elevated CO_2. The improved photosynthetic acclimation responses to elevated CO_2 in the RCSL-89 cultivar were associated with an enhanced flag N assimilation and a consequent increase in organic N compounds. Moreover, the higher sink capacity of the last stem internode and the ears would have facilitated the leaf C/N balance and overcome the photosynthetic down-regulation due to elevated CO_2, confirming the importance of C sink strength for increased crop yields under elevated CO_2.

Experiment 2: a balance in C and N metabolism modulates adaptability to CO_2 conditions

As reported in the previous experiment, photosynthesis in plants grown under elevated CO_2 conditions is limited by the ability to adjust photosynthetic activity according to leaf C demand (Ziska *et al.*, 2004). To evaluate the adaptation capacity of both barley cultivars to changing environmental CO_2, plants were exposed to a different CO_2 after an initial adaptive environmental CO_2.

Increasing CO_2 conditions (400-700) caused a similar response in the A_N, g_s and C_i and relative Rubisco content in both barley cultivars with respect to 700 ppm-adapted plants. Harrington plants maintained their photosynthetic capacity compared to 700 ppm-adapted plants as shown by the similarity of the Vc_{max} to the 400 ppm-adapted plants, whereas no stimulation was detected in RCSL-89. The ability to overcome photosynthetic acclimation would be linked to the up-regulation of genes encoding proteins involved in light harvesting and the maintenance of Rubisco gene expression and protein content (Vicente *et al.*, 2015). According to that, our findings suggest that Harrington plants did not suffer photosynthetic down-regulation or, at least, that it showed a better photosynthetic capacity than RCSL-89 under such growth conditions.

In agreement with Stitt *et al.* (2010), the higher starch content detected in Harrington plants (compared to RCSL-89) could be considered as a symptom of C overflow generated when the rate of photosynthesis exceeds the rate of leaf C demand. This imbalance may be associated with the down-regulation of amino acid storage, in agreement with previous studies (Yamakawa and Hakata, 2010; Midorikawa *et al.*, 2014). Interestingly, the starch content did not differ in either cultivar after increasing the initial CO_2, but RCSL-89 showed higher storage-capacity of fructans in leaves and last stem internodes than Harrington cultivar.

In the second experiment, a late increase in CO_2 improved the NR activity in flag leaves of both Harrington and RCSL-89 plants with respect to 700 ppm-adapted plants. These data suggest that CO_2 enrichment does not restrict leaf nitrate reduction, which is at variance with the reduction in the N pool reported in other plant species grown under elevated CO_2 (Bloom *et al.*, 2002, 2010; Vicente *et al.*, 2015). More notably than in the first experiment, CO_2 enrichment induced the expression of nitrate reductase genes and nitrate content (Stitt and Krapp, 1999; Vicente *et al.*, 2016), while increasing the amino acid content and reducing the sucrose and starch contents relative to the 700 ppm-adapted plants. The competition for reductants in the chloroplast stroma has been described as a factor that conditions C and N assimilation (Rachmilevitch *et al.*, 2004; Vicente *et al.*, 2016). For this reason, the leaf light-harvesting complexes and proteins involved in electron transport may have special relevance in maintaining the energy necessary for balancing both N and C metabolism. In agreement with Vicente *et al*. (2017), we observed that the exposure to elevated CO_2 induced the expression of photosystem II light-harvesting complexes. In addition, more than 50% of the N that is assimilated by roots is allocated to leaves and comprises Rubisco, light-harvesting complexes and others proteins involved in electron transport (Kitaoka and Koike, 2004). Our results suggest that increasing CO_2 from 400 to 700 ppm caused concomitant increases in the A_N and nitrate content and reduction in carbohydrate content by increasing energy availability for coordinating C and N assimilation under elevated CO_2. These findings suggest that this stimulation in N assimilation could be involved in the increase in the amino acid content and the capacity to overcome the initial photosynthetic down-regulation found in Harrington under elevated CO_2.

Decreasing the CO_2 from 700 to 400 ppm (700-400) after ear emergence caused a severe stomatal closure that reduced the photosynthetic rates associated with the lower biomass of Harington plants. Stomatal limitations are, among others, responsible for the photosynthetic down-regulation that reduces the photosynthetic rates (Xu *et al.*, 2016). Bloom *et al*. (2002, 2010) reported that the reduction in A_N would increase nitrate assimilation because NR had access to a higher NADH available for reducing nitrate to nitrite. Moreover, the results reported here suggest that plants exposed to decreasing CO_2 suffered energy limitations due to a lower expression of light-harvesting complexes and reaction centres when compared to 400 ppm-adapted plants. The photosynthetic limitation of these plants was reflected by a decrease in the leaf carbohydrate content under these conditions. However, the last stem internodes of RCSL-89 plants showed a greater starch accumulation, which is associated with long-term carbohydrate storage. In concordance with the photosynthetic limitations, genes related to photosynthesis, such as light harvesting, Rubisco and chlorophyll synthesis, were down-regulated, or at least showed similar expression to 700 ppm-adapted plants. Comparing both Harrington and RCSL-89 plants, the higher fructan content in RCSL-89 internodes could be linked to the repression of fructosyltransferases (particularly sucrose:sucrose 1-fructosyltransferase), which are involved in the fructans synthesis. Moreover, the lower sucrose and starch-storage capacity in leaves, or their accumulation as fructans in internodes, revealed that the lower photosynthetic capacity decreased the modified C/N balance. In this sense, the lower biomass, and specially the ear weight, along with the lower amino acid and protein contents and the down-regulation of photosynthetic related-genes suggested that the plants attempted to adapt to the new environment.

Concluding remarks

In summary, our study highlighted the relevance of internode sink capacity in leaf C assimilation and balance, and their implications in photosynthesis and N assimilation in two barley cultivars exposed to elevated CO_2. The study showed that the larger internode carbohydrate storage capacity of RCSL-89 plants exposed to elevated CO_2, mainly in the form of fructans, allowed the carbohydrate levels to be balanced and consequently photosynthetic down-regulation was overcome due the capacity for maintaining Rubisco protein in leaves. On the other hand, when growth CO_2 was modified it was observed that expression of the light-harvesting complex and the CO_2 diffusion were significant to conditioning the responsiveness of plants to changing CO_2. In cases where CO_2 increased from 400 to 700 ppm, a diminishment in leaf carbohydrate content and an improvement in N assimilation was detected. Increased C/N was associated with the up-regulation of photosynthetic genes and N assimilation. On the other hand, when decreasing the CO_2 from 700 to 400 ppm our study revealed that both stomatal closure and the inhibited expression of light-harvesting proteins were major factors involved in the inhibition of photosynthetic machinery and crop development.

6

Exposure to elevated CO_2 delays the senescence and permits the extension of the vegetative stage and the later remobilisation of metabolites toward ears

6.1. Introduction

According to the Intergovernmental Panel on Climate Change, it is predicted that the global atmospheric concentration of carbon dioxide CO_2 reach 700 ppm, or even more (IPCC, 2014). On C_3 plants, which photosynthetic metabolism is limited by ambient CO_2 the primary effects of increased CO_2 include enhanced plant biomass, leaf net photosynthetic rates, and decreased stomatal conductance (Long *et al.*, 2004; Ainsworth and Long, 2005). However, prolonged exposure to elevated CO_2 usually depleted photosynthetic activity and plant development due to the carbohydrate accumulation in leaves that cannot be remobilised to sinks. Developing C demanding organs/processes has been described (Ainsworth and Rogers, 2007; Aranjuelo *et al.*, 2009, 2013*a*) to be target aspects conditioning leaf carbohydrate sink/source balance. Therefore, plants with a large C demand (i.e. large ears in the case of cereals) will benefit more from CO_2 enrichment than those with a small sink size (Aranjuelo *et al.*, 2009, Manderscheid and Weigel., 1997). Such aspect is especially relevant in wheat where grains represent a major C sink during grain filling period (Uddling *et al.*, 2008).

N availability has been identified as a second factor crop performance under elevated CO_2 (Ainsworth and Long, 2005). The link between N content in plants performance under elevated CO_2 has been the object of an intense. Furthermore, under elevated CO_2 conditions, it has been noted mineral content reduction in different plant species (Cotrufo *et al.*, 1998) and growth conditions (Poorter *et al.,* 1997). Depleted N observed under elevated CO_2 would constrain Rubisco availability, with the consequent effect on photosynthetic performance (Long *et al.*, 2004; Taub and Wang, 2008). Although it has not been characterized in the past, when considering CO_2 effect in photosynthetic performance, it should be considered that target factors conditioning leaf carbohydrate build-up and protein availability will be also conditioned by the phenological stage. During grain filling period, ears represent a major C and N sink in wheat plants. As mentioned above, leaf C sink/source and therefore photosynthetic performance is also conditioned by the sink strength of other organs such as grains (Uddling *et al*., 2008; Aranjuelo *et al*., 2011). C required for grain filling is mostly provided by flag leaf photosynthesis (Evans, 1983), translocation of C assimilated before anthesis (mainly stored in the internodes) (Gebbing and Schnyder, 1999), and ear photosynthesis (Tambussi *et al.*, 2007; Maydup *et al.*, 2012). Therefore, compared to the vegetative stage period, the fact that during grain filling period a “new” C sink organ, such as ears, is developed implies that during the late phonologic period, wheat plants will be less susceptible to show leaf C accumulation. In addition, during this period, developing ears also demand N content. Nitrogen sources feeding grain filling include current N uptake, assimilation, translocation, recycling and remobilization (Masclaux-Daubresse *et al.*, 2010). The proportion of remobilized N in the harvested grain is environment-dependent and can account for 60 to 92% of the total grain N in wheat (Austin *et al.*, 1977; Masclaux-Daubresse *et al.,* 2010). Rubisco might represent up to 50 % of the total soluble protein (TSP) and 25 % of the nitrogen (N) content in leaves (Aranjuelo *et al*., 2013a). Although it function is mostly related with CO_2 assimilation during the Calvin cycle, its larger amounts in leaves confers a role as a source of N for sustaining grain N demand (Masclaux-Daubresse *et al.*, 2008; Erice *et al.*, 2014).

During senescence period, proteins are degraded and activity of proteins involved in N assimilation such as cytosolic glutamine synthetase (GS1) and glutamate dehydrogenase (GDH) have been described to be stimulated (Masclaux-Daubresse *et al.,* 2001; Martin *et al.*, 2006). Amino acids are the major form of N remobilization from wheat leaves to grain during grain filling period. While aspartate (Asp) and glutamate (Glu) represent (approximately) 50 % of total amino acids (Hayashi and Chino, 1986) at the vegetative stage, during leaf senescence, Asp and Glu content decreases and glutamine (Gln) availability increases (Simpson and Dalling, 1981). N assimilation and later remobilization have been studied through the 'apparent remobilization' method based on the determination of differences in N content during the pre/post-anthesis period in different plant organs, but is susceptible to commit large experimental errors. Moreover, this method does not enable the identification of N sources such as N uptake from soil and remobilization from senescent organs (Masclaux-Daubresse *et al.*, 2008).

While wheat physiologic and agronomic performance under elevated CO_2 has been extensively characterized on the past, the role of changing C and N sinks-sources in leaf N and C status has comparatively received minor attention. However, taking into account that leaf C/N ratio represents a target parameter conditioning physiologic performance under elevated CO_2 it is crucial to characterize metabolite and protein profile of leaves at different phonologic stages. The progressive degradation of Rubisco during leaf senescence, together with the development of a C and N demanding to emerging organs causes major modifications in carbon and N assimilatory pathways that will affect crop responsiveness to elevated CO_2. In order to better understand the relevancy of phenological stages on leaf C/N and crop responsiveness to elevated CO_2, here a metabolomics study was carried out. For this purpose durum wheat plants (*Triticum durum* Def. cv. Amilcar) were exposed to two CO_2 levels (ambient versus elevated; 400 -700 ppm) and leaf metabolite contents were compared at two phenological stages (vegetative and grain filling).

6.2. Material and methods

Plant growth conditions

Wheat plants (*Triticum durum* Def. cv. Amilcar) were growth under the same controlled environmental conditions that plants of chapter 4. Plants grown under different atmospheric controlled CO_2 of 400 ppm and 700 ppm CO_2 levels and Hoagland solution (Arnon and Hoagland, 1940) were replaced three times by week. Wheat plants were watered with ammonium nitrate (NH_4NO_3) at a rate of 10mM of total N. For metabolic analysis, four flag leaves of two developmental stages (vegetative stage and grain filling), were harvested and stored at −80 °C until further measurements.

Metabolite extraction

For metabolites extraction, 10mg of dry leaves were homogenized at 4°C with 0.7ml of ice cold methanol:chloroform:water (MCW) extraction mixture (2.5:0.5:1, v/v/v), agitated vigorously for 10 sec and incubated at 4°C for 15 min. After the incubation period, samples were centrifuged at 14000 g for 4 min at 4°C and the supernatant were transferred to a new 2ml tube. The extraction procedure was repeated twice using the resultant pellet with 300 µl of MCW and the supernatants were combined. For separate both polar and unpolar phases, 300 µl of ultrapure water was added, the samples were agitated and centrifuged again at 14000 g for 2 min at 4°C. The upper polar phase was transferred to a new Eppendorf tube and samples were dry in a in a speed-vac concentrator (Scan Vac, LaboGene APS, Denmark) (Weckwerth *et al.*, 2004). After thus, dry samples were derivatized by adding 20 µl of a methoximation reagent consisting in 40 mg methoxyamine hydrochloride per 1 ml of pyridine. Samples were incubated for 90 min at 30°C using a thermo shaker. Then, 80 µl of a silylation mixture (1ml of N-methyl-N-trimethylsilyltrifluoroacetamid (MSTFA; Machery Nagel, Düren, Germany) spiked with 30 µl of alkane mixture markers) was added and the samples were incubated for 30 min at 37°C using a thermo shaker. The derivatized samples were centrifuged and 70 µl were transferred to GC-microvials with microinserts and closed with crimp caps (Strehmel *et al.* 2008).

GC–TOF/MS analysis:

Metabolites were identified using a Agilent 6890 gas chromatograph coupled to a LECO Pegasus 4D mass spectrometer (LECO Corporation, USA). GS-MS components, temperatures ramps and other parameters were set up according to Doerfler *et al.,* (2013). Data obtained from the analysis were performed with the software LECO CHROMATOF (http://de.leco-europe.com/category/separation-science-mass-spectrometry/). Retention time (RT) of the peaks was converted into retention indices (RI) throughout the retention times of the spiked alkanes. RI and mass spectra from the different peaks were compared with those annotated in the GMD Golm database (Kopka et al., 2005) with a minimum match factor of 700. A reference list was created manually containing the information of all the annotated compounds to all the samples. Peak areas were used for relative quantification.

Protein quantification

Powder flag leaves were homogenised with a protein extraction buffer described by Gibon *et al.* (2004): 50 mM Tris–HCl pH 7.5, 1 mM EDTA, 1mM EGTA, 10 mM DTT, 10 mM $MgCl_2$, 0.1% Triton X-100, 10% glycerol, 0.5% PVPP in a proportion 1/20 (w:v). Protein extract were centrifuged at 4000 g for 30 min at 4°C and the supernatants was transferred to a new tubes. Total soluble protein was quantified by the Bradford assay (Bradford, 1976).

Statistics

Data were analysed using IBM SPSS statistic 22 software (Armonk, NY, USA). Analysis of significant differences between both CO_2 conditions for each developmental stage were analysed by one-way ANOVA with a Kruskal-Wallis post hoc-test. Significant differences of soluble protein contents were analysed by one-way ANOVA with a Duncan´s post hoc-test. Phenological differences at the same CO2 were analysed by comparisons of means by t-test analysis. Significant differences were considered at $p<0.05$.

6.3. Results and Discussion

Metabolomics (GS-MS) analyses showed that, at both developmental stage, elevated CO_2 condition affect the leaf metabolite profile (Table 1). In addition, elevated CO_2 causes general changes in the relative content of amino acids, carbohydrates and tricarboxylic acids, regardless the developmental stage, which would conditioning grain yield. Our data highlighted that for both phenological periods (vegetative and grain filling), elevated CO_2 conditions caused a general amino acid suppression (Aranjuelo *et al.*, 2011). In this sense, exposure to elevated CO_2 showed a clear effect over wheat leaves metabolites, reducing the relative content of asparagine and glutamine amino acids, that are the main N-form assimilated into amino acids (Table 1). In general, the effect of CO_2 was more pronounced at vegetative stage than post-anthesis corresponding to grain filling period, except for asparagine content that it was so much repressed at grain filling period. The lower leaves amino acids contents detected during these periods were in accordance with the fact that leaves become in sources for new developing organs. N contents were by the far provided from the remobilization of amino acids product of the protein degradation (Patric and Offler, 2001; Triboi and Triboi-Blondel, 2002), but also a small proportion is usually assimilated before the anthesis period and translocated directly to developing ears (Masclaux-Daubresse *et al.*, 2010). The C required for developing organs is provided from the remobilisation of C assimilated during the vegetative stage, but also from the posterior assimilation in flag leaves or ears by the photosynthetic process (Evans, 1983; Gebbing and Schnyder, 1999; Tambussi *et al.*, 2007; Maydup *et al.*, 2012). In this sense, the depletion of the tricarboxylic acid cycle organic acids (such as oxaloacetate, citrate and fumarate), would be contextualized in plants were energy availability might have been limited. Moreover, consequence of the lower availability of organic acids provided lower carbon skeletons for amino acid synthesis.

Table 1. Heat-map of elevate CO_2 (700 *versus* 400 ppm) effect on metabolite profile of wheat leaves at vegetative and grain filling stages. The values are expressed as the ratio of each metabolite contents at 700 over 400 ppm CO_2. Asterisk (*) indicates significant differences of elevate CO_2 (700 *versus* 400 ppm).

Amino acids	Vegetative stage		Grain filling	
	(700 / 400 ppm CO_2)			
Asparagine	-6.40	*	-12.9!	*
Aspartic acid	-2.05	*	-1.86	*
Glutamic acid	-0.61		-0.89	
Glutamine	-3.97	*	-4.18	*
Glycine	-2.63	*	-2.63	*
Isoleucine	-1.33		0.52	
Leucine	-0.97		-1.10	
Lysine	-4.79	*	-2.09	*
Methionine	-5.25	*	-3.06	*
Ornithine	-7.96	*	-2.82	*
Phenylalanine	-2.38	*	-1.90	*
Proline	-2.08	*	-1.73	*
Serine	-1.16	*	-1.45	*
Threonine	-1.00		-0.84	
Tryptophan	-7.67	*	-2.21	*
Tyrosine	-2.30	*	-1.57	*
Valine	-0.74		-1.46	*

Carbohydrates	Vegetative stage		Grain filling	
	(700 / 400 ppm CO_2)			
Fructose	1.39		-0.07	
Galactose	3.28	*	1.96	*
Glucose	0.81		-0.62	
Maltose	6.83	*	0.31	
Sucrose	0.05		-0.08	

Tricarboxilic acids	Vegetative stage		Grain filling	
	(700 / 400 ppm CO_2)			
Citrate	-1.77	*	-1.82	*
2-oxo-glutarate	-0.03		3.38	*
Oxaloacetate	-5.61	*	-1.11	
Fumarate	-6.03	*	-2.09	*
Succinate	-0.30		-0.89	
Malate	-1.30		-1.63	*

When analyzing the impact of phenology, our data showed different responses on metabolites and protein content contents depending on CO_2 condition (Table 2, Figure 1). Regardless of CO_2, the amino acid relative content asparagine was lower in leaves after the anthesis stage than during the vegetative period. According to Hayashi and Chino, (1986) during leaf senescence, Asp and Glu content were described to decrease and glutamine availability increases.

The proportion of remobilized N in the harvested grain is might represent up to 92% of the total grain N in (Austin *et al*., 1977; Masclaux-Debresse *et al*., 2010). Moreover, the larger amounts of Rubisco protein contents (up to 50% in C_3 plants) is the major source of N for remobilized for supporting grain filling. In this sense, leaf protein senescence during grain filling period has been linked with the presence of reactive oxygen species (ROS), which initiated the leaf proteolysis and nutrient remobilisation to developing sink organs (Kong *et al.*, 2016*b*). In this sense, wheat plants grown at ambient CO_2 showed lower leaf protein content after the anthesis period (Figure 1).

Regarding leaf soluble sugar availability, obtained data revealed that in plants grown under ambient CO_2 conditions increased soluble sugar (fructose, galactose, glucose and maltose) contents increased during post-anthesis, but in plants exposed to elevated CO_2 conditions did no phenological derived differences were detected. Although we did not determine the starch content in the current study, the higher availability of maltose (main product of starch breakdown) would suggest that the storage C compounds were degraded for being remobilised to developing organs in plants grown at ambient CO_2. Therefore, the lower amino acid and soluble protein contents together the higher carbohydrate contents detected during post-anthesis period in plants grown at ambient CO_2 conditions could be linked with a higher remobilization in these plants. Indeed, the fact that under elevated CO_2 conditions tricarboxylic cycle showed higher 2-oxo-glutarate and fumarate contents suggest that CO_2 delay the leaf senescence, favouring C assimilation by leaves for longer period. Whereas the effect of elevated CO_2 showed similar metabolite profile at both vegetative and grain-filling periods (Table 1). Leaves of plants grown at elevated CO_2 conditions showed lower protein degradation and thus, the senescence was delayed. This permitted continue fixing C in leaves even during the grain filling period.

Table 2. Heat-map of phenology effect (grain filling *versus* vegetative stages) on metabolite profile of wheat leaves at 400 and 700 ppm CO_2. The values are expressed as the ratio of each metabolite contents at Grain filling over vegetative stage. Asterisk (*) indicates significant differences of phenological stage (grain filling *versus* vegetative stages).

Amino acids	400 ppm (Grain filling / Vegetative stage)		700 ppm (Grain filling / Vegetative stage)	
Asparagine	-1.94	*	-8.52	*
Aspartic acid	-0.79		-0.60	
Glutamic acid	-0.51		-0.80	
Glutamine	-0.56		-0.77	
Glycine	0.02		0.01	
Isoleucine	-0.33		1.52	*
Leucine	0.02		-0.11	
Lysine	-1.45	*	1.25	
Methionine	-0.89		1.31	
Ornithine	-3.27	*	1.86	*
Phenylalanine	0.24		0.72	
Proline	-0.36		-0.02	
Serine	-1.01	*	-1.30	
Threonine	-0.84		-0.68	
Tryptophan	1.23	*	6.69	*
Tyrosine	-0.12		0.62	
Valine	0.25		-0.47	

Carbohydrates	400 ppm (Grain filling / Vegetative stage)		700 ppm (Grain filling / Vegetative stage)	
Fructose	1.65	*	0.19	
Galactose	3.00	*	1.68	
Glucose	1.56		0.13	
Maltose	8.00	*	1.48	
Sucrose	0.16		0.04	

Tricarboxilic acids	400 ppm (Grain filling / Vegetative stage)		700 ppm (Grain filling / Vegetative stage)	
Citrate	0.66		0.61	
2-oxo-glutarate	1.05		4.45	*
Oxaloacetate	-4.51	*	-0.01	
Fumarate	1.05		4.99	*
Succinate	1.48		0.90	
Malate	1.29		0.95	

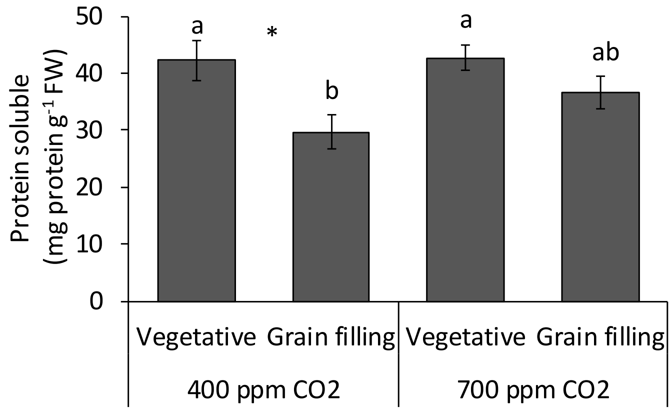

Figure 1. Total soluble protein content of wheat leaves collected at vegetative and grain filling stages that were grown at 400 and 700 ppm CO_2. Significant differences between phenological stage and CO_2 conditions were indicated with letters. Asterisk (*) indicates significant differences of elevate CO_2 condition (700 *versus* 400 ppm CO_2).

In accordance with this, the principal component assay (PCA) remarked the fact that (regardless of harvest factor) the wheat plants grown at elevated CO_2 conditions were very similar. In the other hand, in case of plants grown at ambient CO_2, were clear differences were detected between samples collected during vegetative and grain filling period (Figure 2).

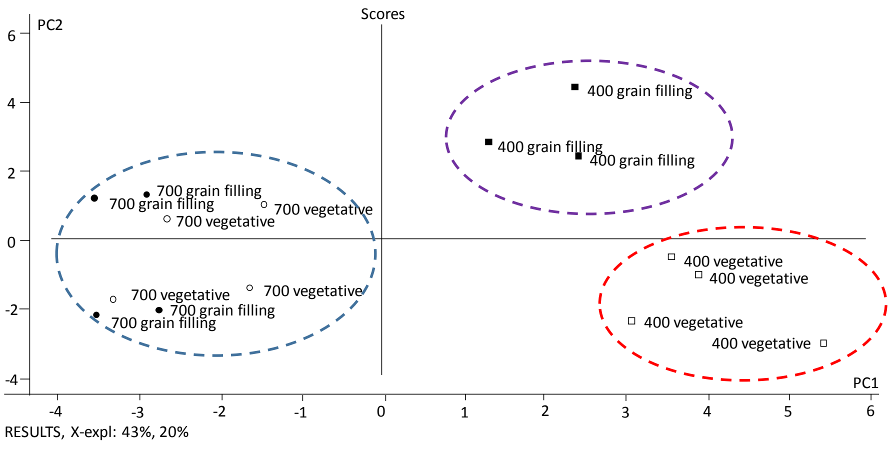

Figure 2. Principal component analysis of leaves metabolites of wheat leaves collected at vegetative and grain filling stages that were grown at 400 and 700 ppm CO_2. The analysis was done using the Portable Unscrambler 9.7 software.

Previous studies observe that, under elevated CO_2, there might be an acceleration on leaf senescence. However, it should be noted that, usually, those assumptions are based on the use of physiological markers such as chlorophyll content (Ommen *et al.*, 1999) or photosynthesis (Garcia *et al.*, 1998). Our data are in line with Buchner *et al*. (2015), who cannot confirm an acceleration of the senescence under elevated CO_2. According to what described by those authors, elevated CO_2 decreased the expression of carbohydrate-related genes as advance the phenology. In agreement with this finding, our study also remarked the higher carbohydrate contents detected (Table 1). More specifically, obtained data showed that during grain filling period, plants grown under ambient CO_2 had higher maltose content (probably by a higher starch breakdown) and lower protein contents in leaves. The fact that in leaves of plants grown at elevated CO_2 levels protein degradation was lower would suggest that in these conditions the senescence was delayed. This permitted continue in a green stage for longer period, enabling the assimilation of more C for the later grain filling period.

Metabolite remobilisation from leaves to developing ears requires a highly synchronised regulation of cellular metabolite transports, thus further studies on metabolite transporters and the metabolite pattern in ears and, more especially in grains, are required to understand how C and N remobilisation are conditioned by elevated CO_2.

7

General conclusions

- Both nitrification inhibitors (NIs), DMPP and DMPSA, showed similar efficiency reducing N_2O emissions under aerobic conditions (40% WFPS) by inhibiting bacterial ammonia oxidation (AOB).
- Under anaerobic conditions (80% WFPS), both NIs reduced N_2O emissions by inhibiting nitrification, evidenced by the persistence of NH_4 in soil jointly with the decrease in the AOB population, but also by the stimulation of nosZ population.
- The application of DMPP and DMPSA stimulated the reduction of N_2O to N_2 by the nitrous oxide reductase activity under denitrifying conditions.
- Durum wheat plants grown under nitrate nutrition presented C-assimilation imbalance that causes the accumulation of starch at elevated CO_2.
- Mixed ammonium nitrate nutrition allowed that wheat plants grown at elevated CO_2 overcome the limitations derived to unique N-source nutrition of starch accumulation and photochemical imbalance associate to nitrate and ammonium nutrition, respectively. Exposure to elevated CO_2 reduced ammonium toxicity by higher rates of photorespiration and enhanced GS and GDH activities.
- The higher internode carbohydrate-storage capacity of RSCL-89 barley cultivar permitted improved photosynthetic machinery under elevated CO_2, overcoming the photosynthetic down-regulation observed in Harrington.
- Under changing growth CO_2, the expression of the light-harvesting complex and the CO_2 diffusion conditioning the responsiveness of plants to changing CO_2.
- Growth under elevated CO_2 delayed the senescence and permitted extend the vegetative stage for assimilate longer amounts of C in leaves for posterior remobilisation to ear developing sinks.

- Obtained results remark the need to better understand the impact of N fertilization form and crop C sink increase strategies so to develop a more environmentally friendly crop production during the next decades.

8

References

Ainsworth EA, Long SP. 2005. What have we learned from 15 years of free-air CO_2 enrichment (FACE)? A meta-analytic review of the responses of photosynthesis, canopy properties and plant production to rising CO_2. New Phytologist 165, 351–372.

Ainsworth EA, Rogers A. 2007. The response of photosynthesis and stomatal conductance to rising [CO_2]: Mechanisms and environmental interactions. Plant, Cell and Environment 30, 258–270.

Ainsworth EA, Rogers A, Leakey ADB, Heady LE, Gibon Y, Stitt M, Schurr U. 2006. Does elevated atmospheric [CO_2] alter diurnal C uptake and the balance of C and N metabolites in growing and fully expanded soybean leaves? Journal of Experimental Botany 58, 579–591.

Ainsworth EA, Rogers A, Nelson R, Long SP. 2004. Testing the 'source-sink' hypothesis of down-regulation of photosynthesis in elevated [CO_2] in the field with single gene substitutions in Glycine max. Agricultural and Forest Meteorology 122, 85–94.

Andrews M, Raven JA, Lea PJ. 2013. Do plants need nitrate? The mechanisms by which nitrogen form affects plants. Annals of Applied Biology 163, 174–199.

Aranjuelo I, Araus JL, Nogués S. 2013a. Carbon and nitrogen partitioning during the post-anthesis period is conditioned by N fertilisation and sink strength in three cereals. Plant biology 15, 135–143.

Aranjuelo I, Cabrera-Bosquet L, Morcuende R, Avice J-C, Nogués S, Araus JL, Martínez-Carrasco R, Pérez P. 2011. Does ear C sink strength contribute to overcoming photosynthetic acclimation of wheat plants exposed to elevated CO_2? Journal of experimental Botany 62, 3957–69.

Aranjuelo I, Erice G, Sanz-Sáez Á, *et al*. 2015. Differential CO_2 effect on primary carbon metabolism of flag leaves in durum wheat (*Triticum durum* Desf.). Plant, Cell & Environment 38, 2780–2794.

Aranjuelo I, Pardo A, Biel C, Savé R, Azcón-Bieto J, Nogués S. 2009. Leaf carbon management in slow-growing plants exposed to elevated CO_2. Global Change Biology 15, 97–109.

Aranjuelo I, Sanz-Sáez Á, Jauregui I, Irigoyen JJ, Araus JL, Sánchez-Díaz M, Erice G. 2013b. Harvest index, a parameter conditioning responsiveness of wheat plants to elevated CO_2. Journal of Experimental Botany 64, 1879–1892.

Ariz I, Artola E, Asensio AC, Cruchaga S, Aparicio-Tejo PM, Moran JF. 2011. High irradiance increases NH_4^+ tolerance in *Pisum sativum*: Higher carbon and energy availability improve ion balance but not N assimilation. Journal of Plant Physiology 168, 1009–1015.

Arnon DI, Hoagland DR. 1940. A comparison of water culture and soil as media for crop production. Science 89, 512–514.

Arp WJ. 1991. Effects of source-sink relations on photosynthetic acclimation to elevated CO_2. Plant, Cell and Environment 14, 869–875.

Arp DJ, Stein LY. 2003. Metabolism of inorganic N compounds by ammonia-oxidizing bacteria. Critical reviews in biochemistry and molecular biology 38, 471–495.

Aulakh MS, Doran JW, Walters DT, Mosier AR, Francis DD. 1991. Crop residue type and placement effects on denitrification and mineralization. Soil Science Society of America Journal 55, 1020–1025.

Austin RB, Edrich JA, Ford MA, Blackwell RD. 1977. The nitrogen economy of winter wheat. Journal Agricultural Science 88: 159–167

Bahaji A, Sánchez-López AM, De Diego N, et al. 2015. Plastidic phosphoglucose isomerase is an important determinant of starch accumulation in mesophyll cells, growth, photosynthetic capacity, and biosynthesis of plastidic cytokinins in Arabidopsis. PLoS ONE 10, 1–35.

Baki GKA, Siefritz F, Man H, Weiner H, Kaldenhoff R, Kaiser WM. 2000. Nitrate reductase in *Zea mays* L. under salinity. Plant, Cell & Environment 23, 515–521.

Barrena I, Menéndez S, Bedmar EJ, Correa-Galeote D, Vega-Mas I, González-Murua C, Estavillo JM. 2017. Soil water content modulates the effect of the nitrification inhibitor 3,4-Dimethylpyrazole Phosphate (DMPP) on nitrifying and denitrifying bacteria. Geoderma 303, 1–8.

Barrena I, Menéndez S, Duñabeitia M, Merino P, Florian Stange C, Spott O, González-Murua C, Estavillo JM. 2013. Greenhouse gas fluxes (CO_2, N_2O and CH_4) from forest soils in the Basque Country: Comparison of different tree species and growth stages. Forest Ecology and Management 310, 600–611.

Baslam M, Baroja-Fernández E, Ricarte-Bermejo A, et al. 2017. Genetic and isotope ratio mass spectrometric evidence for the occurrence of starch degradation and cycling in illuminated Arabidopsis leaves. PLoS ONE 12: e0171245.

Behrens S, Azizian MF, McMurdie PJ, Sabalowsky A, Dolan ME, Semprini L, Spormann AM. 2008. Monitoring abundance and expression of 'Dehalococcoides' species chloroethene-reductive dehalogenases in a tetrachloroethene-dechlorinating flow column. Applied and Environmental Microbiology 74, 5695–5703.

Benckiser G, Schartel T, Weiske A. 2015. Control of NO_3^- and N_2O emissions in agroecosystems: A review. Agronomy for Sustainable Development 35, 1059–1074.

Bittsánszky A, Pilinszky K, Gyulai G, Komives T. 2015. Overcoming ammonium toxicity. Plant Science 231, 184–190.

Bloom AJ, Burger M, Asensio JSR, Cousins AB. 2010. Carbon dioxide enrichment inhibits nitrate assimilation in wheat and Arabidopsis. Science 328, 899–904.

Bloom AJ, Burger M, Kimball BA, Pinter PJ. 2014. Nitrate assimilation is inhibited by elevated CO_2 in field-grown wheat Nitrate assimilation is inhibited by elevated CO_2 in field-grown wheat. Nature Climate Change, 477–480.

Bloom AJ, Smart DR, Nguyen DT, Searles PS. 2002. Nitrogen assimilation and growth of wheat under elevated carbon dioxide. Proceedings of the National Academy of Sciences of the United States of America 99, 1730–1735.

Bloom AJ, Sukrapanna SS, Warner RL. 1992. Root respiration associated with ammonium and nitrate absorption and assimilation by barley. Plant physiology 99, 1294–301.

Bradford MM. 1976. A rapid and sensitive method for the quantitation of microgram quantities of protein utilizing the principle of protein-dye binding. Analytical chemistry 72, 248–254.

Braker G, Conrad R. 2011. Diversity, structure, and size of N_2O-producing microbial communities in soils-What matters for their functioning? Advances in Applied Microbiology. 33–70.

Britto DT, Kronzucker HJ. 2002. NH_4^+ toxicity in higher plants: a critical review. Journal of Plant Physiology 159, 567–584.

Buchner P, Tausz M, Ford R, Leo A, Fitzgerald GJ, Hawkesford MJ, Tausz-Posch S. 2015. Expression patterns of C- and N-metabolism related genes in wheat are changed during senescence under elevated CO_2 in dry-land agriculture. Plant Science 236, 239–249.

Butterbach-Bahl K, Baggs EM, Dannenmann M, Kiese R, Zechmeister-Boltensternan S. 2013. Nitrous oxide emissions from soils: how well do we understand the processes and their controls? Philosophical transactions of the Royal Society of London. Series B, Biological sciences 368, 20130122.

Cataldo DA, Schrader LE, Youngs VL. 1974. Analysis by digestion and colorimetric assay of total nitrogen in plant tissues high in nitrate. Crop Science 14, 854–856.

Cawse PA. 1967. The determination of nitrate in soil solutions by ultraviolet spectrophotometry. Analyst 92, 311–315.

Chen H, Mothapo N V., Shi W. 2014a. Soil Moisture and pH Control Relative Contributions of Fungi and Bacteria to N_2O Production. Microbial Ecology 69, 180–191.

Chen Q, Qi L, Bi Q, Dai P, Sun D, Sun C, Liu W, Lu L, Ni W, Lin X. 2014b. Comparative effects of 3,4-dimethylpyrazole phosphate (DMPP) and dicyandiamide (DCD) on ammonia-oxidizing bacteria and archaea in a vegetable soil. Applied Microbiology and Biotechnology 99, 477–487.

Chien SH, Prochnow LI, Cantarella H. 2009. Recent Developments of Fertilizer Production and Use to Improve Nutrient Efficiency and Minimize Environmental Impacts. Elsevier Inc. Advances in Agronomy, Chapter 8, 267-322

Cohen SA, De Antonis KM. 1994. Applications of amino acid derivatization with 6-aminoquinolyl-N-hydroxysuccinimidyl carbamate. Analysis of feed grains, intravenous solutions and glycoproteins. Journal of Chromatography 661, 25–34.

Cohen SA, Michaud DP. 1993. Synthesis of a fluorescent derivatizing reagent, 6-aminoquinolyl-N-hydroxysuccinimidyl carbamate, and its application for the analysis of hydrolysate amino acids via high-performance liquid chromatography. Analytical Biochemistry 211, 279–287.

Córdoba J, Molina-Cano JL, Martínez-Carrasco R, Morcuende R, Pérez P. 2016. Functional and transcriptional characterization of a barley mutant with impaired photosynthesis. Plant Science 244, 19–30.

Córdoba J, Pérez P, Morcuende R, Molina-Cano JL, Martínez-Carrasco R. 2017. Acclimation to elevated CO_2 is improved by low Rubisco and carbohydrate content, and enhanced Rubisco transcripts in the G132 barley mutant. Environmental and Experimental Botany 137, 36–48.

Correa-Galeote D, Tortosa G, Bedmar EJ. 2013. Determination of Denitrification Genes Abundance in Environmental Samples. Metagenomics 2, 1–14.

Coskun D, Britto DT, Kronzucker HJ. 2016. Nutrient constraints on terrestrial carbon fixation: The role of nitrogen. Journal of Plant Physiology 203, 95–109.

Coskun D, Britto DT, Li M, Becker A, Kronzucker HJ. 2013. Rapid ammonia gas transport accounts for futile transmembrane cycling under NH_3/NH_4^+ toxicity in plant roots. Plant Physiology 163, 1859–1867.

Coskun D, Britto DT, Shi W, Kronzucker HJ. 2017. How Plant Root Exudates Shape the Nitrogen Cycle. Trends in Plant Science 22, 661–673.

Cotrufo MF, Ineson P, Scoot A. 1998. Elevated CO_2 reduces the nitrogen concentration of plant. Global Change Biology, 43–54.

Dawson IK, Russell J, Powell W, Steffenson B, Thomas WTB, Waugh R. 2015. Barley: a translational model for adaptation to climate change. New Phytologist 206, 913–931.

Di HJ, Cameron KC. 2011. Inhibition of ammonium oxidation by a liquid formulation of 3,4-Dimethylpyrazole phosphate (DMPP) compared with a dicyandiamide (DCD) solution in six new Zealand grazed grassland soils. Journal of Soils and Sediments 11, 1032–1039.

Di HJ, Cameron KC. 2016. Inhibition of nitrification to mitigate nitrate leaching and nitrous oxide emissions in grazed grassland: a review. Journal of Soils and Sediments 16, 1401–1420.

Di HJ, Cameron KC, Podolyan A, Robinson A. 2014. Effect of soil moisture status and a nitrification inhibitor, dicyandiamide, on ammonia oxidizer and denitrifier growth and nitrous oxide emissions in a grassland soil. Soil Biology and Biochemistry 73, 59–68.

Doerfler H, Lyon D, Nägele T, Sun X, Fragner L, Hadacek F, Egelhofer V, Weckwerth W. 2013. Granger causality in integrated GC-MS and LC-MS metabolomics data reveals the interface of primary and secondary metabolism. Metabolomics 9, 564–574.

Domeignoz-Horta LA, Spor A, Bru D, Breuil M, Bizouard F, Léonard J, Philippot L. 2015. The diversity of the N_2O reducers matters for the N_2O:N_2 denitrification end-product ratio across an annual and a perennial cropping system. Frontiers in Microbiology 6.

Drake BG, Gonzàlez-Meler MA. 1997. More efficient plants: A consequence of rising atmospheric CO_2? Annu. Rev. Plant. Physiol. Plant. Mol. Bio 48, 609–639.

Duan Y-F, Kong X-W, Schramm A, Labouriau R, Eriksen J, Petersen SO. 2017. Microbial N transformations and N_2O emission after simulated grassland cultivation: effects of the nitrification inhibitor 3,4-dimethylpyrazole phosphate (DMPP). Applied and Environmental Microbiology 83, e02019-16.

Ellis RP, Forster BP, Robinson D, Handley LL, Gordon DC, Russell J, Powell W. 2000. Wild barley: a source of genes for crop improvement in the 21st century? Journal of Experimental Botany 51, 9–17.

Van den Ende W. 2013. Multifunctional fructans and raffinose family oligosaccharides. Frontiers in Plant Science 4, 1–11.

Erice G, Sanz-sáez A, Urdiain A, Araus JL, Irigoyen JJ, Aranjuelo I. 2014. Harvest index combined with impaired N availability constrains the responsiveness of durum wheat to elevated CO_2 concentration and terminal water stress. Functional Plant Biology 41, 1138–1147.

Esteban R, Ariz I, Cruz C, Moran JF. 2016. Review: Mechanisms of ammonium toxicity and the quest for tolerance. Plant Science 248, 92–101.

Evans JR. 1983. Nitrogen and photosynthesis in the flag leaf of wheat (*Triticum aestivum* L.). Plant Physiology 72, 297–302.

FAO. 2015. World fertilizer trends and outlook to 2018.

Flexas J, Ribas-Carbo M, Hanson DT, Bota J, Otto B, Cifre J, McDowell N, Medrano H, Kaldenhoff R. 2006. Tobacco aquaporin *NtAQP1* is involved in mesophyll conductance to CO_2 *in vivo*. the Plant Journal 48, 427–439.

Florio A, Clark IM, Hirsch PR, Jhurreea D, Benedetti A. 2014. Effects of the nitrification inhibitor 3,4-dimethylpyrazole phosphate (DMPP) on abundance and activity of ammonia oxidizers in soil. Biology and Fertility of Soils 50, 795–807.

Fowler D, Coyle M, Skiba U, et al. 2013. The global nitrogen cycle in the twenty-first century. Philos. Trans. R. Soc. Lond. B. Biol. Sci. 368, 1–13.

Fuertes-Mendizabal T, Setién I, Estavillo JM, González-Moro MB. 2010. Late nitrogen fertilization affects carbohydrate mobilization in wheat. Journal of Plant Nutrition and Soil Science 173, 907–919.

Fukayama H, Sugino M, Fukuda T, et al. 2011. Gene expression profiling of rice grown in free air CO_2 enrichment (FACE) and elevated soil temperature. Field Crops Research 121, 195–199.

Galloway JN, Leach AM, Bleeker A, Erisman JW, B PTRS, Galloway JN, Leach AM, Bleeker A, Erisman JW. 2013. A chronology of human understanding of the nitrogen cycle. Philos. Trans. R. Soc. Lond. B. Biol. Sci. 368, 20130120.

Garcia RL, Long SP, Wall GW, Osborne CP, Kimball BA, Nie GY, Jr PJP. 1998. Photosynthesis and conductance of spring-wheat leaves : field response to continuous free-air atmospheric CO_2 enrichment. Plant Cell and Environment 21, 659–669.

Gebbing T, Schnyder H. 1999. Pre-anthesis reserve utilization for protein and carbohydrate synthesis in grains of wheat. Plant physiology 121, 871–878.

Geiger M, Haake V, Ludewig F, Sonnewald U, Stitt M. 1999. The nitrate and ammonium nitrate supply have a major influence on the response of photosynthesis, carbon metabolism, nitrogen metabolism and growth to elevated carbon dioxide in tobacco. Plant, Cell and Environment 22, 1177–1199.

Gibon Y, Blaesing OE, Hannemann J, Carillo P, Höhne M, Hendriks JHM, Palacios N, Cross J, Selbig J, Stitt M. 2004. A Robot-Based Platform to Measure Multiple Enzyme Activities in Arabidopsis Using a Set of Cycling Assays:

Comparison of Changes of Enzyme Activities and Transcript Levels during Diurnal Cycles and in Prolonged Darkness. the Plant Cell 16, 3304–3325.

Gilsanz C, Báez D, Misselbrook TH, Dhanoa MS, Cárdenas LM. 2016. Development of emission factors and efficiency of two nitrification inhibitors, DCD and DMPP. Agriculture, Ecosystems and Environment 216, 1–8.

Guardia G, Cangani MT, Andreu G, Sanz-Cobena A, García-Marco S, Álvarez JM, Recio-Huetos J, Vallejo A. 2017. Effect of inhibitors and fertigation strategies on GHG emissions, NO fluxes and yield in irrigated maize. Field Crops Research 204, 135–145.

Guo S, Zhou Y, Shen Q, Zhang F. 2007. Effect of ammonium and nitrate nutrition on some physiological processes in higher plants- Growth, photosynthesis, photorespiration, and water relations. Plant Biology 9, 21–29.

Hachiya T, Sakakibara H. 2017. Interactions between nitrate and ammonium in their uptake, allocation, assimilation, and signaling in plants. Journal of Experimental Botany 68, 2501–2512.

Hallin S, Philippot L, Löffler FE, Sanford RA, Jones CM. 2018. Genomics and Ecology of Novel N_2O-Reducing Microorganisms. Trends in Microbiology 1, 43–55.

Hare PD, Cress W. 1997. Metabolic implications of stress-induced proline accumulation in plants. Plant Growth Regulation 21, 79–102.

Harter J, Krause H-M, Schuettler S, Ruser R, Fromme M, Scholten T, Kappler A, Behrens S. 2013. Linking N_2O emissions from biochar-amended soil to the structure and function of the N-cycling microbial community. The ISME Journal 8, 660–674.

Hatch D, Trindade H, Cardenas LM, Carneiro J, Hawkins J, Scholefield D, Chadwick D. 2005. Laboratory study of the effects of two nitrification inhibitors on greenhouse gas emissions from a slurry-treated arable soil:

Impact of diurnal temperature cycle. Biology and Fertility of Soils 41, 225–232.

Hawkesford M, Horst W, Kichey T, Lambers H, Schjoerring J, Møller IS, White P. 2012. Functions of Macronutrients. In: Marschner P, ed. Marschner's mineral nutrition of higher plants, 3rd edn. San Diego: Academic Press, 135–189.

Hayashi H, Chino M. 1986. Collection of pure phloem sap from wheat and its chemical composition. Plant Cell Physiology 27, 1387–93.

Huérfano X, Fuertes-Mendizabal T, Duñabeitia MK, González-Murua C, Estavillo JM, Menéndez S. 2015. Splitting the application of 3,4-dimethylpyrazole phosphate (DMPP): Influence on greenhouse gases emissions and wheat yield and quality under humid Mediterranean conditions. European Journal of Agronomy 64, 47–57.

Huérfano X, Fuertes-Mendizabal T, Fernández-Diez K, Estavillo JM, González-Murua C, Menéndez S. 2016. The new nitrification inhibitor 3,4-dimethylpyrazole succinic (DMPSA) as an alternative to DMPP for reducing N_2O emissions from wheat crops under humid Mediterranean conditions. European Journal of Agronomy 80, 78–87.

IPCC, 2014: Climate Change 2014: Synthesis Report. Contribution of Working Groups I, II and III to the Fifth Assessment Report of the Intergovernmental Panel on Climate Change [Core Writing Team, R.K. Pachauri and L.A. Meyer (eds.)]. IPCC, Geneva, Switzer.

Jauregui I, Aparicio-Tejo PM, Baroja-Fernández E, Avila C, Aranjuelo I. 2017. Elevated CO_2 improved the growth of a double nitrate reductase defective mutant of Arabidopsis thaliana: The importance of maintaining a high energy status. Environmental and Experimental Botany 140, 110–119.

Jauregui I, Aroca R, Garnica M, Zamarreño ÁM, García-Mina JM, Serret MD, Parry M, Irigoyen JJ, Aranjuelo I. 2015. Nitrogen assimilation and transpiration: key processes conditioning responsiveness of wheat to elevated [CO_2] and temperature. Physiologia Plantarum 155, 338–354.

Jones CM, Graf DRH, Bru D, Philippot L, Hallin S. 2013. The unaccounted yet abundant nitrous oxide-reducing microbial community: a potential nitrous oxide sink. The ISME journal 7, 417–26.

Khalil K, Mary B, Renault P. 2004. Nitrous oxide production by nitrification and denitrification in soil aggregates as affected by O_2 concentration. Soil Biology and Biochemistry 36, 687–699.

Kimball BA, Kobayashi K, Bindi M. 2002. Responses of Agricultural Crops to Free-Air CO_2 Enrichment. Advances in Agronomy 77, 293–368.

Kitaoka S, Koike T. 2004. Invasion of broad-leaf tree species into a larch plantation: seasonal light environment, photosynthesis and nitrogen allocation. Physiologia Plantarum 121, 604–611.

Kong X, Duan Y, Schramm A, Eriksen J, Petersen SO. 2016a. 3,4-Dimethylpyrazole phosphate (DMPP) reduces activity of ammonia oxidizers without adverse effects on non-target soil microorganisms and functions. Applied Soil Ecology 105, 67–75.

Kong L, Xie Y, Hu L, Feng B, Li S. 2016b. Remobilization of vegetative nitrogen to developing grain in wheat (*Triticum aestivum* L.). Field Crops Research 196, 134–144.

Kopka, J., Schauer, N., Krueger, S., Birkemeyer, C., Usadel, B., Bergmuller, E., et al. (2005). GMD@CSB.DB: the golm metabolome database. Bioinformatics 21, 1635–1638. doi: 10.1093/bioinformatics/bti236

Koroleva O, Farrar JF, Deri Tomos A AD, Pollock CJ. 1998. Carbohydrates in individual cells of epidermis, mesophyll, and bundle sheath in barley leaves with changed export or photosynthetic rate. Plant physiology 118, 1525–32.

Kou YP, Wei K, Chen GX, Wang ZY, Xu H. 2015. Effects of 3,4-dimethylpyrazole phosphate and dicyandiamide on nitrous oxide emission in a greenhouse vegetable soil. Plant, Soil and Environment 61, 29–35.

Laemmli UK. 1970. Cleavage of structural proteins during the assembly of the head of bacteriophage T4. Nature 227, 680–685.

Langley JA, Megonigal JP. 2010. Ecosystem response to elevated CO_2 levels limited by nitrogen-induced plant species shift. Nature 466, 96–9.

Lassaletta L, Billen G, Grizzetti B, Anglade J, Garnier J. 2014. 50 year trends in nitrogen use efficiency of world cropping systems: The relationship between yield and nitrogen input to cropland. Environmental Research Letters 9, 105011.

Lea PJ, Miflin BJ. 1974. Alternative route for nitrogen assimilation in higher plants. Nature 251, 614–616.

Lewis JD, Wang XZ, Griffin KL, Tissue DT. 2002. Effects of age and ontogeny on photosynthetic responses of a determinate annual plant to elevated CO_2 concentrations. Plant, Cell & Environment 25, 359–368.

Li J, Almagro G, Muñoz FJ, et al. 2012. Post-translational redox modification of ADP-glucose pyrophosphorylase in response to light is not a major determinant of fine regulation of transitory starch accumulation in Arabidopsis leaves. Plant and Cell Physiology 53, 433–444.

Li Q, Cui X, Liu X, Roelcke M, Pasda G, Zerulla W, Wissemeier AH, Chen X, Goulding K, Zhang F. 2017. A new urease-inhibiting formulation decreases ammonia volatilization and improves maize nitrogen utilization in North China Plain. Scientific Reports 7, 43853.

Li X, Sørensen P, Olesen JE, Petersen SO. 2016. Evidence for denitrification as main source of N_2O emission from residue-amended soil. Soil Biology and Biochemistry 92, 153–160.

Liu R, Hayden H, Suter HC, He J, Chen D. 2015. The effect of nitrification inhibitors in reducing nitrification and the ammonia oxidizer population in three contrasting soils. Journal of Soils and Sediments 15, 1113–1118.

Liu C, Wang K, Zheng X. 2013. Effects of nitrification inhibitors (DCD and DMPP) on nitrous oxide emission, crop yield and nitrogen uptake in a wheat-maize cropping system. Biogeosciences 10, 2427–2437.

Liu Y, Wirén N Von. 2017. Ammonium as a signal for physiological and morphological responses in plants. Journal of Experimental Botany 68, 2581–2592.

Loladze I. 2014. Hidden shift of the ionome of plants exposed to elevated CO_2 depletes minerals at the base of human nutrition. eLIFE, 1–29.

Long SP, Ainsworth EA, Rogers A, Ort DR. 2004. Rising atmospheric carbon dioxide: Plants FACE the Future*. Annual Review of Plant Biology 55, 591–628.

Macadam XMB, del Prado A, Merino P, Estavillo JM, Pinto M, González-Murua C. 2003. Dicyandiamide and 3,4-dimethyl pyrazole phosphate decrease N_2O emissions from grassland but dicyandiamide produces deleterious effects in clover. Journal of plant physiology 160, 1517–1523.

MacNeill GJ, Mehrpouyan S, Minow MAA, Patterson JA, Tetlow IJ, Emes MJ. 2017. Starch as a source, starch as a sink: the bifunctional role of starch in carbon allocation. Journal of Experimental Botany 68, 4433–4453.

Marsden KA, Marín-Martínez AJ, Vallejo A, Hill PW, Jones DL, Chadwick D. 2016. The mobility of nitrification inhibitors under simulated ruminant urine deposition and rainfall: a comparison between DCD and DMPP. Biology and Fertility of Soils.

Marsden KA, Scowen M, Hill PW, Jones DL, Chadwick D. 2015. Plant acquisition and metabolism of the synthetic nitrification inhibitor dicyandiamide and naturally-occurring guanidine from agricultural soils. Plant and Soil 395, 201–214.

Martin, A. Lee J, Kichey T, Gerentes D *et al.* 2006. Two cytosolic glutamine synthetase isoforms of maize are specifically involved in the control of grain production. Plant Cell 18, 3252–3274

Masclaux C, Quillere´I, Gallais A, Hirel B. 2001. The challenge of remobilisation in plant nitrogen economy. A survey of physio-agronomic and molecular approaches. Annals of Applied Biology 138, 68–81.

Masclaux-Daubresse C, Daniel-Vedele F, Dechorgnat J, Chardon F, Gaufichon L, Suzuki A. 2010. Nitrogen uptake, assimilation and remobilization in plants: challenges for sustainable and productive agriculture. Annals of Botany 105, 1141–1157.

Masclaux-Daubresse C, Reisdorf-Cren M, Orsel M. 2008. Leaf nitrogen remobilisation for plant development and grain filling. Plant Biology 10, 23–36.

Matus I, Corey A, Filichkin T, Hayes PM, Vales MI, Kling J, Riera-Lizarazu O, Sato K, Powell W, Waugh R. 2003. Development and characterization of recombinant chromosome substitution lines (RCSLs) using Hordeum vulgare subsp. spontaneum as a source of donor alleles in a Hordeum vulgare subsp. vulgare background. Genome 46, 1010–1023.

Maurel C, Verdoucq L, Luu D, Santoni V. 2008. Plant Aquaporins : Membrane Channels with Multiple Integrated Functions. Annual Review of Plant Biology 59, 595–624.

Maydup ML, Antonietta M, Guiamet JJ, Tambussi EA. 2012. The contribution of green parts of the ear to grain filling in old and modern cultivars of bread wheat (*Triticum aestivum* L.): evidence for genetic gains over the past century. Field Crops Research 134, 208–215.

McTaggart IP, Tsuruta H. 2003. The influence of controlled release fertilisers and the form of applied fertiliser nitrogen on nitrous oxide emissions from an andosol. Nutrient Cycling in Agroecosystems 67, 47–54.

Méndez AM. 2014. Papel de los carbohidratos en la tolerancia al estrés hídrico en líneas recombinantes con sustitución de cromosomas de cebada. Estudio bioquímico y molecular.

Méndez AM, Castillo D, del Pozo A, Matus I, Morcuende R. 2011. Differences in stem soluble carbohydrate contents among recombinant chromosome substitution lines (RCSLs) of barley under drought in a mediterranean-type environment. Agronomy Research 9, 433–438.

Menéndez S, Barrena I, Setien I, González-Murua C, Estavillo JM. 2012. Efficiency of nitrification inhibitor DMPP to reduce nitrous oxide emissions under different temperature and moisture conditions. Soil Biology and Biochemistry 53, 82–89.

Menéndez S, López-Bellido RJ, Benítez-Vega J, González-Murua C, López-Bellido L, Estavillo JM. 2008. Long-term effect of tillage, crop rotation and N fertilization to wheat on gaseous emissions under rainfed Mediterranean conditions. European Journal of Agronomy 28, 559–569.

Menéndez S, Merino P, Pinto M, González-Murua C, Estavillo JM. 2006. 3,4-Dimethylpyrazol phosphate effect on nitrous oxide, nitric oxide, ammonia, and carbon dioxide emissions from grasslands. Journal of environmental quality 35, 973–81.

Midorikawa K, Kuroda M, Terauchi K, Hoshi M, Ikenaga S, Ishimaru Y, Abe K, Asakura T. 2014. Additional nitrogen fertilization at heading time of rice down-regulates cellulose synthesis in seed endosperm. PLoS ONE 9, 1–9.

Moore BD, Cheng S, Sims D, Seemann JR. 1999. The biochemical and molecular basis for photosynthetic acclimation to elevated atmospheric CO_2. Plant, Soil and Environment, 567–582.

Morcuende R, Kostadinova S, Pérez P, Martín Del Molino IM, Martínez-Carrasco R. 2004. Nitrate is a negative signal for fructan synthesis, and the fructosyltransferase-inducing trehalose inhibits nitrogen and carbon assimilation in excised barley leaves. New Phytologist 161, 749–759.

Morcuende R, Krapp A, Hurry V, Stitt M. 1998. Sucrose-feeding leads to increased rates of nitrate assimilation, increased rates of α-oxoglutarate synthesis, and increased synthesis of a wide spectrum of amino acids in tobacco leaves. Planta 206, 394–409.

Mothapo N V., Chen H, Cubeta MA, Grossman JM, Fuller F, Shi W. 2015. Phylogenetic, taxonomic and functional diversity of fungal denitrifiers and associated N_2O production efficacy. Soil Biology and Biochemistry 83, 160–175.

Mothapo N V., Chen H, Cubeta MA, Shi W. 2013. Nitrous oxide producing activity of diverse fungi from distinct agroecosystems. Soil Biology and Biochemistry 66, 94–101.

Müller C, Stevens RJ, Laughlin RJ, Azam F, Ottow JCG. 2002. The nitrification inhibitor DMPP had no effect on denitrifying enzyme activity. Soil Biology and Biochemistry 34, 1825–1827.

Nimesha F, Naoki N, Panozzo J, Tausz M, Norton RM, Seneweera S. 2017. Lower grain nitrogen content of wheat at elevated CO_2 can be improved through post-anthesis NH_4^+ supplement. Journal of Cereal Science 74, 79–85.

Ommen OE, Donnelly A, Vanhoutvin S, Oijen M Van, Manderscheid R. 1999. Chlorophyll content of spring wheat flag leaves grown under elevated CO_2 concentrations and other environmental stresses within the 'ESPACE-wheat' project. European Journal of Agronomy 10, 197–203.

Osuna D, Usadel B, Morcuende R, et al. 2007. Temporal responses of transcripts, enzyme activities and metabolites after adding sucrose to carbon-deprived Arabidopsis seedlings. Plant Journal 49, 463–491.

Pasda G, Hähndel R, Zerulla W. 2001. Effect of fertilizers with the new nitrification inhibitor DMPP (3,4-dimethylpyrazole phosphate) on yield and quality of agricultural and horticultural crops. Biology and Fertility of Soils 34, 85–97.

Patton CJ, Crouch SR. 1977. Spectrophotometric and kinetics investigation of the Berthelot reaction for the determination of ammonia. Analytical chemistry1 49, 464–469.

Patrick J.W., Offler C.E. 2001. Compartmentation of trans- port and transfer events in developing seeds. Journal of Experimental Botany 52, 551–564.

Pérez P, Morcuende R, Molino I, Martínez-Carrasco R. 2005. Diurnal changes of Rubisco in response to elevated CO_2, tempeature and nitrogen in wheat grown under temperature gradient tunnels. Environmental and Experimental Botany 53, 13–27.

Pfab H, Palmer I, Buegger F, Fiedler S, Müller T, Ruser R. 2012. Influence of a nitrification inhibitor and of placed N-fertilization on N_2O fluxes from a vegetable cropped loamy soil. Agriculture, Ecosystems and Environment 150, 91–101.

Philippot L, Andert J, Jones CM, Bru D, Hallin S. 2011. Importance of denitrifiers lacking the genes encoding the nitrous oxide reductase for N_2O emissions from soil. Global Change Biology 17, 1497–1504.

Philippot L, Hallin S. 2005. Finding the missing link between diversity and activity using denitrifying bacteria as a model functional community. Current Opinion in Microbiology 8, 234–239.

Pollock CJ, Cairns AJ. 1991. Fructan metabolism in grasses and cereals. Annu. Rev. Plant. Physiol. Plant. Mol. Bio 42, 77–101.

Poorter H, Berkel YVAN, Baxter R, Hertog JDEN, Dijkstra P, Gifeord RM. 1997. The effect of elevated CO_2 on the chemical composition and construction costs of leaves of 27 C_3 species. Plant cell & environmental, 472–482.

Pozo A del, Castillo D, Inostroza L, Matus I, Méndez AM, Morcuende R. 2012. Physiological and yield responses of recombinant chromosome substitution lines of barley to terminal drought in a Mediterranean-type environment. Annals of Applied Biology 160, 157–167.

Qiao C, Liu L, Hu S, Compton JE, Greaver TL, Li Q. 2015. How inhibiting nitrification affects nitrogen cycle and reduces environmental impacts of anthropogenic nitrogen input. Global Change Biology 21, 1249–1257.

Rachmilevitch S, Cousins AB, Bloom AJ. 2004. Nitrate assimilation in plant shoots depends on photorespiration. Proceedings of the National Academy of Sciences of the United States of America 101, 11506–11510.

Rees RM, Baddeley JA, Bhogal A, et al. 2013. Nitrous oxide mitigation in UK agriculture. Soil Science and Plant Nutrition 59, 3–15.

Reich PB, Hobbie SE. 2012. Decade-long soil nitrogen constraint on the CO_2 fertilization of plant biomass. Nature Climate Change 3, 278–282.

Robredo A, Pérez-López U, Miranda-Apodaca J, Lacuesta M, Mena-Petite A, Muñoz-Rueda A. 2011. Elevated CO_2 reduces the drought effect on nitrogen metabolism in barley plants during drought and subsequent recovery. Environmental and Experimental Botany 71, 399–408.

Rubio-Asensio JS, Bloom AJ. 2017. Inorganic nitrogen form: A major player in wheat and Arabidopsis responses to elevated CO_2. Journal of Experimental Botany 68, 2611–2625.

Rubio-Asensio JS, Rachmilevitch S, Bloom AJ. 2015. Responses of Arabidopsis and wheat to rising CO_2 depend on nitrogen source and nighttime CO_2 levels. Plant Physiology 168, 156–63.

Ruser R, Schulz R. 2015. The effect of nitrification inhibitors on the nitrous oxide (N_2O) release from agricultural soils-a review. Journal of Plant Nutrition and Soil Science 178, 171–188.

Saggar S, Jha N, Deslippe J, Bolan NS, Luo J, Giltrap DL, Kim DG, Zaman M, Tillman RW. 2013. Denitrification and N_2O:N_2 production in temperate grasslands: Processes, measurements, modelling and mitigating negative impacts. Science of the Total Environment 465, 173–195.

Sanz-Cobena A, Lassaletta L, Aguilera E, *et al.* 2016. Strategies for greenhouse gas emissions mitigation in Mediterranean agriculture: A review. Agriculture, Ecosystems and Environment 238, 5–24.

Sarasketa A, González-Moro MB, González-Murua C, Marino D. 2014. Exploring ammonium tolerance in a large panel of *Arabidopsis thaliana* natural accessions. Journal of Experimental Botany 65, 6023–33.

Sarasketa A, González-Moro MB, González-Murua C, Marino D. 2016. Nitrogen source and external medium pH interaction differentially affects root and shoot metabolism in Arabidopsis. Frontiers in plant science 7, 1–12.

Schmid I, Franzaring J, Müller M, Brohon N, Calvo OC, Högy P, Fangmeier A. 2016. Effects of CO_2 Enrichment and Drought on Photosynthesis, Growth and Yield of an Old and a Modern Barley Cultivar. Journal of Agronomy and Crop Science 202, 81–95.

Schmittgen TD, Livak KJ. 2008. Analyzing real-time PCR data by the comparative C_T method. Nature Protocols 3, 1101–1108.

Serrago RA, Alzueta I, Savin R, Slafer GA. 2013. Understanding grain yield responses to source-sink ratios during grain filling in wheat and barley under contrasting environments. Field Crops Research 150, 42–51.

Setién I, Fuertes-Mendizabal T, González A, Aparicio-Tejo PM, González-Murua C, González-Moro MB, Estavillo JM. 2013. High irradiance improves ammonium tolerance in wheat plants by increasing N assimilation. Journal of Plant Physiology 170, 758–771.

Setién I, Vega-Mas I, Celestino N, Calleja-Cervantes ME, González-Murua C, Estavillo JM, González-Moro MB. 2014. Root phosphoenolpyruvate carboxylase and NAD-malic enzymes activity increase the ammonium-assimilating capacity in tomato. Journal of Plant Physiology 171, 49–63.

Sharkey TD, Bernacchi CJ, Farquhar GD, Singsaas EL. 2007. Fitting photosynthetic carbon dioxide response curves for C_3 leaves. Plant, Cell and Environment 30, 1035–1040.

Shen T, Stieglmeier M, Dai J, Urich T, Schleper C. 2013. Responses of the terrestrial ammonia-oxidizing archaeon Ca. *Nitrososphaera viennensis* and the ammonia-oxidizing bacterium *Nitrosospira multiformis* to nitrification inhibitors. FEMS Microbiology Letters 344, 121–129.

Shi X, Hu H, He J, Chen D, Suter HC. 2016a. Effects of 3,4-dimethylpyrazole phosphate (DMPP) on nitrification and the abundance and community composition of soil ammonia oxidizers in three land uses. Biology and Fertility of Soils 52, 927–939.

Shi X, Hu H-W, Kelly K, Chen D, He J-Z, Suter HC. 2016b. Response of ammonia oxidizers and denitrifiers to repeated applications of a nitrification inhibitor and a urease inhibitor in two pasture soils. Journal of Soils and Sediments 17, 974–984.

Šimek M, Cooper JE. 2002. The influence of soil pH on denitrification: Progress towards the understanding of this interaction over the last 50 years. European Journal of Soil Science 53, 345–354.

Simpson RJ, Dalling MJ. 1981. Nitrogen redistribution during grain growth in wheat (*Triticum aestivum* L.). Planta 151, 447–456.

Singh BP, Hatton BJ, Balwant S, Cowie AL, Kathuri A. 2010. Influence of biochars on nitrous oxide emission and nitrogen leaching from two contrasting soils. Journal of Environmental Quality 39, 1224–35.

Snyder CS, Bruulsema TW, Jensen TL, Fixen PE. 2009. Review of greenhouse gas emissions from crop production systems and fertilizer management effects. Agriculture, Ecosystems and Environment 133, 247–266.

Stange CF, Spott O, Arriaga H, Menéndez S, Estavillo JM, Merino P. 2013. Use of the inverse abundance approach to identify the sources of NO and N_2O release from Spanish forest soils under oxic and hypoxic conditions. Soil Biology and Biochemistry 57, 451–458.

Stitt M, Krapp A. 1999. The interaction between elevated carbon dioxide and nitrogen nutrition: the physiological and molecular background. Plant, Cell & Environment 22, 583–621.

Stitt M, Lunn J, Usadel B. 2010. Arabidopsis and primary photosynthetic metabolism- more than the icing on the cake. the Plant Journal 61, 1067–1091.

Stitt M, Müller C, Matt P, Gibon Y, Carillo P, Morcuende R, Scheible W-R, Krapp A. 2002. Steps towards an integrated view of nitrogen metabolism. Journal of Experimental Botany 53, 959–970.

Strehmel N., Hummel J., Erban A., Strassburg K., Kopka J. 2008. Retention index thresholds for compound matching in GC-MS metabolite profiling. Journal of Chromatography. B, Analytical Technologies in the Biomedical and Life Sciences 871, 182-190.

Subbarao G V., Ito O, Sahrawat KL, Berry WL, Nakahara K, Ishikawa T, Watanabe T, Suenaga K, Rondon M, Rao IM. 2006. Scope and Strategies for Regulation of Nitrification in Agricultural Systems—Challenges and Opportunities. Critical Reviews in Plant Sciences 25, 303–335.

Subbarao G V., Sahrawat KL, Nakahara K, Rao IM, Ishitani M, Hash CT, Kishii M, Bonnett DG, Berry WL, Lata JC. 2013. A paradigm shift towards low-nitrifying production systems: the role of biological nitrification inhibition (BNI). Annals of Botany 112, 297–316.

Sweetlove LJ, Burrell MM, ap Rees T. 1996. Starch metabolism in tubers of transgenic potato (*Solanum tuberosum*) with increased ADPglucose pyrophosphorylase. Biochemical Journal 320, 493–498.

Syakila A, Kroeze C, Slomp CP. 2010. Neglecting sinks for N2O at the earth's surface: does it matter? Journal of Integrative Environmental Sciences 7, 79–87.

Szabados L, Savouré A. 2009. Proline: a multifunctional amino acid. Trends in Plant Science 15, 89–97.

Tambussi EA, Bort Pie J, Guiamet JJ, Nogués S, Araus JL. 2007. The photosynthetic role of ears in C_3 cereals: metabolism, water use efficiency and contribution to grain yield. Critical Reviews in Plant Sciences 26, 1–16.

Taub DR, Wang X. 2008. Why are nitrogen concentrations in plant tissues lower under elevated CO_2? A critical examination of the hypotheses. Journal Integrative Plant Biology 50, 1365–1374

Tegeder M, Masclaux-Daubresse C. 2017. Source and sink mechanisms of nitrogen transport and use. New Phytologist 217, 35–53.

Timilsena YP, Adhikari R, Casey P, Muster T, Gill H, Adhikari B. 2015. Enhanced efficiency fertilisers: A review of formulation and nutrient release patterns. Journal of the Science of Food and Agriculture 95, 1131–1142.

Triboi E, Triboi-Blondel AM. 2002. Productivity and grain or seed composition: A new approach to an old problem - Invited paper. European Journal of Agronomy 16, 163–186.

Uddling J, Gelang-Alfredsson J, Karlsson PE, Selldén G, Pleijel H. 2008. Source-sink balance of wheat determines responsiveness of grain production to increased [CO_2] and water supply. Agric. Ecosyst. Environ. 127, 215–222

United Nations, Department of Economic and Social Affairs, Population Division. 2015. World Population Prospects: The 2015 Revision, Key Findings and Advance Tables. Working Paper No. ESA/P/WP.241

Ussiri D, Lal R. 2013. Chapter 3: Formation and release of nitrous oxide from terrestrial and aquatic ecosystems. Soil Emission of Nitrous Oxide and its Mitigation.63–96.

Ussiri D, Lal R, Jarecki MK. 2009. Nitrous oxide and methane emissions from long-term tillage under a continuous corn cropping system in Ohio. Soil and Tillage Research 104, 247–255.

Valentini R, Epron D, Deangelis P, Matteucci G, Dreyer E. 1995. In-situ estimation of net CO_2 assimilation, photosynthetic electron flow and photorespiration in Turkey Oak (*Q. Cerris* L) leaves - diurnal cycles under different levels of water-supply. Plant Cell and Environment 18, 631–640.

Valluru R. 2015. Fructan and hormone connections. Frontiers in Plant Science 6, 1–6.

Vega-Mas I, Marino D, Sánchez-Zabala J, González-Murua C, Estavillo JM, González-Moro MB. 2015. CO_2 enrichment modulates ammonium nutrition in tomato adjusting carbon and nitrogen metabolism to stomatal conductance. Plant Science 241, 32–44.

Vega-Mas I, Pérez-Delgado CM, Marino D, Fuertes-Mendizabal T, González-Murua C, Márquez AJ, Betti M, Estavillo JM, González-Moro MB. 2017. Elevated CO_2 induces root defensive mechanisms in tomato plants when dealing with ammonium toxicity. Plant and Cell Physiology 58, 2112–2125.

Vicente R, Martínez-Carrasco R, Pérez P, Morcuende R. 2018. New insights into the impacts of elevated CO_2, nitrogen, and temperature levels on the regulation of C and N metabolism in durum wheat using network analysis. New BIOTECHNOLOGY 40, 192–199.

Vicente R, Pérez P, Martínez-Carrasco R, Feil R, Lunn JE, Watanabe M, Arrivault S, Stitt M, Hoefgen R, Morcuende R. 2016. Metabolic and transcriptional analysis of durum wheat responses to elevated CO_2 at low and high nitrate supply. Plant and Cell Physiology 57, 2133–2146.

Vicente R, Pérez P, Martínez-Carrasco R, Morcuende R. 2017. Improved responses to elevated CO_2 in durum wheat at a low nitrate supply associated with the upregulation of photosynthetic genes and the activation of nitrate assimilation. Plant Science 260, 119–128.

Vicente R, Pérez P, Martínez-Carrasco R, Usadel B, Kostadinova S, Morcuende R. 2015. Quantitative RT-PCR platform to measure transcript levels of C and N metabolism-related genes in durum wheat: transcript profiles in elevated [CO_2] and high temperature at different levels of N supply. Plant and Cell Physiology 56, 1556–1573.

Weckwerth, W., Wenzel, K., and Fiehn, O. (2004). Process for the integrated extraction, identification and quantification of metabolites, proteins and RNA to reveal their co-regulation in biochemical networks. Proteomics 4, 78–83.

White AC, Rogers A, Rees M, Osborne CP. 2015. How can we make plants grow faster? A source-sink perspective on growth rate. Journal of Experimental Botany 67, 31–45.

Wrage N, Velthof GL, Van Beusichem ML, Oenema O. 2001. Role of nitrifier denitrification in the production of nitrous oxide. Soil Biology and Biochemistry 33, 1723–1732.

Wu D, Senbayram M, Well R, Brüggemann N, Pfeiffer B, Loick N, Stempfhuber B, Dittert K, Bol R. 2017. Nitrification inhibitors mitigate N_2O emissions more effectively under straw-induced conditions favoring denitrification. Soil Biology and Biochemistry 104, 197–207.

Xu Z, Jiang Y, Jia B, Zhou G. 2016. Elevated-CO_2 response of stomata and its dependence on environmental factors. Frontiers in Plant Science 7, 1–15.

Xue GP, Kooiker M, Drenth J, McIntyre CL. 2011. *TaMYB13* is a transcriptional activator of fructosyltransferase genes involved in β-2,6-linked fructan synthesis in wheat. Plant Journal 68, 857–870.

Yamakawa H, Hakata M. 2010. Atlas of rice grain filling-related metabolism under high temperature: Joint analysis of metabolome and transcriptome demonstrated inhibition of starch accumulation and induction of amino acid accumulation. Plant and Cell Physiology 51, 795–809.

Yang M, Fang Y, Sun D, Shi Y. 2016. Efficiency of two nitrification inhibitors (dicyandiamide and 3,4-dimethypyrazole phosphate) on soil nitrogen transformations and plant productivity: a meta-analysis. Scientific Reports 6, 22075.

Yoshinari T, Hynes R, Knowles R. 1977. Acetylene inhibition of nitrous oxide reduction and measurement of denitrification and nitrogen fixation in soil. Soil Biology and Biochemistry 9, 177–183.

Zaghdoud C, Carvajal M, Ferchichi A, del Carmen Martínez-Ballesta M. 2016. Water balance and N-metabolism in broccoli (*Brassica oleracea* L. var. Italica) plants depending on nitrogen source under salt stress and elevated CO_2. Science of the Total Environment 571, 763–771.

Zanella M, Borghi GL, Pirone C, Thalmann M, Pazmino D, Costa A, Santelia D, Trost P, Sparla F. 2016. β-amylase 1 (BAM1) degrades transitory starch to sustain proline biosynthesis during drought stress. Journal of Experimental Botany 67, 1819–1826.

Zerulla W, Barth T, Dressel J, Erhardt K, Horchler von Locquenghien K, Pasda G, Rädle M, Wissemeier A. 2001. 3,4-Dimethylpyrazole phosphate (DMPP) - A new nitrification inhibitor for agriculture and horticulture. Biology and Fertility of Soils 34, 79–84.

Zhou B, Serret MD, Elazab A, Bort Pie J, Araus JL, Aranjuelo I, Sanz-Sáez Á. 2016. Wheat ear carbon assimilation and nitrogen remobilization contribute significantly to grain yield. Journal of Integrative Plant Biology 58, 914–926.

Zhu C, Ziska LH, Zhu J, Zeng Q, Xie Z, Tang H, Jia X, Hasegawa T. 2012. The temporal and species dynamics of photosynthetic acclimation in flag leaves of rice (*Oryza sativa*) and wheat (*Triticum aestivum*) under elevated carbon dioxide. Physiologia Plantarum 145, 395–405.

Ziska LH, Morris CF, Goins EW. 2004. Quantitative and qualitative evaluation of selected wheat varieties released since 1903 to increasing atmospheric carbon dioxide: Can yield sensitivity to carbon dioxide be a factor in wheat performance? Global Change Biology 10, 1810–1819.

Zumft W. 1997. Cell biology and molecular basis of denitrification. Cell Biology and Molecular Basis of Denitrification 61, 533–616.

9

Supplementary information

Chapter 3

Supplementary Table 1. Primers pairs and thermal conditions used for real-time qPCR.

Target group	Primer name	Sequence	Thermal profile	bp length	Efficiency (%)	References
16S rRNA Bacteria	341F 534R	5´-CCTACGGGAGGCAGCAG-3´ 5´-ATTACCGCGGCTGCTGGCA-3´	95ºC for 2 min – x 1 cycle 95ºC for 15 sec , 60 °C for 30 sec , 72 °C for 30 sec , 80 °C for 30sec – x 40 cycles	174	95	Lopez-Gutiérrez *et al.*, (2004)
16S rRNA Archaea	771F 957R	5´-ACGGTGAGGGATGAAAGCT-3´ 5´ -CGGCGTTGACTCCAATTG-3´	95 °C for 2 min – x 1 cycle 95 °C for 15 sec , 58 °C for 30 sec , 72 °C for 30 sec , 80 °C for 30sec – x 40 cycles	226	93	Ochsenreiter *et al.*, (2003)
Bacterial *amoA*	amoA1F amoA2R	5´-GGGGTTTCTACTGGTGGT-3´ 5´-CCCTCKGSAAAGCCTTCTTC-3´	95 °C for 2 min – x 1 cycle 95 °C for 15 sec, 54 °C for 60 sec , 72 °C for 60 sec – x 40 cycles	491	91	Rotthauwe *et al.*, (1997)
Archaea *amoA*	Arch-amoAF Arch-amoAR	5´-STAATGGTCTGGCTTAGACG-3´ 5´-GCGGCCATCCATCTGTATGT-3´	95 °C for 2 min - x 1 cycle 95 °C for 45 sec, 54 °C for 45 sec, 72 °C for 45 sec; 85 °C for 20 sec - x 40 cycles	635	86	Francis *et al.*, (2005)
narG	NarG-f NarG-r	5'-TCGCCSATYCCGGCSATGTC-3' 5'-GAGTTGTACCAGTCRGCSGAYTCSG-3'	95 °C for 2 min – x 1 cycle 95 °C for 15 sec, 63 °C for 30 sec (-1 °C /cycle), 72 °C for 30 sec, 80 °C for 30 sec – x 6 cycles 95 °C for 15 sec, 58 °C for 30 sec, 72 °C for 30 sec, 80 °C for 30sec – x 40 cycles	173	97	Bru *et al.*, (2007)
nirS	cd3aF R3cd	5´-GTSAACGTSAAGGARACSGG-3 ´ 5´-GASTTCGGRTGSGTCTTGA-3´	95 °C for 2 min - x 1 cycle 95 °C for 45 sec, 55 °C for 45 sec, 72 °C for 45 sec; 85 °C for 20 sec - x 40 cycles	410	92	Michotey *et al.*, (2000) Throbäck *et al.*, (2004)
nirK	NirK 876 NirK1040	5´-ATYGGCGGVCAYGGCGA-3´ 5´-GCCTCGATCAGRTTRTGGTT-3´	95 °C for 2 min – x 1 cycle 95 °C for 15 sec, 63 °C for 30 sec (-1 °C /cycle), 72 °C for 30 sec, 80 °C for 15 sec – x 6 cycles 95 °C for 15 sec, 58 °C for 30 sec, 72 °C for 30 sec, 80 °C for 30sec – x 40 cycles	165	86	Henry *et al.*, (2004)
nosZI	nosZ-F nosZ-R	5´-CGCRACGGCAASAAGGTSMSSGT-3´ 5´-CAKRTGCAKSGCRTGGCAGAA-3´	95 °C for 2 min – x 1 cycle 95 °C for 15 sec, 65 °C for 30 sec (-1 °C /cycle), 72 °C for 30 sec, 80°C for 30 sec – x 6 cycles 95 °C for 15 sec, 60 °C for 30 sec, 72 °C for 30 sec, 80 °C for 30sec – x 40 cycles	267	88	Henry *et al.*, (2006)

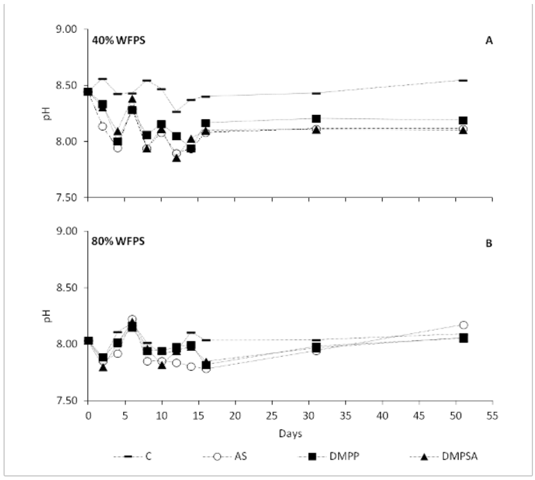

Supplementary Figure 1. Evolution of soil pH at 40% WFPS (A) and 80% WFPS (B) during the whole experiment.

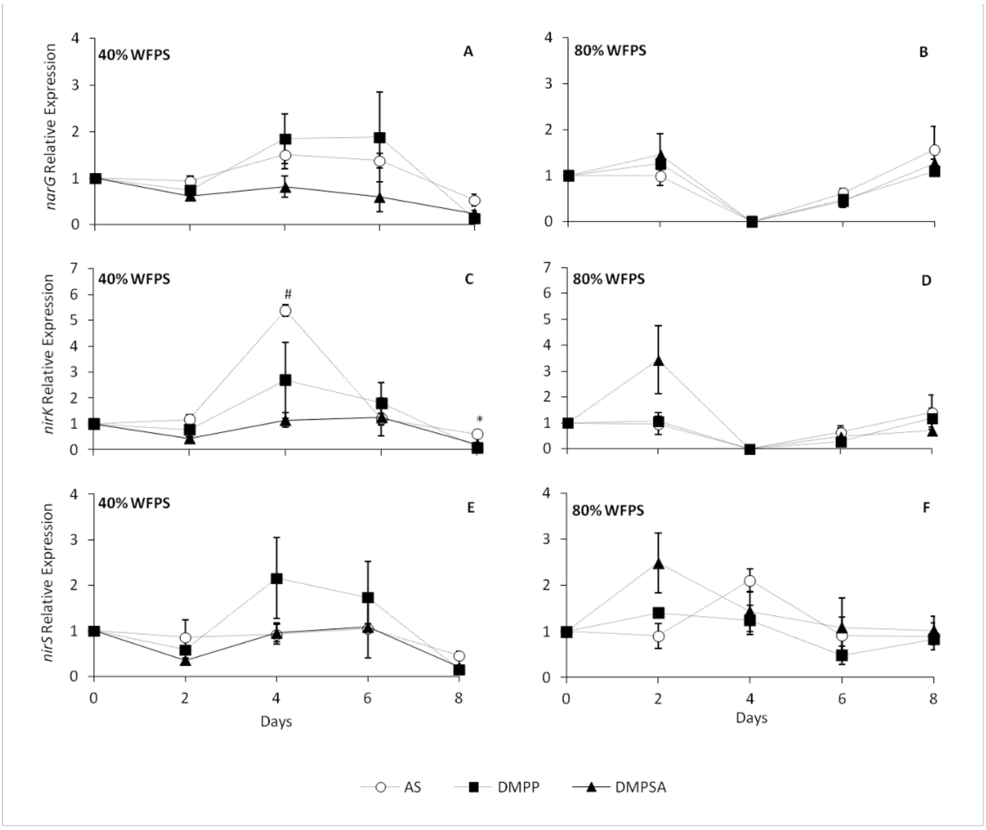

Supplementary Figure 2. Relative expression of denitrifying genes *narG* (A, B), *nirK* (C, D) and *nirS* (E, F) at 40% WFPS (A, C, E) and 80% WFPS (B, D, F) for the first 8 days. Significant differences ($p<0.05$) between DMPP and DMPSA with respect to AS are represented by * and #, respectively. Values represent mean ± SE (n=3).

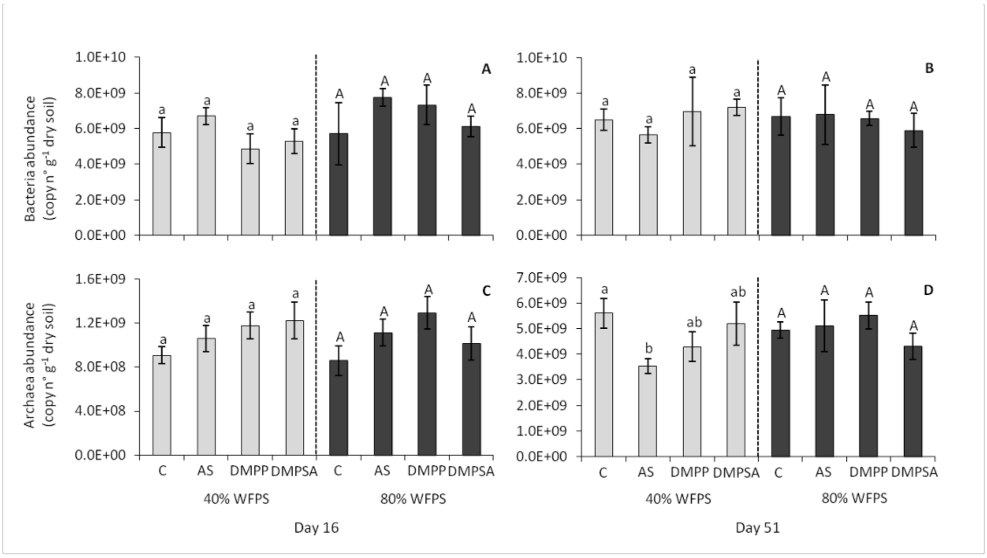

Supplementary Figure 3. Bacteria (A, B) and archaea (C, D) abundances expressed as *16S rRNA* gene copy number per gram of dry soil at 40% WFPS (grey bars) and 80% of WFPS (black bars) 16 (A, C) and 51 days (B, D) after treatment application. Significant differences ($p<0.05$) between treatments within each WFPS condition are indicated with different letters. Asterisk (*) indicates significant WFPS effect for each fertilised treatment ($p<0.05$). Values represent the mean ± SE (n=4). C = unfertilised control; AS = ammonium sulphate; DMPP = ammonium sulphate + DMPP; and DMPSA = ammonium sulphate + DMPSA.

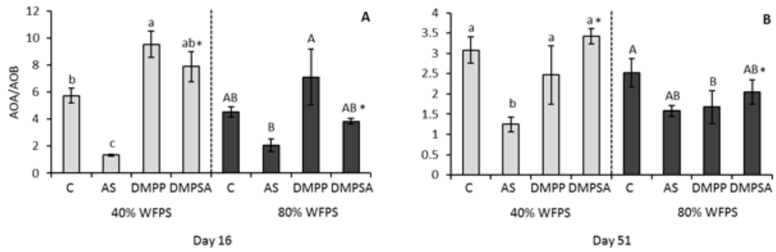

Supplementary Figure 4. Ratio of AOA over AOB at 40% WFPS (grey bars) and 80% of WFPS (black bars) 16 (A, C) and 51 days (B, D) after treatment application. Significant differences ($p<0.05$) between treatments within each WFPS condition are indicated with different letters. Asterisk (*) indicates significant WFPS effect for each fertilised treatment ($p<0.05$). Values represent the mean ± SE ($n=4$). C = unfertilised control; AS = ammonium sulphate; DMPP = ammonium sulphate + DMPP; and DMPSA = ammonium sulphate + DMPSA.

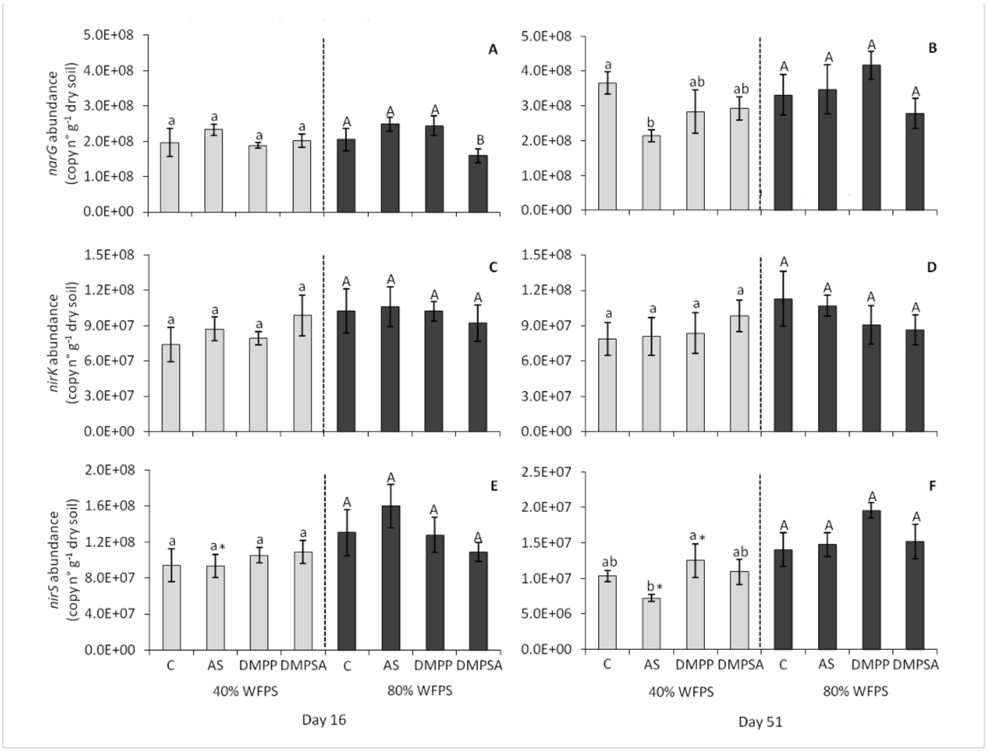

Supplementary Figure 5. Denitrifying abundances expressed as *narG* (A, B), *nirK* (C, D) and *nirS* (E, F) gene copy number per gram of dry soil at 40% WFPS (grey bars) and 80% of WFPS (black bars) 16 (A, C, E) and 51 days (B, D, F) after treatment application. Significant differences ($P < 0.05$) between treatments within each WFPS condition are indicated with different letters. Asterisk (*) indicates significant WFPS effect for each fertilization treatment ($P < 0.05$). Values represent mean ± SE (n=4). C means unfertilized control, AS ammonium sulphate, DMPP ammonium sulphate + DMPP and DMPSA ammonium sulphate + DMPSA.

Chapter 4

Supplementary Table 1. Primers pairs used for real-time qPCR.

Acc. No.	Description	Foward and reverse primer (5´- 3´)		Product (bp)	Reference
AK331207	Similar to A. thaliana RNase L inhibitor protein	Fw	TTGAGCAACTCATGGACCAG	86	(Giménez et al., 2010)
		Rv	GCTTTCCAAGGCACAAACAT		
Ta2291	ADP-ribosylation factor	Fw	TCTCATGGTTGGTCTCGATG	81	(Giménez et al., 2010)
		Rv	GGATGGTGGTGACGATCTCT		
AB181991	Actin	Fw	AGAGTCGGTGAAGGGGACTTA	97	(Jauregui et al., 2017)
		Rv	TCCTGTACCCCTTATTCCTCTGA		
BE213258	Putative carbonic anhydrase, plastidial, CA	Fw	CGACCGATGTGGATCCATTGCCA	65	(Vicente, R. et al., 2015)
		Rv	ATCCCGGCATCCAGTCGTGGAA		
TC389217	Putative carbonic anhydrase, plastidial, CA	Fw	GGTCGGCGGTCACTACGACTTC	173	(Vicente, R. et al., 2015)
		Rv	AAACAACGAGTACGCACTCCCATG		
TC393400	Putative carbonic anhydrase, plastidial, CA	Fw	GCAGAACCTCCTGACCTACCCGTTC	82	(Vicente, R. et al., 2015)
		Rv	GAAGTCGTAATGACCGCCGACCAG		
TC442386	Putative carbonic anhydrase, plastidial, CA	Fw	TGGAGTAAAGTTGGACACAGCGAAC	126	(Vicente, R. et al., 2015)
		Rv	CTGGCCGCCATTTCACGATTCTAG		
HF544985	Low affinity nitrate transporter, NRT1 (NRT1.1A)	Fw	CCTTCACCTACATCGGCCAG	112	(Vicente, R. et al., 2015)
		Rv	CTGACGAAGAATCCGAGCGA		
AY587264	Low affinity nitrate transporter, NRT1 (NRT1.2)	Fw	ATACCTGGGGAAGTACCGGACAGC	133	(Vicente, R. et al., 2015)
		Rv	AGGATCTGCCCAAAGAGTCCAAGCA		
HF544995	Low affinity nitrate transporter, NRT1 (NRT1.7B)	Fw	ATCGTATGCTTCGTCGCGT	147	(Vicente, R. et al., 2015)
		Rv	CGGCAAGAATGCAGTTAGGG		
AY428038	Ammonium transporter, AMT (AMT2;1)	Fw	GAGCCGAACCTCTGCAATCT	123	(Vicente, R. et al., 2015)
		Rv	GTTCCACCCGATCACGAAGA		
DQ345446	Aquaporin (PIP 1.1)	Fw	CCGCCTCGCCTCCGCTACCA	127	(Jauregui et al., 2017)
		Rv	CTGGATTCAGTCAGGAGAGAACAT		
AY525641	Aquaporin (PIP 2.3)	Fw	TCTCATCCTCCCCAGCTCGGT	141	(Jauregui et al., 2017)
		Rv	ACGAAGATGAGGGTGGAGATGAA		
EU177566	Aquaporin (TIP 1)	Fw	CTCAGCGCAGCCAGCCTGCTT	132	(Jauregui et al., 2017)
		Rv	CCACAAACTGATCGACCCAGGAAG		

Supplementary Table 2. Nitrogen source on individual amino acid content (µmol g DW^{-1}) in flag leaves of wheat grown under ambient (400 ppm) and elevated (750 ppm) CO_2 concentration fertilised with nitrate (NO_3^-), ammonium (NH_4^+) and ammonium nitrate (NH_4NO_3). Data represent mean values ±SE (n=3). Letters represent significant differences between treatments analysed by non-parametric test ($p<0.05$). Asterisk (*) indicates significant CO_2 differences ($p<0.05$).

	400 ppm CO_2			700 ppm CO_2		
	NO_3^- T1	NH_4^+ T1	NH_4NO_3 T1	NO_3^- T0	NH_4^+ T1	NH_4NO_3 T1
asp	63.7 ± 8.1 a	76.0 ± 3.8 a*	67.0 ± 18.0 a	50.7 ± 2.6 A	42.3 ± 9.0 A	71.3 ± 11.9 A
asn + ser	193.3 ± 59.1 a*	296.5 ± 29.7 a*	254.7 ± 83.4 a	73.0 ± 19.6 B	91.3 ± 18.7 B	178.7 ± 28.8 A
glu	189.7 ± 11.3 a*	214.0 ± 12.0 a*	193.7 ± 30.1 a	143.7 ± 6.6 B	91.3 ± 6.9 B	213.7 ± 29.2 A
gly	10.7 ± 0.7 a*	12.7 ± 2.7 a	7.3 ± 1.8 a	2.0 ± 0.0 A	4.5 ± 2.0 A	3.5 ± 0.3 A
his + gln	127.3 ± 65.9 a*	585.7 ± 179.4 a*	242.0 ± 130.7 a	14.3 ± 2.7 B	120.0 ± 27.0 A	48.0 ± 9.1 AB
arg	13.3 ± 9.8 a	76.7 ± 23.8 a	21.0 ± 5.8 a	10.0 ± 6.0 B	36.7 ± 5.2 A	16.0 ± 3.1 B
thr	21.3 ± 4.3 a	30.3 ± 2.4 a*	32.0 ± 8.9 a	17.3 ± 3.8 AB	15.3 ± 2.9 B	28.3 ± 3.5 A
ala	70.3 ± 8.8 a*	67.7 ± 5.6 a	49.7 ± 11.5 a	31.7 ± 2.0 B	51.3 ± 10.2 AB	66.7 ± 11.2 A
pro	25.7 ± 7.1 b	333.0 ± 55.4 a*	331.7 ± 55.3 a*	8.3 ± 4.9 B	35.5 ± 2.6 A	16.7 ± 4.3 B
gaba	15.3 ± 5.5 a*	19.0 ± 2.5 a*	23.0 ± 6.4 a	5.0 ± 0.6 A	9.3 ± 2.2 A	12.0 ± 3.0 A
val	8.7 ± 4.7 b	68.7 ± 14.3 a	25.0 ± 8.5 b	7.0 ± 4.0 B	28.5 ± 3.5 A	20.0 ± 4.6 AB
lys	4.7 ± 2.7 b	28.3 ± 8.1 a	13.0 ± 4.0 ab	8.0 ± 5.0 A	23.0 ± 5.5 A	14.0 ± 3.5 A
ile	3.7 ± 1.7 a	20.7 ± 6.7 a	30.3 ± 14.1 a	5.0 ± 3.0 B	16.0 ± 0.6 A	12.3 ± 3.2 AB
leu	2.0 ± 1.0 a	9.7 ± 3.7 a	25.3 ± 12.9 a	7.7 ± 4.7 A	13.7 ± 2.6 A	14.3 ± 3.7 A
phe	2.0 ± 0.0 b	6.3 ± 1.7 ab	18.0 ± 5.7 a	3.7 ± 2.2 B	13.0 ± 2.3 A*	9.7 ± 2.8 AB

Chapter 5

Supplementary Table 1. Primer pairs for barley sequences associated with photosynthesis, carbohydrate metabolism and nitrogen assimilation.

Acc. No.	Description		Sequence	Product (bp)	Reference
AY145451	Actin (reference gene)	Fw	GGCACACTGGTGTCATGG	134	(Córdoba *et al.*, 2016)
		Rv	CTCCATGTCATCCCAGTT		
AK356022	Photosystem II light harvesting chlorophyll a/b binding protein	Fw	CATCCCCTCACGGCTTTCTT	67	(Córdoba *et al.*, 2016)
		Rv	CGCCGCCATTGTAGAGCTAA		
AK361860	Photosystem II light harvesting chlorophyll a/b binding protein	Fw	CGCCACCAACTTTGTTCCTG	147	(Córdoba *et al.*, 2016)
		Rv	ATCGAAGGCGGGCAAATCTT		
AK365564	Photosystem II subunit R	Fw	GCGGATTATAACCGTCAGGACA	140	(Córdoba *et al.*, 2016)
		Rv	TGTGAGAGAGCTTAGCACTGAA		
AK360942	Oxygen evolving enhancer protein 3, PsbQ	Fw	AAAGGGGACTACGCAGAAGC	73	(Córdoba *et al.*, 2016)
		Rv	AGCTCTTGATCCGGCAAACA		
AK252670	Photosystem II reaction center, PsbP	Fw	GACCTAGGCCCTCCTGAGAA	141	(Córdoba *et al.*, 2016)
		Rv	ATAGAGCTTGCCATCGTCCG		
KC912689	Photosystem I P700 apoprotein A1, PsaA	Fw	CGCAAGGAAAGCGAAAACCT	62	(Córdoba *et al.*, 2016)
		Rv	ATTTGCTCGGAGTTCCCGTT		
AGP50910	Photosystem I P700 apoprotein A2	Fw	CATTGAAAGCGGGGCCATTC	68	(Córdoba *et al.*, 2016)
		Rv	TGCTCATGGCAAGACGACAT		
X15869	Protochlorophyllide oxidoreductase, POR	Fw	CGTGTACTGGAGCTGGAACA	100	(Córdoba *et al.*, 2016)
		Rv	GGATTTGCGGTGGATCATGC		
AGP50919	Rubisco large subunit, RbcL	Fw	ACGTGCTCTACGTTTGGAGG	65	(Córdoba *et al.*, 2016)
		Rv	GCGGGCCTTGGAAAGTTTTT		
U43493	Rubisco small subunit, RbcS	Fw	ACCAACATGCTCGAGAAAGCA	141	(Córdoba *et al.*, 2016)
		Rv	GTGTGGGCGTGCAAAGATGT		
AK366020	Sucrose:sucrose 1-fructosyltransferase, 1-SST	Fw	GGCCAGGAAACAATCTACCCA	87	(Córdoba *et al.*, 2016)
		Rv	GGGATGAGAATGACGCGAGA		
X83233	Sucrose:fructan 6-fructosyltransferase, 6-SFT	Fw	CGTATCAGGAGGCAAGAGTC	98	(Méndez, 2014)
		Rv	GTTGTGTGCCGAGTCCAT		
JQ411253	Fructan:fructan 1-fructosyltransferase, 1-FFT	Fw	GACCGGCGAGACTATTACGC	110	(Méndez, 2014)
		Rv	CTGCCATAGTCGTAGCGCA		
AJ605333	Fructan 1-exohydrolase, 1-FEH	Fw	GGATTACGGCATTTCTACGC	69	(Méndez, 2014)
		Rv	CCCCATACAATCCTCCTGCC		
AK357958	Fructan 6-exohydrolase, 6-FEH	Fw	GTCAGAGGAGGAACTACGCAC	70	(Córdoba *et al.*, 2016)
		Rv	GGCGGTCGAGTCTGTCATAA		
AJ534444	Cell wall invertase, cwinv2	Fw	AGACGTTGAGGAGCAAACGA	140	(Méndez, 2014)
		Rv	GGTTTCTGCCTCTTCCAGGG		
AK359654	Structural constituent of cell wall	Fw	CATAGATCGAGCGGTGGCTA	75	(Córdoba *et al.*, 2016)
		Rv	AATCCGGGCCATCATGCTC		
X57845	Nitrate reductase, NR	Fw	ACCAACTGCGTCATCACCAC	135	(Méndez, 2014)
		Rv	GGATGGATGGATGGAGGAGGA		